THE C-TERMINUS OF TRANSMEMBRANE HELIX 2 (TM2) OF THE *ESCHERICHIA COLI* TAR CHEMORECPTOR DETERMINES SIGNAL OUTPUT AND LIGAND SENSITIVITY

A Dissertation

by

CHRISTOPHER A. ADASE

Submitted to the Office of Graduate Studies of
Texas A&M University
in partial fulfillment of the requirements for the degree of

DOCTOR OF PHILOSOPHY

Approved by:

Chair of Committee,	Michael D. Manson
Committee Members,	Gregory D. Reinhart
	Michael Polymenis
	Michael Benedik
Head of Department,	Gregory D. Reinhart

December 2012

Major Subject: Biochemistry

ABSTRACT

Methyl-accepting chemotaxis proteins MCPs can bind one or more receptor-specific ligands. In the case of the Tar MCP of *Escherichia coli* (Tar_{Ec}), a primary attractant ligand is aspartate. Its binding to the periplasmic domain of Tar generates a conformational change that is transmitted via helix 4 transmembrane helix 2 (TM2). An inward movement of TM2 initiates a transmembrane signal to the cytoplasmic HAMP (histidine kinases, adenyl cyclases, methyl-accepting proteins, phosphatases) domain. Baseline CheA kinase-stimulating activity and ligand-induced responses are both strongly influenced by residues at the C-terminus of transmembrane helix 2 (TM2). The cytoplasmic aromatic anchor, composed of residues Trp-209 and Tyr-210 in Tar_{Ec}, is of particular importance. These residues are not highly conserved among transmembrane receptors having a HAMP domain, although there are almost always some aromatic residues in this region. The question thus becomes what properties of this aromatic anchor are necessary for proper signal transduction.

In this dissertation, I studied the effect on Tar_{Ec} function by substituting all possible combinations of Ala, Phe, Tyr, and Trp at positions 209 and 210. This library of Tar_{Ec} variants allowed the direct assessment of the effect of the residue composition of the aromatic anchor and led to a model of how the wild-type anchor maintains the base-line signaling state in Tar_{Ec}. Additional receptor variants containing double aromatic tandems and Ala substitutions for the periplasmic Trp residue were created, and the aromatic residues were also shifted in position within the six residues 207-212.

Trp, Tyr, and Phe, in that order, had the greatest effect on function when they were moved to novel positions. It was also discovered that Gly-211 plays a critical role in maintaining receptor function. A model was generated that proposes that Gly-211 plays a role in maintaining the flexibility of the TM2-HAMP domain connector. The results suggest that the signaling properties of the transmembrane sensor kinases of two-component systems can be predicted by the nature of their TM2-HAMP connections. It may also be possible to modulate their activity in a controlled way by manipulating the amino acid sequences that comprise those connections.

DEDICATION

This work is dedicated to my mother Linda, Grandpa Jay his wife my Grandmother Nora, and my Grandfather Frank who all passed before they could see me graduate. It is also dedicated to my father and brother who were there for me. Finally this is dedicated to my family who are not with me yet, my success was a struggle but it was worth it so you could have a better life.

ACKNOWLEDGEMENTS

I would like to thank the many good friends and colleagues I have made over the years for making my time at Texas A&M University enjoyable while I worked tirelessly for nearly eight years. I also wish to thank the undergraduates that worked with me in the Manson lab, sometimes the made my life easier, sometimes not.

Finally, I would like to thank my committee chair and members for putting the time and effort to improve my writing and scientific abilities.

TABLE OF CONTENTS

CHAPTER

LIST OF FIGURES

LIST OF TABLES

CHAPTER I

INTRODUCTION TO THE CHEMOTAXIS SYSTEM OF *ESCHERICHIA COLI*

A general overview of the *E.coli* chemotaxis system

Escherichia coli is a gram-negative, rod-shaped bacillus that is 2-4 μm long and 0.7-1 μm in diameter. Flagella arise at random points from the cell surface in a pattern that is known as peritrichous. Each flagellum is attached to a rotary motor that can turn either clockwise (CW) or counterclockwise (CCW). If every flagellum rotates CCW, the left-handed helical flagellar filaments coalesce into a single helical bundle (**Figure 1**) that propels the cell in a gently curved path known as a run (*1*). A running cell swims at 20-40 μm/sec (*2*). The duration of a run is determined by the frequency of switching from counterclockwise (CCW) to clockwise (CW) rotation of the motor. A change in direction of one or more a flagella from CCW to CW rotation disrupts the helical bundle and results in a random reorientation of the cell known as a tumble (*3*). Either pole of the cell can lead, as it has no set front or back end (*4*).

In a homogeneous environment, cells alternate between runs, which last several seconds, and brief tumbles. The resulting movement is described as a three-dimensional random walk. The three-dimensional random walk allows a cell to sample the local environment and compare it to its environment from several seconds ago. The ability to compare the environment at two points in space-time allows gradients to be detected in a heterogeneous environment. Thus, when in a heterogeneous environment, the random walk can be biased by extending the duration of a run in the direction of an increasing

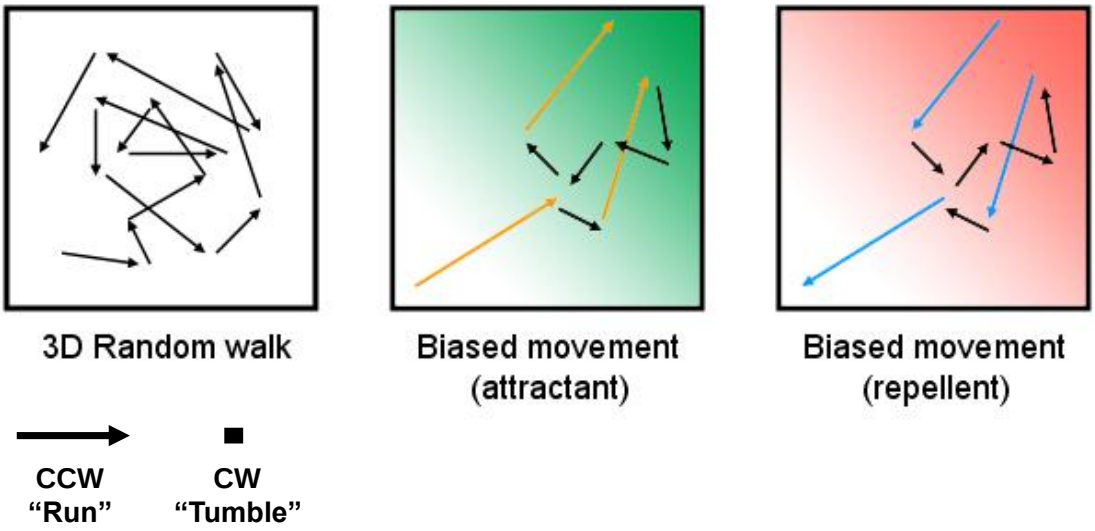

Figure 1. Behavior of an *E. coli* cell in homogenous and non-homogenous environments. The cell normally swims in a vector (run) until it randomizes its direction (tumbles). This behavior yields a three-dimensional random walk (left) unless an attractant (middle) or a repellent (right) gradient is present, in which case the run is lengthened in the favorable direction.

attractant concentration the direction of a decreasing repellent concentration (**Figure 1**).

The chemoreceptors that are responsible for detecting attractant and repellent are typically located in clusters near the poles of an *E.coli* cell, usually in one large sub-polar patch (*4*). The different chemoreceptors integrate responses when multiple ligands are detected and work in a synergistic fashion to stimulate the CheA kinase (*5-7*).

The chemotactic response has three distinct phases: stimulus detection, intracellular signal transduction, and adaptation. Detection involves binding of the chemoeffector to its cognate receptor and a conformational change in the receptor that is transmitted through the membrane to alter the output of the signaling pathway. Intracellular signal transduction converts the regulation of the activity of the CheA kinase, which is controlled by the chemoreceptor, into a change in the intracellular concentration of the phosphorylated (active) form of the response regulator CheY. Adaptation is the result of a more gradual change in the activity of the receptor/kinase complex that restores the pre-stimulus level of receptor-coupled kinase activity. This adaptation is accomplished by the covalent modification, through methylation and demethylation, of certain glutamyl residues in the cytoplasmic portion of the receptor. The difference in kinetics between ligand detection by the receptor and changes in methylation state of the receptor that compensates for the bound ligand is the basis of the "memory" of an *E.coli* cell of its past environment.

Chemoreceptors in *E.coli*

In *E. coli*, there are four methyl-accepting chemoreceptors (MCPs) that recognize

specific attractants and repellents. The MCPs were named for the chemicals to which they mediate responses: taxis to aspartate and away from certain repellents (Tar); taxis to serine and away from certain repellents (Tsr); taxis to ribose and galactose (Trg); and taxis-associated protein for dipeptides (Tap). The aerotaxis receptor (Aer) is an additional MCP-like protein that mediates redox responses in the cell and undergoes methylation-independent adaptation, unlike the methylation-dependent adaptation of the MCPs (*8-13*). The two major transducers in *E.coli* are Tar and Tsr, which are found in approximately 3-5 fold greater abundance than the minor transducers Tap, Trg, and Aer (*14*). The major transducers do not require another chemoreceptor to be present in order to carry out chemotaxis. In contrast, the minor transducers (Tap, Trg, and Aer) are unable to mediate chemotaxis by themselves and require the presence of one of the major transducers (Tar and/or Tsr). There is no requirement that a ligand sensed by the major transducer is needed for a minor transducer to mediate chemotaxis to its ligands.

The chemotaxis system of *E.coli* is relatively simple, as it has fewer chemoreceptors and a simpler downstream signaling pathway compared to other well-studied γ proteobacteria, such as *Vibrio cholerae* (*15*). Although the chemotaxis circuit of *E.coli* is relatively simple and is one of the model systems to study signal transduction in bacteria, new responses, such as the ability of Tap to detect pyrimidines (*16*) or Tsr to detect the autoinducer AI-2 (*17*), are still being discovered. Even for many known chemoeffectors (*18*), the precise interactions between the ligand and protein that initiate the transmembrane signal are unknown. The situation is complicated by the fact that some ligands interact directly with the MCP, whereas others first bind to a periplasmic

binding protein that then interacts with the cognate MCP (*8, 19-23*). **Table 1** gives the full set of known MCPs and auxiliary co-receptors and their respective ligands.

MCPs exist as homodimers whether a ligand is bound or not. The basic functional unit needed to bind to a ligand requires a homodimeric MCP periplasmic domain. Each subunit of a receptor dimer has a molecular weight of approximately 60,000 daltons. Aspartate binds directly to the receptor (*24-26*), as was shown in the atomic structure of the crystallized periplasmic domain of the ligand-bound Tar protein of *Salmonella typhimurium* (*27*). This structure showed the periplasmic domain as two four-helix bundles with the aspartate binding site at the interface of the two subunits. The specific residues involved in binding aspartate by Tar (Tar_{Ec}) are different in each subunit (*28*) (**Figure 2**). When aspartate binds to Tar, it interacts with residues R64, Y149, Q152, and T154 on one subunit and R69 and R73 on the other subunit (*28*). Aspartate binds directly to one of two rotationally symmetric binding sites in an *E. coli* Tar (Tar_{Ec}) homodimeric periplasmic domain (*8, 25, 29*). Each site contains residues from each monomer, but once a single aspartate binds, a strong negative cooperativity either decreases the affinity for binding (Tar_{St}) or virtually prevents binding (Tar_{Ec}) of a second aspartate molecule (*26, 29*).

Tar_{Ec} also has the ability to detect and respond to the disaccharide maltose (*8*). Unlike aspartate, which directly interacts with Tar_{Ec}, maltose must first bind to maltose-binding protein (MBP) (*21, 30, 31*), which then undergoes a conformation change from an "open" to a "closed" form (*31, 32*). The "closed" form of MBP can interact with Tar and thereby elicit a chemotaxis response (*33, 34*). Bound MBP contacts both monomers

Gene	Attractants	Repellents	Binding proteins
Tar	**Aspartate (*35-37*)** **Maltose (*8*)** **Warm temp (*38*)**	**Nickel (*39, 40*)** **Cobalt (*39*)**	**MBP (*30*)**
Tsr	**Serine (*8, 37*)** **AI-2 (*17, 41*)** **Warm temp (*38*)**	**N/A**	**LsrB (*17, 42*)**
Trg	**Ribose (*23*)** **Galactose (*43*)** **Warm temp (*44*)**	**N/A**	**GBP (*45*)**
Tap	**Dipeptides (*46*)** **Pyrmidines (*16*)** **Cold temp (*44*)**	**N/A**	**DBP (*46, 47*)**
Aer	**Molecular oxygen (*48*)** **Temperature (*49*)**	**N/A**	**N/A**

Table 1. Chemoreceptors of *E.coli* with known attractants, repellents, and binding proteins used to elicit a chemotaxis response. The table lists the five chemoreceptors of *E. coli.* with known attractants and repellents that interact with a specific chemoreceptor. There are multiple repellents for E. coli. their exact mechanism of function and specificity with only a single receptor have not been shown.

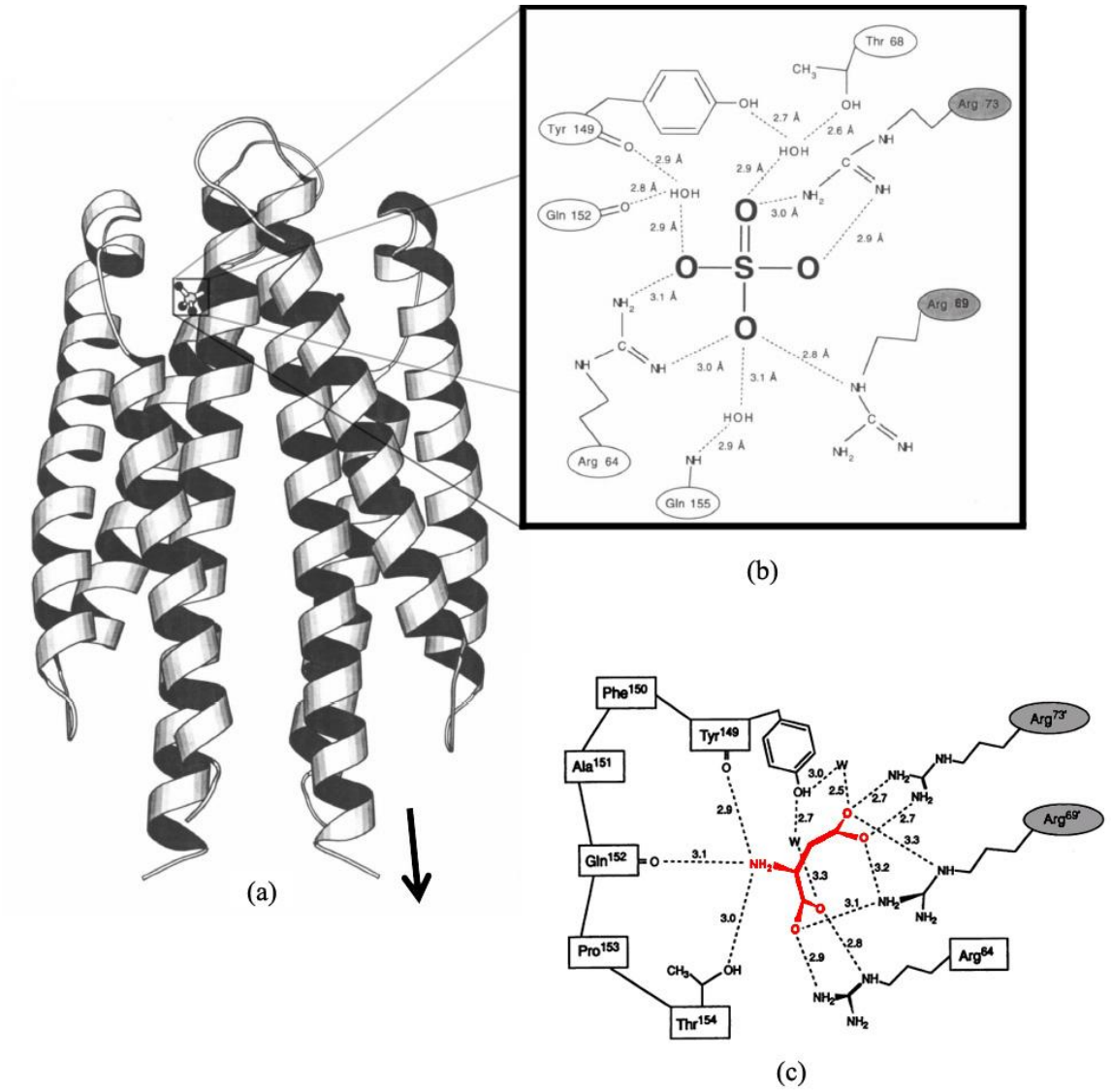

Figure 2. Binding pocket and transduction method of Tar_{Ec}. (A) Ribbon structure of Tar_{Ec} viewed from the side. The arrow indicates which subunit would signal if the bound sulfur was instead an aspartate. **(B)** A detailed view of the binding pocket of Tar with hydrogen bonds to the sulfate ion. Shaded ovals indicate residues from one subunit of Tar_{Ec} while unshaded ovals indicate residues from the other subunit (*50*). (C) A detailed view of the binding pocket of Tar with aspartate bound from *Salmonella typhimurium*. Aspartate is colored red, while dashed lines indicate hydrogen bonds, residues composing the Tar homodimers in indicated in black. Shaded ovals indicate residues from one subunit of Tar_{Ec} while unshaded squares indicate residues from the other subunit (*27*).

of Tar_{Ec} simultaneously (*28, 34, 51*). The signal elicited by either attractant is transduced asymmetrically (*51*) as explained in **Figure 2**. In Tar_{Ec} there is partial sensory additivity when both aspartate and maltose are present (*52*). Several models have been proposed to explain the transduction of a signal from the periplasmic domain through TM2 to the HAMP (histidine kinases, adenyl cyclases, methyl-accepting proteins, phosphatases) domain (*53*). These models will be discussed in a later section.

The HAMP domain lies between TM2 and the cytoplasmic signaling domain and is responsible for transmitting the displacement of TM2 when a ligand binds into an output that affects the signaling domain. Our current understanding of HAMP function is limited, as no structure has been experimentally determined for an *E.coli* HAMP domain. A crystal structure of the HAMP domain of unknown function has been determined for protein Af1503 of the thermophilic Archaeon *Archaeoglobus fulgidus.* It reveals a homodimeric four-helix bundle with a parallel coiled-coil packing in a knobs-on-knobs (x-da) mode (*54*) (**Figure 3**). The authors of the paper describing this crystal structure proposed that the signal is transduced by a 26° rotation between the AS1 and AS2 helices that converts the x-da packing into the more common knobs-into-holes (d-a) packing. This binary alternative for the packing state would provide an all-or-none output signal. Competing models envision either a change in the helix tilt angles within the HAMP domain (*55*), changes in the tightness of the packing of the four-helix bundle (*56*), or sliding movements of the AS1 and AS2 helices relative to one another (*57*). Any model for HAMP function must take into account the fact that the primary conformation change in response to ligand binding seems to be a piston-like movement of

transmembrane helix 2 (TM2) roughly perpendicular to the plane of the cell membrane. Obviously, some combination of different conformational changes is also a possibility.

The extended four-helix bundle of the cytoplasmic domain consists of three major regions; an adaptation domain where methylation occurs (*58*), a flexible connecter (*59*), and a protein-interaction domain where the receptor interacts with the CheA kinase and the adaptor protein CheW (*60*). The first structure of the dimeric cytoplasmic domain was determined for the Tsr protein of *E. coli* (*61*). Each subunit contained two anti-parallel helices that combined to make a four-helix with a length of approximately 200 Å (**Figure 4**). All MCPs are thought to have very similar cytoplasmic domains because of their conserved amino acid sequences and their ability to cross-react with antibodies generated against the cytoplasmic domain of Tsr. Additionally, chimeric receptors comprised of the periplasmic ligand-binding domain from one MCP and the cytoplasmic signaling domain of a different MCP are still able to detect ligands and effect a response (*25, 62*).

An evolutionary genomics study of MCPs from many different species has shown that the helices in the cytoplasmic domain maintain symmetry in length and register (*59*). Seven-residue long heptads are present in the cytoplasmic region of all chemoreceptors, although the number of heptad repeats can vary between MCPs with a range from 24 to 64 heptad repeats (*59*). In *E. coli* all four MCPs and the methylation independent chemoreceptor Aer have 36 heptad repeats (*59*).

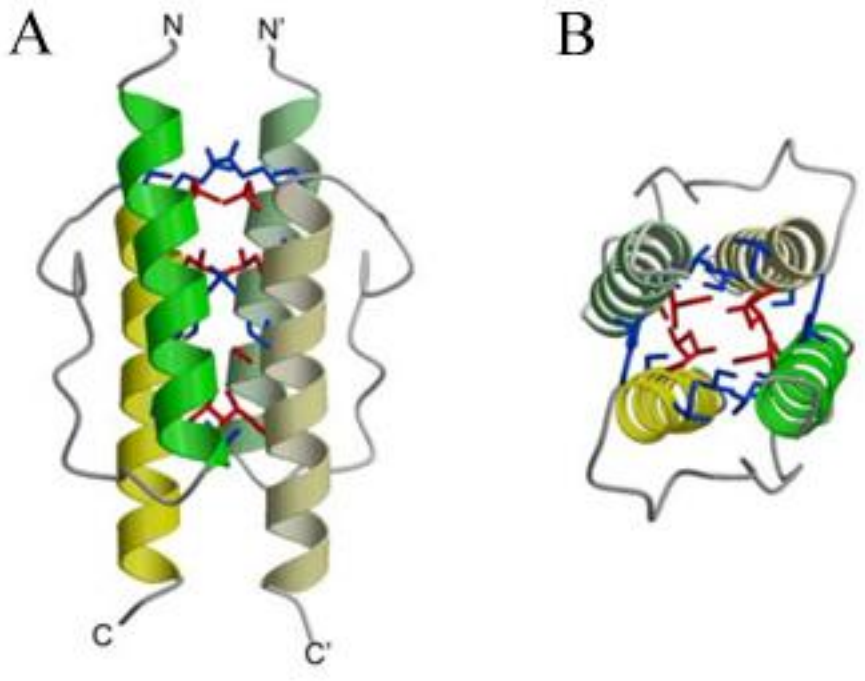

Figure 3. Crystal structure of the HAMP domain from protein Af1503 of the Archaeon *Archaeoglobus fulgidus*. (A) Graphic representation of the side view of the crystal structure of the HAMP domain of *A. fulgidus* where the α-helices are shown as green (α1) and yellow (α2) ribbon structure with monomers separate HAMP domains distinguished by bold and faint colors. Side chain residues involved in packing interactions within the core of the domain are shown in red (residues in x-layer geometry) and blue (da-layer geometry). **(B)** View from (A) rotated 90° around the horizontal axis yielding a top down view of the domain (*54*).

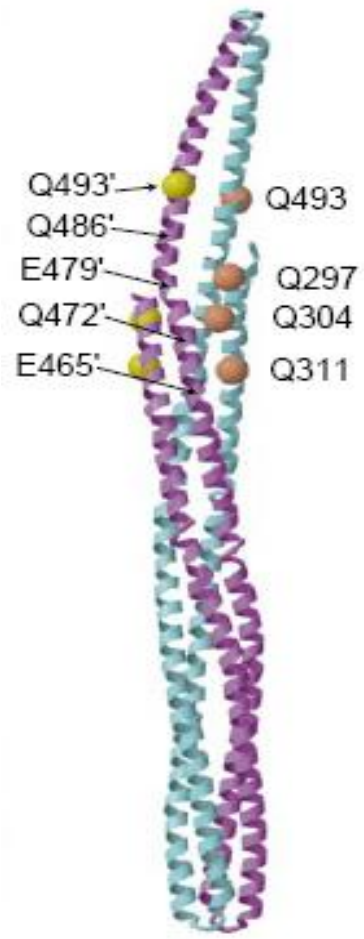

Figure 4. Crystal structure of Tsr cytosolic domain. A ribbon diagram of the Tsr cytoplasmic domain from approx. residues 294-520 reveals a 200Å long coiled-coil of two antiparallel helices connected by a `U-turn'. Each monomer is separately colored with a corresponding set of globes representing its methylation sites (*61*).

The signal transduction pathway of *E.coli*

When an attractant ligand binds to Tar_{Ec}, it causes an inward axial displacement of helix 4 of the periplasmic binding domain. Helix 4 extends through the inner membrane as TM2 (*63-69*). Repellents are proposed to have an opposite effect, causing TM2 to move outward. In either case, the movement of TM2 is propagated to the HAMP domain. Through whatever mechanism HAMP works, the net result is that a small, piston-like displacement of helix 4 in the periplasmic domain exerts a major influence on the CheA kinase-stimulating activity of the cytoplasmic domain.

The HAMP, adaptation, and protein-interaction domains are coupled in a yin-yang fashion. A change in the conformation of HAMP alters the packing of the AS1 and AS2 helices to create a "compact" conformation (*56, 70, 71*). This change in conformation is propagated to the adaptation domain, which assumes a "looser" packing conformation. A "loose" adaptation region generates a "tighter" packing in the protein interaction region (**Figure 5**). The CheW protein acts as a coupling factor between the receptor and CheA, a histidine kinase in which the CheA-stimulating activity of the receptor in inhibited.

CheA and CheW interact with a highly conserved region of the receptor located between residues 370-420 at the membrane-distal tip of the cytoplasmic domain (*58, 60, 72*). The combined binding of CheW and CheA is required to stimulate the activity of CheA, which phosphorylate itself on the His-48 residue of its N-terminal P1 domain (*73, 74*). The phosphoryl group of pospho-CheA can be transferred to a conserved aspartyl residue in either the response regulator CheY or to the methylesterase CheB (*75-77*).

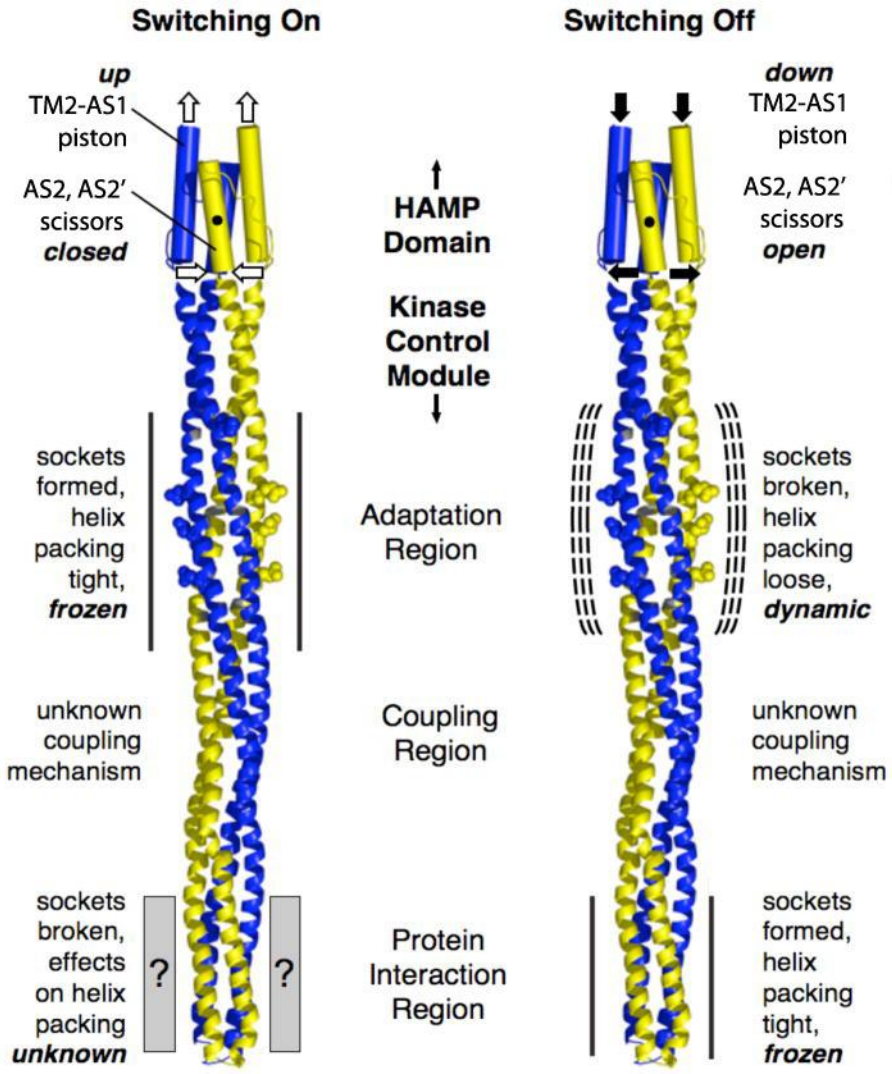

Figure 5. Ying-yang model of signal transduction from TM2 to the protein-interaction signaling domain. Attractant binding to the periplasmic ligand binding domain triggers a transmembrane conformational change converted by the HAMP domain into a different type of conformational signal. HAMP on-off switching triggers a scissors-type displacement of its C-terminal AS2-AS2' helices that directly couple to the N-terminal helices of the kinase control module. In the kinase-activating on state, four-helix bundle packing is more stable (sockets formed) in the adaptation region, but less stable (sockets broken, at least partially) in the protein interaction region. The reverse is true in the kinase-inhibiting off state. The space-filling side chains represent the four adaptation Glu residues of each subunit, which can also drive yin-yang signaling via an electrostatic mechanism (*56*).

CheA and CheY, as well as CheA and CheB, form two-component histidine kinase/response-regulator systems, with the former involved in the control of the rotational direction of the flagellar motor and the latter essential to adaptation to ligand-induced signaling (**Figure 6**).

When CheY is phosphorylated at Asp-57, it undergoes a conformational change that greatly increases its affinity for the FliM protein of the flagellar switch/motor complex (*1, 78, 79*). The more CheY-P that is bound to the motor, the higher the probability that the flagella will switch to CW rotation (*80*). Attractants, which inhibit CheA activity, promote CCW rotation, and repellents, which enhance CheA activity, promote CW rotation (**Figure 6**). The turnover of CheY-P is intrinsically rapid because of the self-phosphatase activity of CheY. However, in the enteric bacteria like *E. coli* and *S.*Typhimurium, the decay of CheY-P is hastened by the activity of the phosphatase CheZ (*75, 81*). The combined effect of inhibition of CheA activity and the destruction of CheY-P by CheZ leads to a rapid drop in CheY-P levels after addition of an attractant. This situation creates a high probability of CCW-only rotation of its flagella motors. Thereby runs become longer in the direction of increasing attractant concentration. The adaptation system composed of the methylesterase CheB and methyltransferase CheR restores a new equilibrium of CW to CCW rotation of the flagella motors. (See next section.)

The adaptation system

At the same time as the CheY-P levels rapidly fall, there is a more gradual

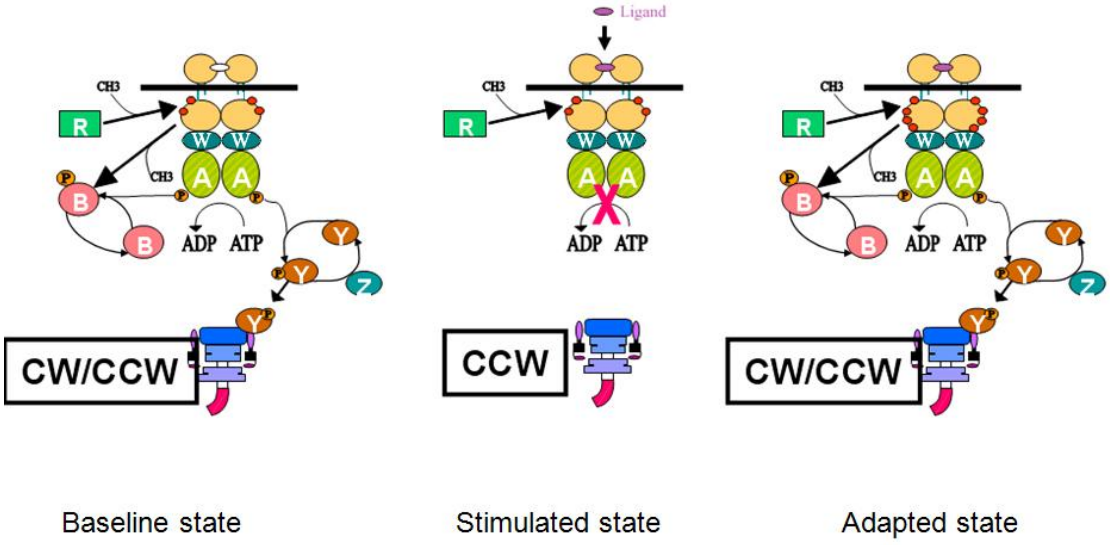

Figure 6. Chemotaxis signaling circuit. A) Homodimeric chemoreceptors complex with the histidine-kinase CheA and the coupling protein CheW. CheA autophosphorylation is stimulated in the complex, and the phosphoryl group is transferred to the CheY response regulator or the CheB methylesterase. CheY-P binds to the FliM protein in the switch/motor complex and stimulates CW rotation. The methyltransferase CheR and the methylesterase CheB-P add and remove, respectively, methyl groups at specific glutamyl residues on in the receptors. **B)** Attractant (red oval) binding to the receptor inhibits CheA activity and decreases the production of CheY-P and CheB-P. The autodephosphorylation of CheY-P is accelerated by the CheZ phosphatase. **C)** CheR continues to add methyl groups to the receptor, and the decrease in methylesterase activity accompanying the decrease in CheB-P results in increased methylation of the receptor. Since methylation enhances the CheA-stimulating activity of the receptor, this process compensates for the effect of attractant binding on CheA activity. A, B, R, W, Y, and Z represent CheA, CheB, CheR, CheW, CheY, and CheZ, respectively.

decrease in CheB-P, which is the active form of the methylesterase CheB. An attractant bound-receptor also serves as a better substrate for the CheR methyltransferase. The combination of lower amounts of CheB-P and the higher susceptibility of the attractant-bound receptor to become methylated lead to an increased level of methylation of the receptor. This increased methylation reverses the conformation change caused by attractant binding and restores the CheA-stimulating activity of the receptor (**Figure 6**). The timescale of methylation is significantly longer than the timescale of ligand association and dissociation. The delay between the current ligand occupancy of the receptor and its adaptation allows the cell to compare environmental conditions encountered a few seconds in the past with the current conditions, giving *E. coli* its approximate 3-second memory. This comparison allows for the detection of changes in ligand concentration, allowing for the cell to move in a gradient (**Figure 1**). In a repellent gradient, the process is reversed; "runs" become extended as the cell moves down the repellent gradient.

CheR is constitutively active in methylating specific glutamyl residues. In Tar_{Ec}, the specific residues that are methylated are Q295, E302, Q309, and E491 (*82*, *83*). CheB-P has a deamidase activity that converts Q295 and Q309 to E295 and E309 and also removes the methyl groups added by CheR as long as CheA is actively phosphorylating CheB (*82*, *84*). CheB has autophosphatase activity, and when CheA is inactive, the concentration of phosphorylated CheB will decrease until the increased methylation level of the receptor restores the activity of CheA.

In their unmodified state, the unmethylated glutamyl residues exert electrostatic repulsion within the four-helix bundle of the adaptation domain that loosens its packing , according to the yin-yang model, tightens the packing of the protein-interaction domain and inhibits CheA stimulation (*56, 70, 71*). Methylation removes the electrostatic repulsion to restore tighter packing of the adaptation and a looser packing of the protein-interaction domain that restore CheA activity.

The CheR methyltransferase, and perhaps the CheB methylesterase, are confined within the receptor patch by binding to the NWETF pentapeptide at the extreme C-terminus of the major receptors Tsr and Tar (*85*). This pentapeptide is attached to the four-helix bundle of the cytoplasmic domain by a flexible linker of about 30 residues (*86-89*). The complex of the adaptation enzymes with these receptors has been said to create an "assistance neighborhood" (*90*). The adaptation enzymes bound to the major receptors within a neighborhood can interact with one another allowing, the adaptation enzymes to interact with the minor MCPs that lack the NWETF motif (*90, 91*). CheR and CheB are thought to be able to move through the receptor patch by "brachiating" from one C-terminal NWETF residue to another (*86-91*). **Figure 7** shows a structural overview of the different structural and functional domains of a chemoreceptor.

Transduction of signal through TM2

Multiple models have been proposed to explain how the binding of a ligand to the periplasmic domain of an MCP is transmitted through TM2 to the HAMP domain. Several of the alternatives are shown in **Figure 8**. The two major models involve a

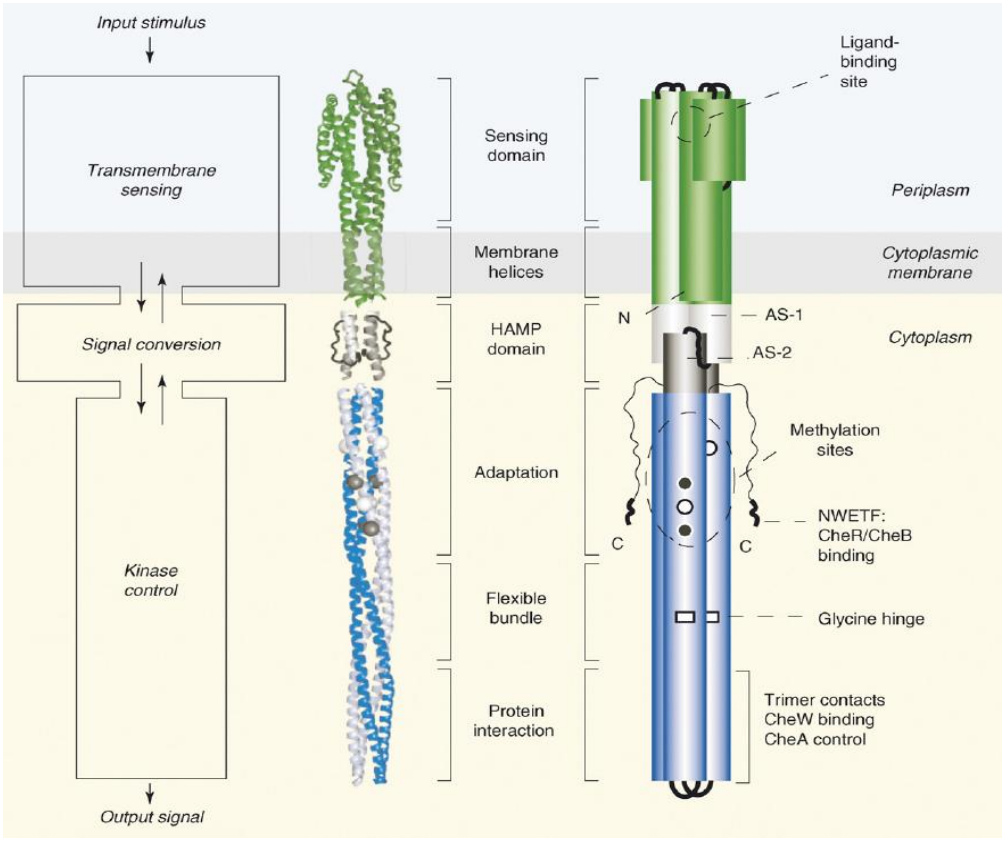

Figure 7. The chemoreceptor dimer. A ribbon diagram of known structures of Tsr obtained through various methods shows its 3D organization. Structural regions are indicated on the left, functional segments are shown in the middle, and notable features are listed on the right (*92*).

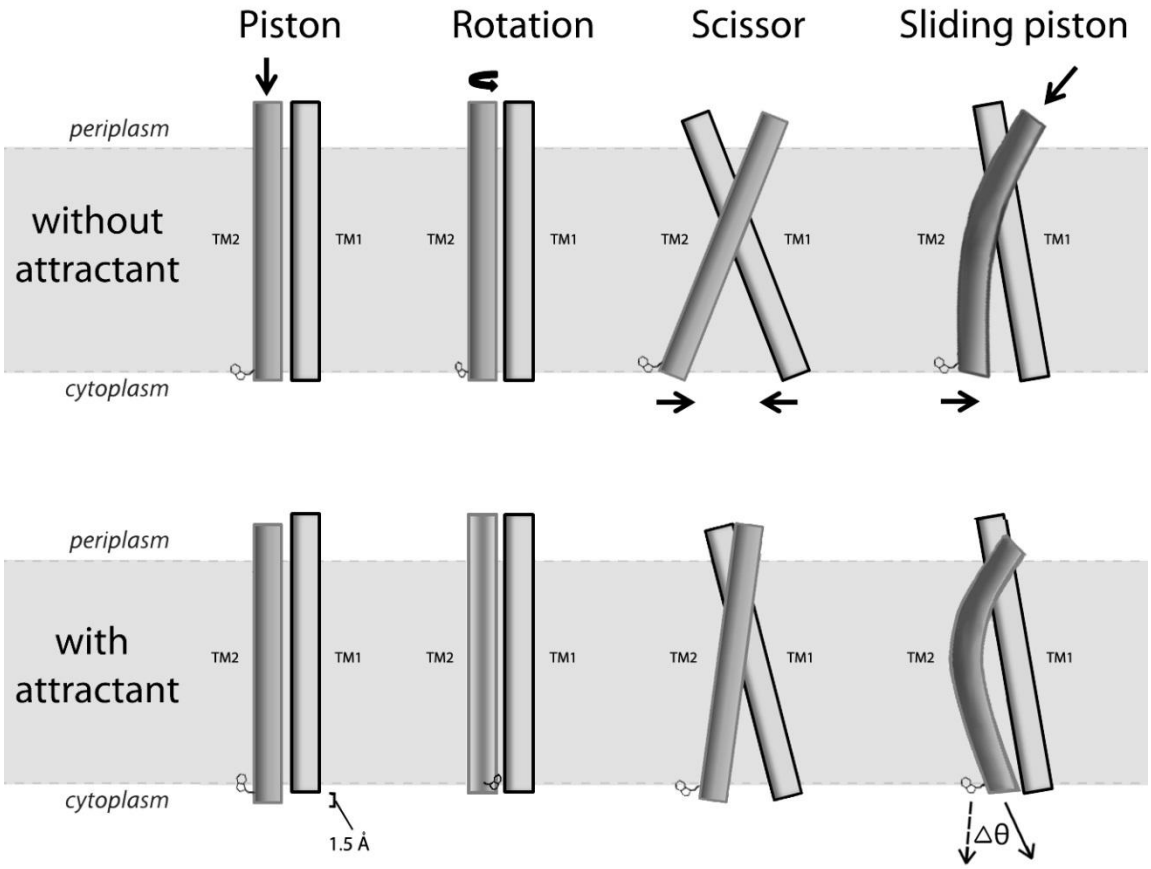

Figure 8. Models of signal transduction through TM2 into the HAMP domain. Multiple models of transduction of signal through the second transmembrane domain have been proposed. The models diagramed above have multiple sources of data that can be used to support the model's mechanism of action.

rotation of TM2 and a piston-like motion perpendicular to the cell membrane. Although there is evidence supporting both models, data consistent with the piston model include studies utilizing ESR, disulfide-crosslinking, and mutational analysis of the aromatic anchor at the cytoplasmic end of TM2 (*63-69*). The piston model envisions the attractant-induced signal as a small (1-2 ångström) downward displacement of helix 4 of the periplasmic (*65*).

Higher-order structures of the chemotactic circuit

The five chemoreceptors of *E. coli* each have a monomeric molecular weight of approximately 60,000 daltons. They form homodimers, which are able to bind ligands and undergo adaptive methylation. However, the homodimers is not the minimal functional unit. As seen in the crystal structure of the cytoplasmic domain of Tsr, homodimers of Tsr form trimmers of dimers (**Figure 9**) (*61*). These trimers can contain different chemoreceptor homodimers (*7*), and the trimers form networks with one another within a chemoreceptor patch (*93*). Mutations in the trimer contact sites of the Tsr protein that disrupt receptor function can be rescued by compensating mutations in the trimer-contact region of Tar, providing further evidence for the existence of mixed trimers (*7*). The minimal functional unit of a receptor patch consists of two trimers of dimers joined by a bridge of CheW bound to one receptor trimer of dimers, a CheA dimer, and a second CheW bound to the other receptor timer of dimers (*94, 95*).

Typically there is one large receptor patch at the old pole of the cell, a smaller, and growing, one at the new pole, and sometimes smaller patches along the lateral cell

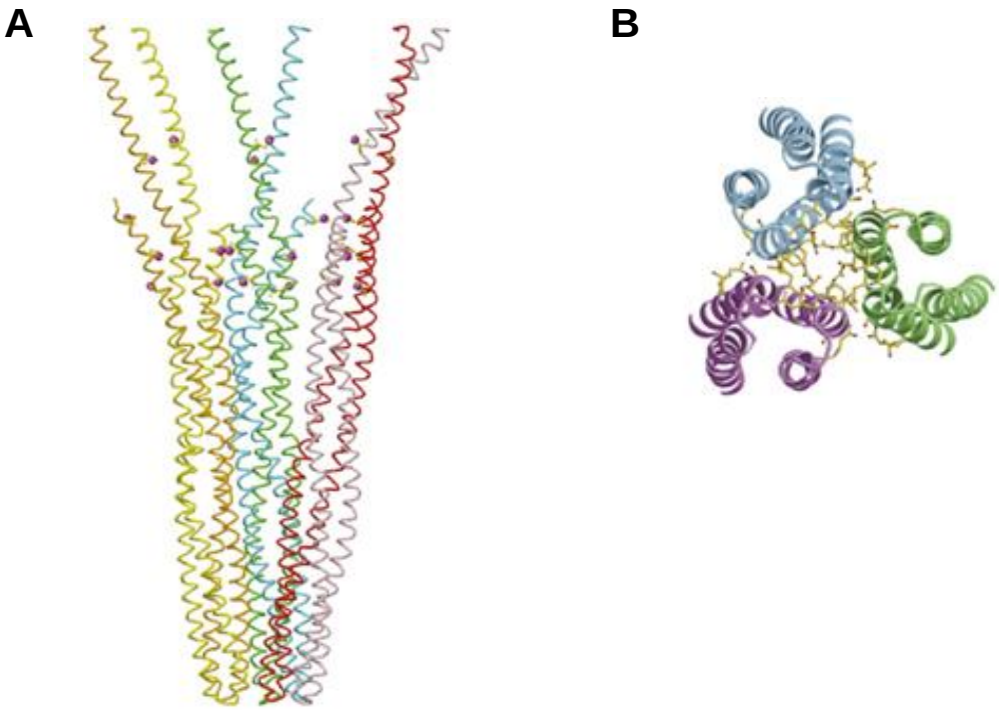

Figure 9. Crystal structure of trimer of Tsr dimers (A) A side view of the crystal structure of a trimer of Tsr cytosolic domains with globes representing methylation sites. **(B)** Top view of the crystal structure (*61*).

wall. The large majority of the chemoreceptors in a cell are present in these well-ordered clusters, whose existence requires the presence of CheA and CheW, which interconnect the trimers within a patch (*72*).

Because of its high connectivity, stimuli sensed by different receptors can be amplified and integrated within the receptor patch. As a result, the binding of one attractant ligand can shut off as many as 30 CheA molecules, creating a very high gain in the signal (*5-7, 91, 93, 96-98*). Transmission Electron Microscopy images of the receptor patches revealed a hexagonal lattice formed in the receptor patch (*99*). The hexagonal packing is also visualized by cryo-electron tomography in the overexpressed Tsr chemoreceptor in *E. coli* as well as in the wild-type receptor patches of *Caulobacter crescentus* and many other bacteria leads to the conclusion that receptor patch structure is universal in bacteria (**Figure 10)** (*95, 98, 100-104*). Analysis of data collected from *E. coli* lead to the creation of models detailing the receptor patch (**Figure 11**) (*95, 104*). These data provide further evidence supporting the proposed binary HAMP domain output model (*54*) in that the authors of one study propose a packing model where the periplasmic domain can be in a compact or expanded state (*102*). Depending on the model of transduction (**Figure 8**) changes caused by ligand binding could alter the exposure of hydrophobic regions of TM2 to the aqueous environment and the interaction of aromatic residues with polar head groups of the phospholipid bilayer. Recent computer simulations indicate that changes due to ligand binding or the composition of the aromatic anchor will alter a receptor's conformation leading to an adjustment in its positioning in the membrane to achieve a more energetically favorable state (*105*).

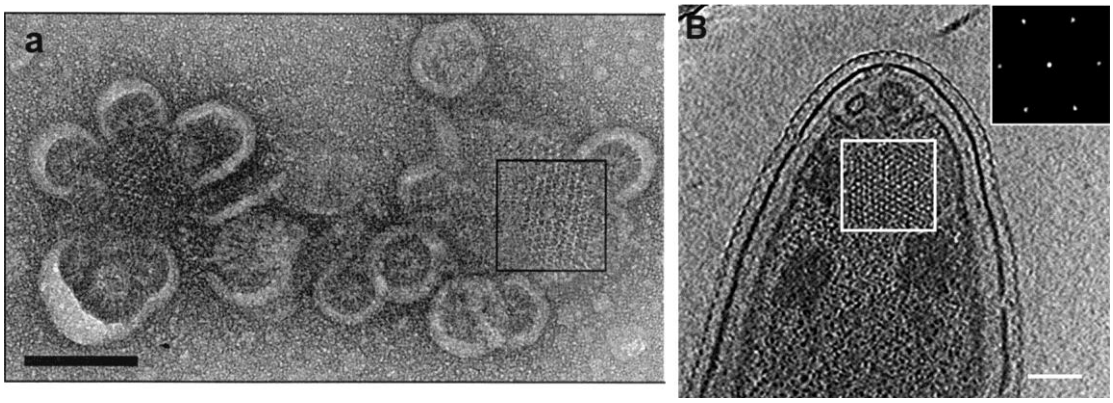

Figure 10. Cryo-electron Tomography of chemoreceptor lattices in *Caulobacter crescentus* and *Escherichia coli*. (A) An electron micrograph of a negatively stained, ordered two-dimensional array of Tsr in a membrane sample that was incubated with detergent. Scale bar is 100nm (*100*). **(B)** In the face-on orientation, chemoreceptor arrays are characterized by a distinct, partially ordered pattern ~32 nm below the cytoplasmic membrane that corresponds to the signaling scaffold. (Inset) The power spectrum of this region clearly demonstrates the ~12-nm hexagonal spacing. The scale bars in panels A and B are 100 nm; the panel A inset scale bar is 50 nm (*102*).

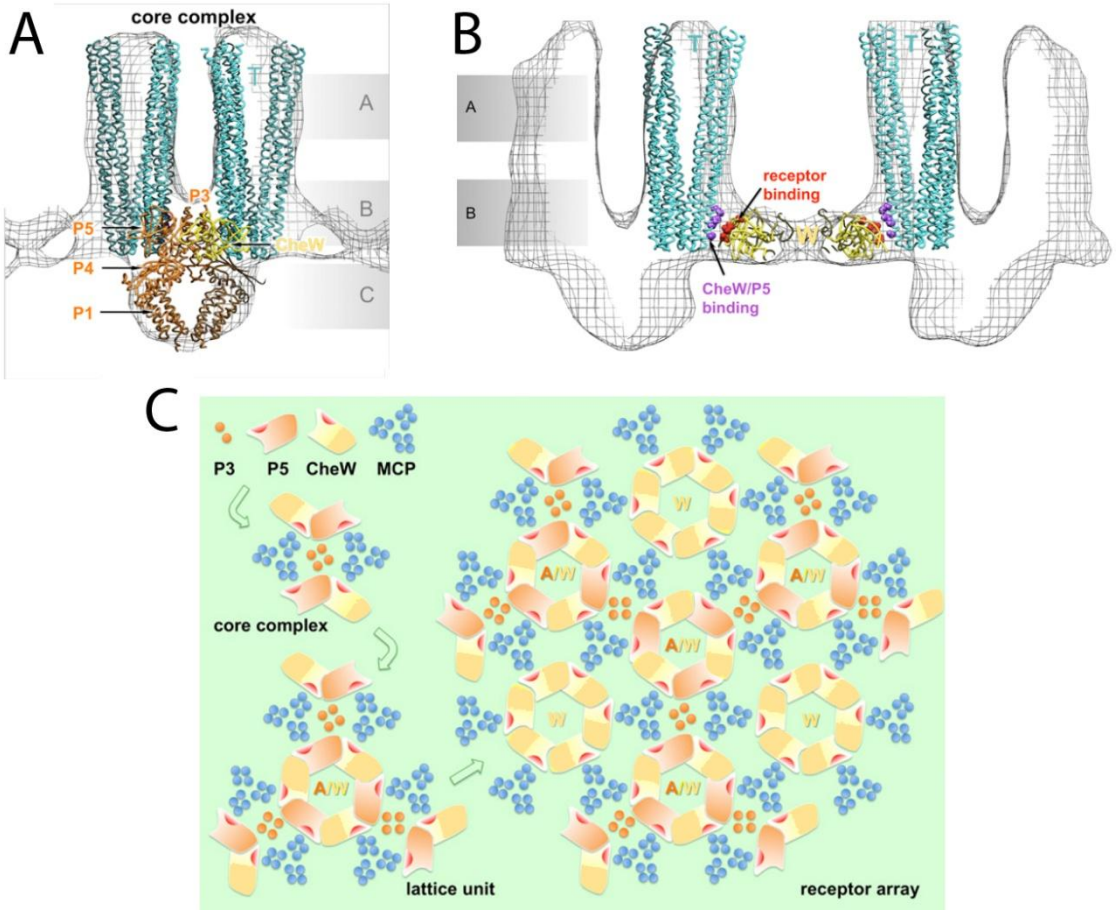

Figure 11. Model of an extended chemoreceptor array in *Escherichia coli*. Six Tsr trimers (residues 300–480; cyan ribbons) were fitted into a density map as rigid bodies where the cytoplasmic tips of the Tsr trimers were embedded into the density layer corresponding to CheA and/or CheW. **(A)** In a CheA/CheW ring two Tsr trimmers that belong to one complex interact with one CheA dimer (Orange ribbon) and two CheW (Yellow ribbon) monomers. **(B)** In a CheW-only ring in the receptor array each CheW interacts with one dimer subunit of a Tsr trimer, which is free to form a core complex with an adjacent MCP trimer, and a P3/P3′ dimer serves as the central core. At the interface between one Tsr trimer and one CheW monomer, residues I33, E38, I39, and V87 of CheW (colored in red) form a hydrophobic pocket adjacent to hydrophobic residues (F373, I377, L380, and V384; purple) from Tsr. **(C)** Illustration of an assembled chemoreceptor receptor array. The initial components, consisting of the P3 and P5 domains of CheA (orange), MCP trimers (blue), and CheW (yellow) form a core complex. Three core complexes are interconnected by P5/CheW interactions to form a lattice unit, which can assemble further to form an indefinitely large array. Rings containing only CheW may play a role in reinforcing the network to achieve optimal cooperativity and sensitivity (*104*).

Localized warping of the membrane around receptors is another possible explanation of how a receptor is in its minimized energetic state. The face of the membrane phospholipid bilayer is extended around a receptor's exposed hydrophobic region or aromtatic anchor, stretching the membrane slightly around the receptor.

Protein-membrane interactions in signaling systems

A phospholipid bilayer consists of hydrophobic center flanked on either side by polar hydrophilic regions. The hydrophobic center is composed of nonpolar acyl chains of the phospholipids from either side of the bilayer, whereas hydrophilic phospholipid head groups interact with the aqueous environment and shield the nonpolar center from solvation (*106*). Depending on the R group, the polar region of a phospholipid can vary in size; a typical lipid bilayer occupies roughly the 15Å on each side of the bilayer, with the hydrophobic core spanning another 30Å (*106*). Solvation by water likely reaches a maximum at the polar head groups of each phospholipid, but it penetrates to the carbonyl group of the ester linkage that attaches the fatty acids to the glycerol moieties (*106*).

Two protein secondary structures, an α-helix and a β-strand, are able to traverse the phospholipid bilayer. These elements of secondary structure must maintain a low energy state to prevent disruption of the phospholipid bilayer. The side chains of an α-helix protrude laterally and interact with the local environment, whereas hydrogen bonding within the α-helix helps to stabilize it. Energetically unfavorable protein-membrane interactions are minimized in membrane-spanning α-helices by controlling the amino acyl residues that occupy critical positions within the membrane-spanning helix.

Comparison of the predicted α-helix transmembrane regions of integral membrane proteins suggests that a core of hydrophobic, mostly aliphatic residues is flanked by amphipathic residues at the polar-hydrophobic interface (*107*). Partitioning of Trp analogs from water to cyclohexane (*108*) and to phosphocholine bilayer interfaces (*109*) is driven mostly entropically by the hydrophobic effect, though interfacial partitioning also has a very favorable enthalpic component, supporting the idea that Trp forms energetically favorable interactions the bilayer interface. Flanking the aromatic residues positively charged or other uncharged polar residues can be found (*107*). The four MCPs of *E. coli* have two hydrophobic transmembrane domains denoted as TM1 and TM2 which contain transmembrane segments that are typically flanked by tryptophan residues (**Figure 12**).

Trp residues preferentially localize to the interface of phospholipid bilayers (*107, 109, 110*), as shown by the positioning of synthetic transmembrane helices (*111*). Altering the distance between flanking Trp residues by varying the length of a hydrophobic core of artificial WALP peptides also demonstrates the preference of the flanking Trp residues to be at the bilayer interface (*112, 113*). This effect is so strong that the local lipid bilayer environment around inserted WALP peptides can be compressed or stretched to accommodate the separation between the flanking Trp residues (*107*).

Interaction of *E. coli* Tar with the lipid bilayer interface

Work with Tar_{Ec} has shown that the Trp residues at positions 192 and 209 are

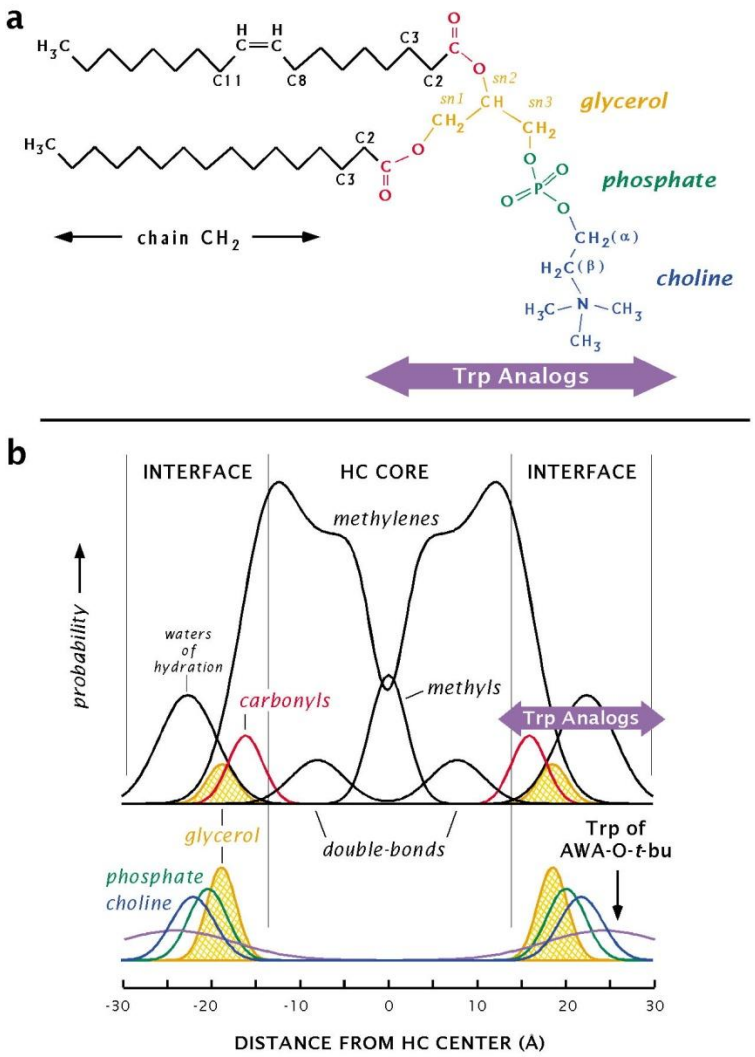

Figure 12. Boundary of water solvation in a lipid bilayer. (A) Chemical structure of a POPC molecule showing the location with the strongest interactions with Trp analogues as indicated by the arrow. **(B)** The structure of a fluid-phase dioleoylphosphatidylcholine (DOPC) bilayer consisting of time-averaged transbilayer distributions of the principal lipid structural groups and water representing time-averaged projections of the motions of the various groups composing the lipid and their probability of finding these groups in a particular location within the bilayer. The area under each distribution is the number of groups in the lipid (one glycerol, two carbonyls, etc.). The methylene distribution is the sum of three Gaussian distributions, and the water distribution is the water of hydration of the head group. Also shown is the distribution of the Trp residue of Ala-Trp-Ala-O-*tert*butyl. The Trp located in the same region as the water of hydration of the head group spends little time in the hydrocarbon core of the bilayer (*110*).

likely at the interface region of the lipid bilayer and that the Trp residue at position 209 is critical in maintaining a normal signaling state (*68, 69*). Repositioning the Trp 209 residue and the Tyr 210 residue as a tandem pair can mimic the binding of attractants or repellents by altering the output of the kinase CheA depending on the direction and number of residue positions shifted (**Figure 13)** (*68*). The WY tandem pair was termed the cytoplasmic aromatic anchor. In different transmembrane sensors of two-component systems, the cytoplasmic anchor can consist of different aromatic residues present singly or in a pair.

In Tar_{Ec}, if the aromatic anchor is moved more than one residue toward the N-terminus, which mimics attractant signaling, enhanced methylation fails to restore full function. Similarly, if the aromatic anchor is moved more than two residues toward the C-terminus, which mimics repellent signaling, decreased methylation can no longer restore full function (**Figure 13)** (*69*). When the receptor remains in the original QEQE form in a Δ*cheRB* strain, a shift of just one residue in the N-terminal direction locks the receptor in the off (CCW) signaling state (*68*). Thus, methylation can compensate for a displacement of TM2 only within the range that is predicted to arise from attractant-induced signaling (*65*).

Recent molecular simulations (*105*) that alter the position/orientation of TM2 of Tar_{Ec} relative to a lipid bilayer and the effects of mutations in the TM2 region. This simulation suggests that alterations in TM2 can affect signaling across the membrane by altering the tilt of the transmembrane helix, although there is still a piston-like displacement (*65*) with little rotation of the TM2 α helix. Another computational model

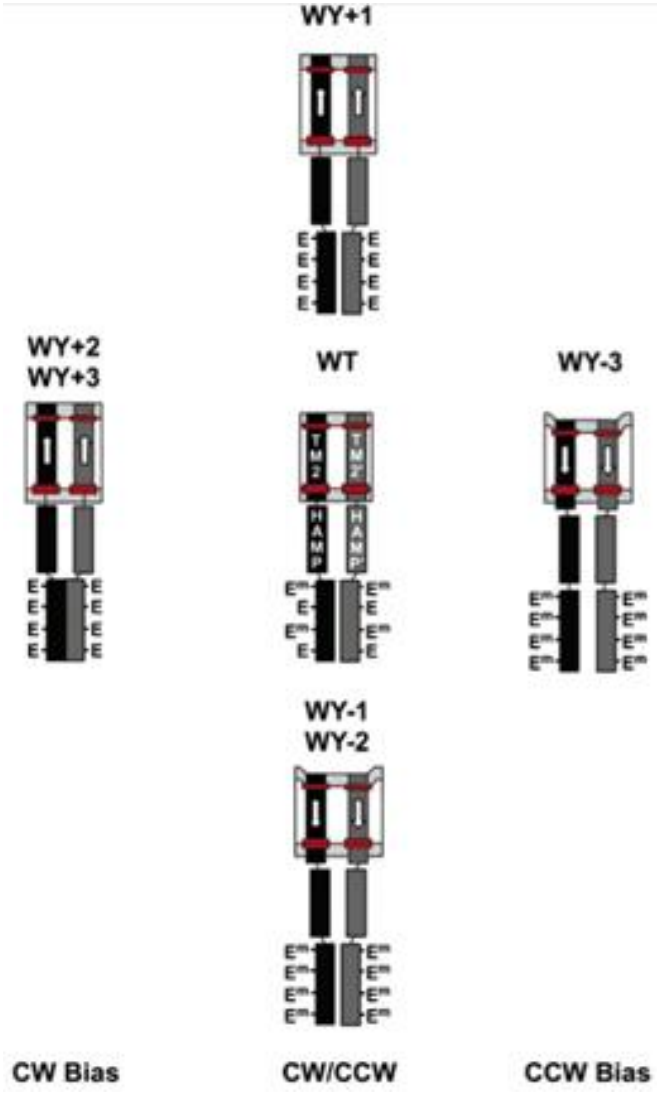

Figure 13. Repositioning the aromatic anchor modifies the output of the *E. coli* chemoreceptor Tar. (A) Repositioning of TM2 by moving the tandem Trp-209/Tyr-210 residues generates conformational changes similar to those that occur when an attractant or a repellent interacts with the receptor. Ligands create relatively small displacements which are similar to the repositioned tandems that mimic attractants (WY minus series) and repellent (WY plus series) conformational states. The methylation system can compensate the small displacements to restore nearly normal levels of CheA kinase stimulation *in* v*ivo* as seen in (WY-1 and WY-2, and WY+1). The displacements of TM2 in WY-3, WY+2, and WY+3 are too large to be completely compensated by the adaptation system. Therefore, these receptors are strongly biased toward the off state (WY-3, right) or the on state (WY+2 and WY+3, left). Note that both TM2s are displaced within the dimer, unlike the asymmetrical displacement of TM2 by normal attractant or repellent binding (*69*).

proposes a mechanism of transmembrane signal transduction that depends on the angle of the transmembrane helix entering and exiting the lipid bilayer (*55*).

Dissertation overview

During the past twenty years, a number of models have been proposed to explain how both individual elements of the signal transduction pathway and the integrated activity of the receptor patch function. The research presented in this dissertation examines signal transfer from the periplasmic domain to the cytoplasmic domain of the *E. coli* Tar chemoreceptor. The focus of the research is on the role of the aromatic groups of TM2 on the signaling output of the Tar_{Ec} receptor.

Chapter II describes my research in altering the residue composition of the aromatic anchor. The prediction that altering the composition of the anchor could generate a gradation of altered signal output proved to hold under normal conditions. The results reveal that the adaptation system can restore CW signal output to the a variety of Tar_{Ec} mutants and that non-aromatic anchors lacking aromatic residues can still function properly to some extent as long as the adaptation system can compensate for any bias an altered anchor exerts upon the baseline signaling state of the receptor (*114*).

In Chapter III, the mutant library created in the work described in Chapter II was used, in the context of the results of previous work (*68, 69*) to alter the position of specific mutant anchors. Monitoring of the signal output of the receptors constructed should predict that position shifts of mutants anchors could either compensate for or

exacerbate the innate biases associated with the mutant anchors. Additionally, it was found that the Gly-211 residue plays a critical role in the proper function of the Tar_{Ec} receptor. Chapter IV describes investigating the importance of the Trp residue (W192) present at the periplasmic end of Tar_{Ec}. Both residue changes and shifts in the position of the residue at position 192 were examined.

Chapter V summarizes the conclusions from the research and proposes potential future experiments, some of which were started but not finished. Finally, future avenues of research based upon this dissertation and the future of the field are discussed.

The work reviewed in this dissertation builds upon research that dates back more than thirty-five years. The lineage of researchers whose accomplishments made the current work possible is vast. It is my hope that this research regarding the function and composition of the aromatic anchor of Tar_{Ec} and the region surrounding it will lead to practical developments for modifying transmembrane signaling by two-component systems.

One of the more interesting aspects of this research is that a defective receptor can be made functional by changing a single, adjacent non-aromatic residue. The discovery of new variables that can control receptor function may allow for the development of design rules that can be used to create rationally designed receptors possessing desired signaling properties.

CHAPTER II

RESIDUE COMPOSITION OF THE AROMATIC ANCHOR OF TM2 DETERMINES THE SIGNALING PROPERTIES OF THE ASPARTATE/MALTOSE CHEMORECEPTOR TAR OF *E.COLI*[*]

Overview

The work detailed in this chapter was designed by and a vast majority of the experiments were performed by myself utilizing techniques originally developed within our laboratory by Dr. Roger R. Draheim and Dr. Run-Zhi Lai. Assisting me with this research was Dr. Roger R. Draheim who helped to create half of the mutants used in the experiments, performed the *in vitro* kinase assay experiments, and provided assistance reviewing this manuscript published in the ACS journal Biochemistry (*114*).

Summary

Repositioning of the tandem aromatic residues (Trp-209 and Tyr-210) at the cytoplasmic end of the second transmembrane helix (TM2) modulates the signal output of the aspartate/maltose chemoreceptor of *Escherichia coli* (Tar_{Ec}). Here, we directly assessed the effect of the residue composition of the aromatic anchor by studying the function of a library of Tar_{Ec} variants that possess all possible combinations of Ala, Phe, Tyr, and Trp at positions 209 and 210. We identified three important properties of the

aromatic anchor. First, a Trp residue at position 209 was required to maintain clockwise (CW) signal output in the absence of adaptive methylation, but adaptive methylationrestored the ability of all of the mutant receptors to generate CW rotation. Second, when the aromatic anchor was replaced with tandem Ala residues, signaling was less compromised than when an Ala residue occupied position 209 and an aromatic residue occupied position 210. Finally, when Trp was present at position 209, the identity of the residue at position 210 had little effect on baseline signal output or aspartate chemotaxis, although maltose taxis was significantly affected by some substitutions at position 210. All of the mutant receptors we constructed supported some level of aspartate and maltose taxis in semisolid agar swim plates, but those without Trp at position 209 were overmethylated in their baseline signaling state. These results show the importance of the cytoplasmic aromatic anchor of TM2 in maintaining the baseline Tar_{Ec} signal output and responsiveness to attractant signaling.

Introduction

In a chemically homogeneous environment, *Escherichia coli* moves in a three-dimensional random walk that consists of a series of smooth-swimming "runs" interspersed with brief "tumbles" that reorient the bacterium in three-dimensional space. Runs are produced when the flagella rotate counterclockwise (CCW), which causes the left-handed helical flagellar filaments to coalesce into a bundle at one end of the cell (*1*, *3*). Tumbles occur when one or more flagella switch from CCW to clockwise (CW)

rotation, which disrupts the helical bundle and causes a random reorientation of the cell (*3*).

E. coli possesses several transmembrane chemoreceptors, known as methyl-accepting chemotaxis proteins (MCPs), that mediate behavioral responses to specific sets of compounds. These MCPs, along with the aerotaxis (Aer) receptor, utilize a common signal transduction pathway that modulates the rotational bias of the flagella motors. By decreasing CCW rotation, a cell can extend the duration of runs in a favorable direction, either up an attractant gradient or down a repellent gradient (*115, 116*).

Attractant binding induces covalent modification of the cognate MCP (*92*). Methyl groups are added by a methyltransferase, CheR, and removed by a methylesterase, CheB (*70, 71*). CheB also removes the amide groups from the two glutaminyl residues that comprise two of the modification sites in the newly translated protein (*82*). Increased methylation of eight specific glutamyl residues (four per subunit) within the receptor homodimer stimulates the activity of the CheA kinase, whereas decreased methylation decreases CheA stimulation (*117*).

The aspartate chemoreceptor of *E. coli* (Tar_{Ec}) detects the presence of attractants both directly (aspartate) and indirectly (maltose). Aspartate binds at one of two rotationally symmetric binding sites in the periplasmic domain of the Tar_{Ec} homodimer. Maltose first associates with the periplasmic maltose-binding protein (MBP), causing MBP to adopt a conformation that facilitates interaction with Tar_{Ec} (*21, 31*). Maltose-bound MBP binds to the apex of the Tar periplasmic four-helix bundle (*28, 51*). Tar_{Ec}

also mediates repellent taxis to Ni^{2+} and Co^{2+}, which also bind directly to its periplasmic domain (*39, 40*).

E. coli MCPs contain two transmembrane helices. Transmembrane helix 1 (TM1) is an N-terminal extension of helix 1 of the periplasmic domain. Transmembrane helix 2 (TM2) is a C-terminal extension of helix 4 of that domain. TM2 communicates the conformational change induced by ligand binding to the cytoplasmic HAMP domain (histidine kinases, adenylyl cyclases, methyl-accepting chemotaxis proteins, and certain phosphatases) (*53*). The mechanism of signal transduction from the periplasmic domain to the HAMP domain is not fully understood, but several hypotheses have been advanced to explain the process (*27, 54, 57*). Whatever the signaling mechanism may be, the preponderance of evidence suggests that a small (~ 1–3 Å) inward displacement of helix 4/TM2 roughly perpendicular to the plane of the membrane occurs upon binding of aspartate (*63-69*).

Repositioning the two aromatic residues (the aromatic anchor) at the cytoplasmic end of TM2 of Tar_{Ec} (Trp-209/Tyr-210) by a single position is sufficient to modulate the signal output of Tar_{Ec} (*69*). Mutant receptors in which the aromatic anchor was moved toward the hydrophobic core of the membrane had decreased CW signal output. This suggests that the well-documented affinity of amphipathic aromatic residues for the polar-hydrophobic interfaces (*107, 110, 112*) within the phospholipid bilayer is sufficient to reposition TM2 toward the cytoplasm in a manner similar to an aspartate-induced displacement (*63-69*). Conversely, mutant receptors in which the aromatic anchor was repositioned toward the polar head groups exhibit increased CW signal

output (*69*), a result consistent with displacement of TM2 away from the cytoplasm. These results demonstrate that aromatic residues can "tune" the output of $Tar_{Ec,}$ and perhaps of other chemoreceptors and members of the sensor histidine kinase superfamily that share a similar mechanism of transmembrane communication (*118-121*).

A variety of chemoreceptors and other two-pass transmembrane sensor proteins have aromatic residues at the cytoplasmic end of TM2 followed by a HAMP domain (**Table 2**). To determine the essential features of the cytoplasmic aromatic anchor of Tar_{Ec}, Trp-209 and Tyr-210 were replaced with all possible combinations of other aromatic residues and Ala. We also looked at the effect of introducing a variety of different residues at position 210 when Trp-209 was still present. Our results indicate that Trp-209 is crucial for the ability of Tar_{Ec} to stimulate CheA activity in a Δ*cheRB* strain. However, adaptive covalent modification can restore sufficient function to enable chemotaxis. When Trp-209 is present, charged or polar uncharged amino acids at position 210 impair function to some extent, but the effect is less than that accompanying the loss of Trp-209. Thus, optimal function of Tar_{Ec} requires a cytoplasmic aromatic anchor of the configuration WX, in which X is a non-polar residue.

Materials and methods

Bacterial strains and plasmids

HCB436 (Δ*tsr7021* Δ*trg100* Δ(*tar-cheB)2234*) (*122*), RP3098 (Δ*(fhlD-flhB)4*) (*123*), and VB13 (Δ*tsr7021* Δ*tar-tap5201 trg*::Tn*10*) (*62*) are derived from the *E. coli* K-

Receptors[a]	Known ligands[b]	N' Seq.[c]	Predicted TM2 core[d]	C' Seq.[e]
Enteric MCPs with C-terminal pentapeptide CheR-binding motif (NWE^{S}/$_{T}$F)				
Tar$_{Ec}$	Asp/Mal*	FAQ	WQLAVIALVVVLILLVAW	YGIRRMLLT**P**(HAMP)
Tar$_{Se}$	Asp	FAQ	WQLGVLAVVLVLILMVVW	FGIRHALLN**P**(HAMP)
Tsr$_{Ec}$	Ser/AI-2*	QAM	WILVGVMIVVLAVIFAVW	FGIKASLVA**P**(HAMP)
Tsr$_{Se}$	Ser/AI-2*	QAM	WVLVSVLIAVLVVIIAVW	FGIKLSLIA**P**(HAMP)
Tsr$_{Ea}$	Ser	QAM	WVLVSVLIAVLVVIIAVW	FGIKLSLIA**P**(HAMP)
Tcp$_{Se}$	Cit/Mg^{2+}-Cit	QMQ	WTLGIILLIVLIVLAFIW	LGLQRVLLR**P**(HAMP)
Enteric MCPs without C-terminal pentapeptide CheR-binding motif (NWE^{S}/$_{T}$F)				
Tap$_{Ec}$	Pyr/Pep*	SAL	VFISMIIVAAIYISSALW	WTRKMIVQ**P**(HAMP)
Tas$_{Ea}$	Asp	**P**IW	LVAGAVLMLLVVTLSAMW	WLRTMLVQ**P**(HAMP)
Trg$_{Ec}$	Gal*/Glu*	LGG	MFMIGAFVLALVMTLITF	MVLRRIVIR**P**(HAMP)
Trg$_{Se}$	Gal*/Glu*	LGM	MFMIGAFTLALVLTLMTF	MVLRRTVIQ**P**(HAMP)
Enteric MCPs with unknown ligands				
McpB$_{Se}$	???	RIL	LITAVILGIAILIFTDRY	LAMMVKP(HAMP)
McpC$_{Se}$	???	NRT	LLITLALISIAAGCVMGW	YIVRSITRP(HAMP)
Enteric redox chemoreceptor with cytoplasmic FAD-binding PAS domain				
Aer$_{Ec}$	Redox	**P**VV	TYILCALVVLLASACFEW	QIVR**P**(HAMP)
Aer$_{Se}$	Redox	SWQ	ALLLGALAMLAGTALLEW	QIVR**P**(HAMP)
Some *E. coli* transmembrane histidine kinases (HPKs) with known periplasmic ligands				
NarX$_{Ec}$	NO_3^-/NO_2^-	VLV	HRVMAVFMALLLVFTIIW	LRARLLQ**P**(HAMP)
NarQ$_{Ec}$	NO_3^-/NO_2^-	KML	LVVAISLAGGIGIFTLVF	FTLRRIRHQVA**P**(HAMP)
PhoQ$_{Ec}$	Mg^{2+}	VWS	WFIYVLSANLLLVI**P**LLW	VAAWWSLR**P**(HAMP)
An enteric transmembrane HPK that can be regulated by an MCP periplasmic domain				
EnvZ$_{Ec}$	???	DFS	PLFRYTLAIMLLAIGGAW	LFIRIQNR**P**(HAMP)

Table 2. Known chemoreceptors of several enteric bacteria.

[a] All of the known chemoreceptors of *Escherichia coli* ($_{Ec}$) and *Salmonella enterica* ($_{Se}$) serovar Typhimurium are listed, as are two chemoreceptors from *Enterobacter aerogenes* ($_{Ea}$) that function in *E. coli* (*125*). We have also included three *E. coli* sensor kinases that have ligands that are known to bind to their periplasmic domains and the *E. coli* EnvZ osmosensor, which forms functional chimeras when joined to the periplasmic, TM, and HAMP domains of Tar$_{Ec}$ (*126*) and Trg$_{Ec}$ *(127)*.

[b] The ligands are abbreviated as: L-aspartate, Asp; maltose, Mal; L-serine, Ser; autoinducer 2, AI-2; citrate, Cit; magnesium-citrate chelate, Mg^{2+}-Cit; galactose/glucose, Gal; ribose, Rib; dipeptides, Pep; pyrimidines, Pyr. Those ligands marked with an asterisk are sensed by periplasmic binding proteins that, in their ligand-bound, closed conformations, interact with their cognate MCPs.

[c] N' seq. refers to the three residues immediately preceding TM2. Some of these residues may still interact with the membrane and thus formally also be part of the transmembrane region (*67*). Aromatic residues are shaded gray.

[d] The core region of TM2 is taken to be the hydrophobic core of the transmembrane helix and the flanking periplasmic and cytoplasmic aromatic anchors (*68*). In Tar and related MCPs, this region encompasses the 18 residues from Trp-192 at the periplasmic face of the membrane to Trp-209 residue at the cytoplasmic face of the membrane. For proteins that lack one or both of these Trp residues, we aligned the aromatic residue at the cytoplasmic face of the membrane with Trp-209. Aromatic residues are shaded gray.

[e] C' seq. refers to the residues between the aromatic anchor and the highly conserved Pro residue near the beginning of the first amphipathic helix (AS1) of the HAMP domain.

12 strain RP437 (*124*). Strain VB13 is deleted for all chemoreceptor genes, as is strain HCB436, which also carries a Δ*cheRcheB* deletion. All *in vivo* assays of receptor activity were conducted with these two strains. Strain RP3098 contains a deletion of the master regulator *flhDC* and therefore fails to produce any Che proteins. Plasmid pRD200 (*68*), derived from pMK113 (*28*), was used to express wild-type or mutant *tar* genes constitutively. In addition, an in-frame coding sequence for a seven-residue linker (GGSSAAG) (*128*) and a C-terminal V5 epitope tag (GKPIPNPLLGLDST) (*129*) was added to the 3' end of *tar*. Plasmid pRD300 (*68*) is a derivative of pBAD18 (*130*) that expresses *tar* with the same C-terminal linker and V5 epitope tag upon induction with L-arabinose. Strain RP3098 was used with pRD300 as previously described (*68*) to produce standards for the *in vivo* methylation assay. Mutations in *tar* were introduced via site-directed mutagenesis (Stratagene).

Observation of tethered cells

HCB436 or VB13 cells containing plasmid pRD200 were grown overnight in tryptone broth (*131*) supplemented with 100 μg/mL ampicillin. Overnight cultures were then back-diluted 1:100 in tryptone broth and grown at 30°C with agitation until an OD_{600nm} ~0.6. A 10 mL aliquot of cells was pelleted, and the cells were resuspended in 10 mL of tethering buffer (10 mM potassium phosphate [pH 7.0], 100 mM NaCl, 10 μM EDTA, 20 μM L-methionine, 20 mM sodium DL-lactate, and 200 μg/mL chloramphenicol). Flagella were sheared in a Waring blender (*132*) during eight repetitions of 7 s intervals of shearing at high speed interspersed with 13 s pauses to

prevent overheating. Cells were collected by centrifugation, washed three times in tethering buffer, and mixed with an equal volume of a 200-fold dilution of anti-flagellar filament antibody. A 40 µL aliquot of the cell/antibody mix was added to the center of the coverslip. Coverslips were then incubated in a humidity chamber for 30 min at 30°C and affixed to a flow chamber (*133*); non-tethered cells were removed by flushing the chamber with chemotaxis buffer. Cells were observed under reverse phase contrast at 1000x magnification, using an Olympus BH-2 microscope. Rotating cells were digitally recorded, and at least 100 cells for each specific receptor were monitored visually during 20 s playback. Cells were assigned to one of five rotational categories: exclusively CCW; mostly CCW with occasional reversals; reversing frequently with no clear bias; mostly CW with occasional reversals; and exclusively CW. Reversal frequency was determined by tallying the number of reversals for each cell during video playback.

Determination of the methylation state of receptors in vivo

HCB436 or VB13 cells containing plasmid pRD200 expressing each one of the different V5-tagged Tar variants were grown overnight at 30ºC in tryptone broth supplemented with 100 μg/mL ampicillin. Overnight cultures were then back-diluted 1:100 in tryptone broth and grown at 30°C to an OD600 nm of ~0.6. Cells were harvested by centrifugation, washed three times with 10 ml of 10 mM potassium phosphate buffer (pH 7.0) containing 0.1 mM EDTA, and resuspended in 5 ml of 10 mM potassium phosphate (pH 7.0) containing 0.1 mM EDTA, 10 mM sodium DL-lactate, and 200 µg/ml of chloramphenicol. One mL aliquots were transferred to 10-mL

scintillation vials and incubated for 10 min at 32°C, with agitation. Cells were then incubated for another 30 min after the addition of L-methionine to 100 μM. A 100 μL aliquot of 100 mM L-aspartate or 10 mM $NiSO_4$ solutions, or 100 μL of buffer as control, were added at this time, and the cells were incubated for an additional 20 min. Reactions were terminated by addition of 100 μL ice-cold 100% TCA, and the samples were then incubated on ice for 15 min. Denatured proteins were pelleted, washed with 1% TCA and acetone, and resuspended in 100 mL 2X SDS-loading buffer. A 15-μL aliquot of each sample was subjected to SDS-PAGE and immunoblotting with antibodies raised against the V5 epitope that were conjugated to alkaline phosphatase (Invitrogen). Standards were run as a mixture of Tar proteins containing equal proportions of V5-tagged versions of the EEEE, QEQE, and QQQQ forms of the Tar receptor produced from RP3098 cells containing pRD300. The Gln residues affect protein migration like methylated Glu residues, so that the standards migrate like the unmethylated, doubly methylated, and quadrupally methylated forms of the receptor, respectively.

Chemotactic swim-plate assays

Semi-solid motility agar contained 3.25 g/L Difco BactoAgar (Difco) in motility medium [10 mM potassium phosphate (pH 7.0), 1 mM $(NH_4)_2SO_4$, 1 mM $MgSO_4$, 1 mM $MgCl_2$, 1 mM glycerol, 90 mM NaCl] and was supplemented with 20 mg/mL of L-threonine, L-histidine, L-methionine, and L-leucine and 1 mg/mL thiamine. Aspartate and maltose were added to final concentrations of 100 μM. Plates were inoculated with toothpicks from isolated colonies of strain VB13 expressing one of the various Tar

receptors from pRD200. Swarm plates were incubated at 30ºC. Once visible chemotaxis rings became visible (typically 8 h for aspartate and 12 h for maltose plates), their diameter was measured every 4 h.

Analysis of receptor function in vitro

Receptor-containing inner membranes were isolated as previously described (*91*). Strain RP3098 (*123*) harboring either pRD100 (*68*) expressing the wild-type, or pRD300 (*68*) expressing the C-terminal V5-epitope tagged variant, was used for production of receptor-containing membranes. Tar expression was induced by the addition of L-arabinose to a final concentration of 0.2% (w/v). Soluble Che proteins were isolated (*91*) and receptor-coupled *in vitro* phosphorylation assays were performed (*68*) as previously described. Our reactions contained 20 pmol Tar, 5 pmol CheA, 20 pmol CheW, and 500 pmol CheY in 9 μL of fresh phosphorylation buffer [50 mM Tris-HCl, 50 mM KCl, 5 mM $MgCl_2$, and 2 mM DTT (pH 7.5)]. Aspartate was added to the desired final concentration, taking care to maintain the same total volume. The reaction was initiated by the addition of 1 μL of [γ-^{32}P]-ATP (3000 Ci/mmol NEN# BLU502A) diluted 1:1 with 10 mM unlabeled ATP. Reactions were terminated by adding 40 μL of 2× SDS−PAGE loading buffer containing 25 mM EDTA. Samples were subjected to SDS−PAGE, dried, and imaged using a phosphorimager (Fuji BAS 5000).

Results

Residue composition of the aromatic anchor affects baseline Tar_{Ec} signal output

Fifteen mutant receptors were generated by making all possible substitutions of Ala, Phe, Trp, and Tyr at residues 209 and 210 of Tar_{Ec} which are Trp and Tyr in the wild-type protein. Flagellar rotational bias and mean reversal frequency (MRF) were measured in transducer-depleted (ΔT) tethered cells (strain VB13; Δ*tsr* Δ*tar-tap* Δ*trg* *aer*$^{+}$) expressing the wild-type or mutant Tar_{Ec} proteins from plasmid pRD200. The effects of a C-terminal V5 tag on ligand sensitivity and adaptation responses are minimal and have been well characterized (**Figure 14**) (*134*). The behavior of these cells should reflect the steady-state Tar_{Ec} signal output, which is modulated by changes both in the position of TM2 relative to the membrane and the resultant compensatory effects of adaptive methylation (*68, 69, 135*).

VB13 cells expressing V5-tagged wild-type Tar_{Ec} (WY anchor) from pRD200 showed a modest CCW rotational bias (**Figure 15**). All mutant receptors supported some CW rotation and ranged from slightly more CW biased (the WA receptor) through somewhat more CCW biased (all receptors with Ala at position 209 and the FA, FW, YF, and YW receptors). The FF, FY, WF, WW, YA, and YY receptors supported essentially wild-type rotational biases in VB13 cells. The MRF values of VB13 cells expressing the mutant receptors (**Figure 16**) were all between 0.15 s^{-1} and 0.45 s^{-1}, with the highest MRF shown by the WA receptor.

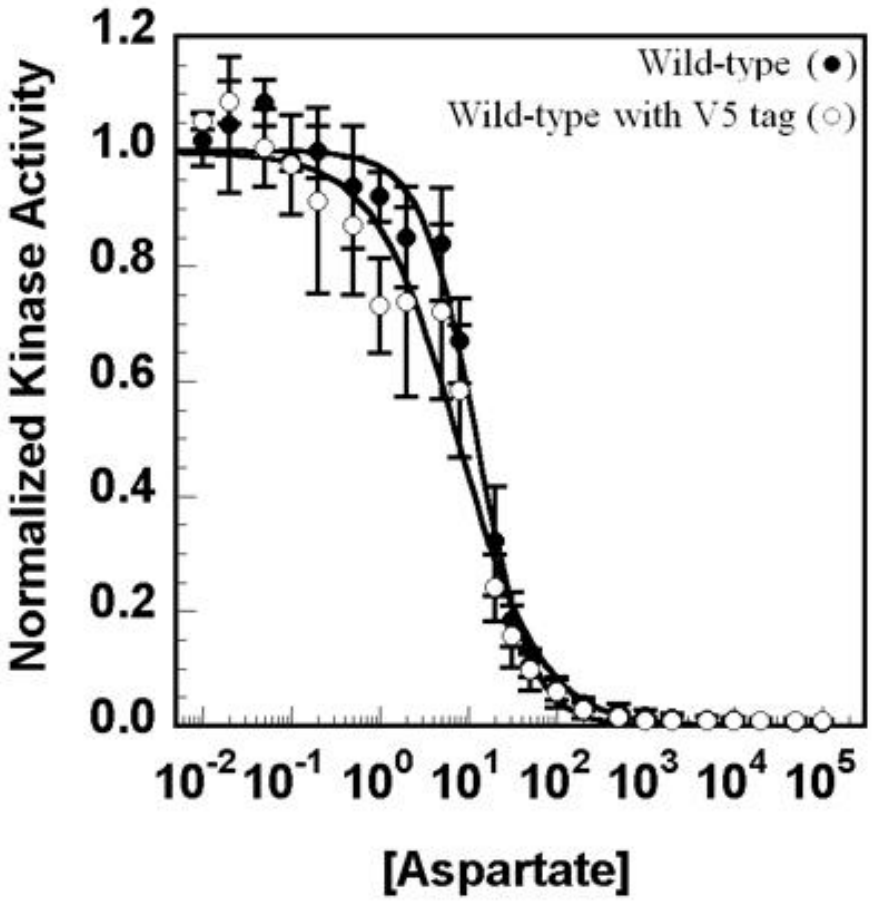

Figure 14. *In vitro* ligand sensitivity of VB13 (ΔT *cheR*$^+$*B*$^+$) cells expressing the wild-type Tar$_{Ec}$ aromatic tandem with or without the V5 epitope tag from pRD100 or pRD300, respectively. Wild-type (●) receptor without the V5 epitope tag has a K_i value of 12 ± 1 μM. The wild-type receptor with a C-terminal V5 epitope tag (○) has a slightly lower K_i of 8 ± 1 μM.

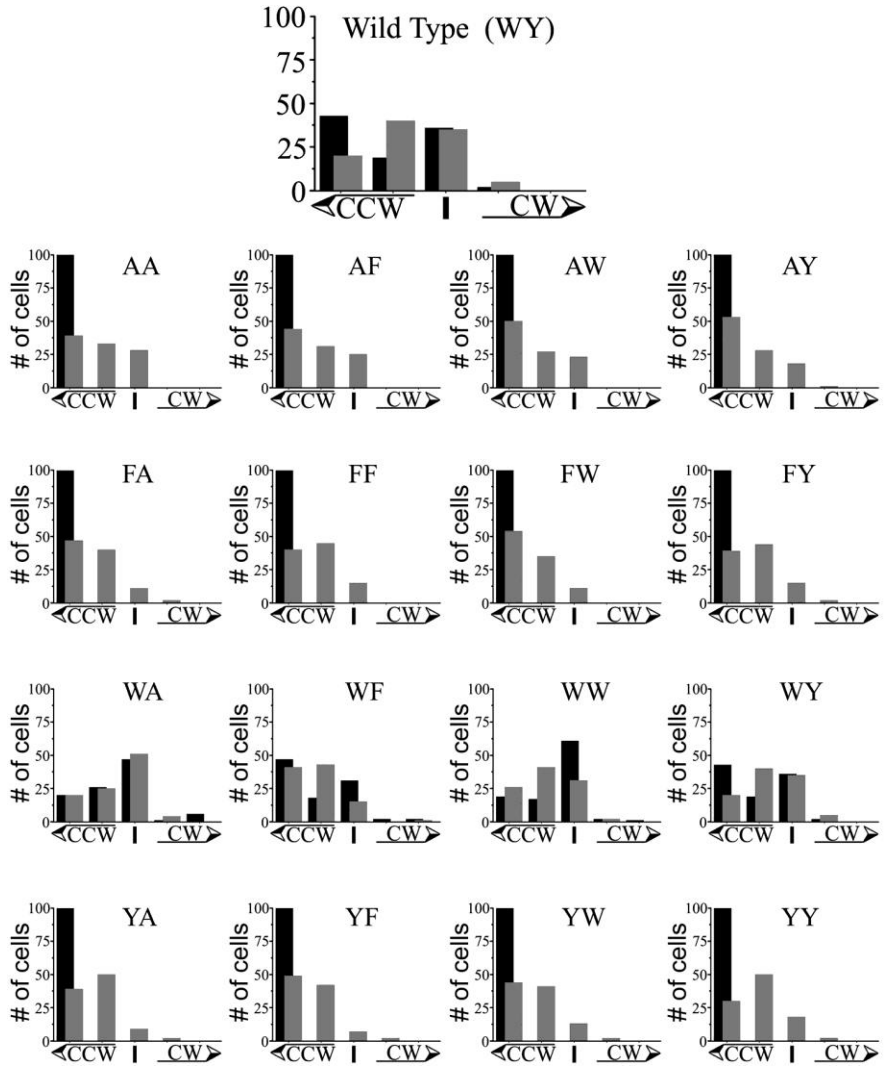

Figure 15. Flagellar rotational bias of cells expressing Tar_{Ec} variants with wild-type or mutant aromatic tandems. VB13 (ΔT *cheR*$^{+}$*B*$^{+}$) or HCB436 (ΔT Δ*cheRB*) cells expressing the wild-type or mutant Tar_{Ec} variants from pRD200 (*68*), posessing a C-terminal epitope V5 tag were tethered, observed for 20 sec and assigned to one of five categories based on their apparent flagellar rotational bias. From left to right, these categories are designated: counterclockwise rotation with no switching (CCW only), counterclockwise-biased with frequent switching (CCW), frequent reversing with no apparent bias (CCW/CW), clockwise-biased with frequent switching (CW) and clockwise rotation with no switching (CW only). Results from VB13 cells are depicted as grey bars in the foreground while results from HCB436 are depicted as black bars in the background. Each histogram contains the classification of one hundred VB13 and one hundred HCB436 cells expressing each Tar_{Ec} variant.

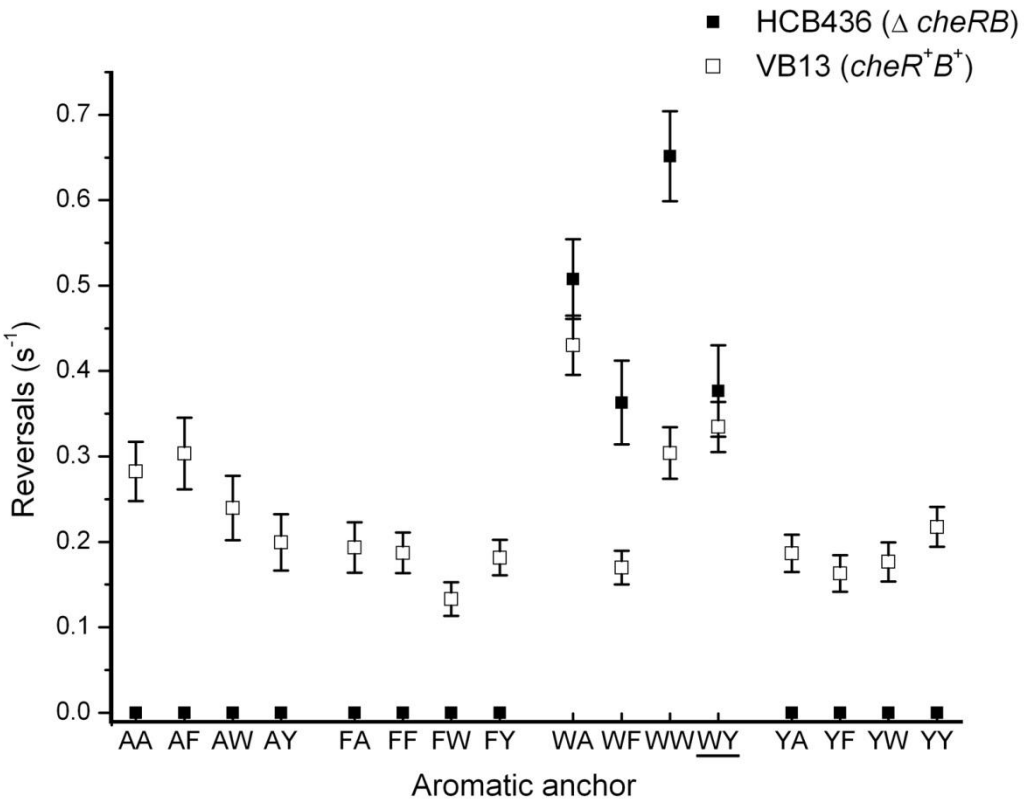

Figure 16. Mean Reversal Frequency (MRF) of flagella in cells expressing $\mathbf{Tar_{Ec}}$ receptors with wild-type or mutant aromatic anchors. The number of flagellar reversals were tabulated from the tethered VB13 (ΔT *cheR*$^+$*B*$^+$) or HCB436 (ΔT Δ*cheRB*) cells whose rotational bias is shown in **Figure 1**. Each data point represents the mean number of reversals for one hundred cells, and the error bars represent the standard error of that mean. The wild-type (WY) aromatic anchor found in Tar_{Ec} is underlined.

Cells lacking adaptive methylation cannot compensate for the absence of Trp-209

A very different picture emerged when receptor performance was analyzed in strain HCB436 (*62*), a ΔT strain that also lacks the adaptation enzymes CheR (methyltransferase) and CheB (methylesterase/deamidase). In these cells, the receptors remain in the QEQE modification state in which they are translated. HCB436 cells expressing receptors with Trp at position 209 supported CCW-biased flagellar rotation (**Figure 15**). The wild-type (WY) and WA receptors had MRF values similar to those in VB13 cells, but the WF and WW receptors expressed in HCB436 cells supported MRF values about twice those seen in VB13 cells (**Figure 16**). HCB436 cells producing receptors with other residues at positions 209 and 210 never rotated CW. Thus, an intact adaptation system is required to compensate for the inherently CCW-locked baseline signal output of these mutant receptors.

Adaptive methylation compensates for changes in the residue composition of the anchor

The level of *in vivo* covalent modification for all of the receptor variants was examined. In strain HCB436, all 16 proteins migrated as a single band with the same motility as wild-type Tar (**Figure 17**). In VB13 cells, all of the receptors with Trp at position 209 migrated as two bands, probably representing the EEEE and singly methylated forms. The WA receptor was shifted slightly toward the least-modified band. In contrast, all but one of the other mutant receptors showed significantly higher levels of covalent modification in their baseline state (**Figure 17**). All of the receptors responded to the addition of 10 mM aspartate by increasing their levels of covalent

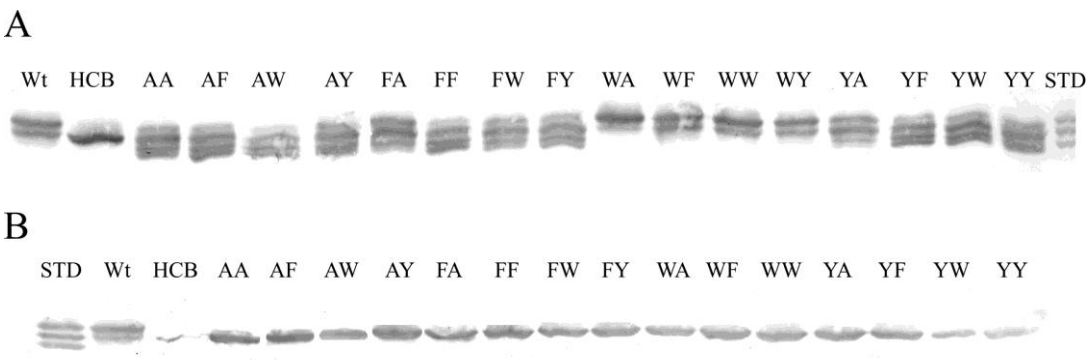

Figure 17. Baseline modification state of Tar_{Ec} receptors with or without the CheRB adaptation system. (A) Proteins from VB13 cells incubated in buffer were analyzed by SDS-PAGE on a single gel. The STD sample consists of the EEEE, QEQE, QQQQ standards. Wt is wild-type Tar_{Ec} with the WY anchor. HCB shows QEQE wild-type Tar_{Ec} from the Δ*cheRB* strain HCB436. **(B)** Proteins from HCB436 cells incubated in buffer were analyzed by SDS-PAGE on a single gel. All of the variants migrate identically.

modification, and all except the WA receptor responded to 10 mM $NiSO_4$ by decreasing their levels of covalent modification (**Figure 18**).

We classified the proteins into three categories with respect to their baseline and attractant-adapted levels of covalent modification (**Figure 19**): wild-type, over-methylated or highly over-methylated. Despite the binning into discrete groups imposed by this classification, the receptors actually were distributed along a continuum of modification states.

Four variants showed levels of covalent modification comparable to those of the wild-type WY receptor. We included the WF, WW, WA and YA receptors in this class, although the WA receptor was somewhat less modified and the YA receptor was slightly more modified than the wild-type receptor (**Figure 17**). Receptors of the second class, exemplified by the AA receptor in **Figure 19**, were significantly more modified in the baseline state and showed more extensive modification in the presence of aspartate. This class included the AA, AF, AY, FA, FW, and FY receptors. Finally, the highly over-methylated class consisted of the AW, FF, YF, YW, and YY receptors. They were highly modified in the baseline state, and their modification increased even more after the addition of aspartate. This third class of receptors decreased modification after the addition of $NiSO_4$. The overall conclusion is that the increases in CCW signaling bias of all receptors are within a range that can be largely accommodated by the adaptation system.

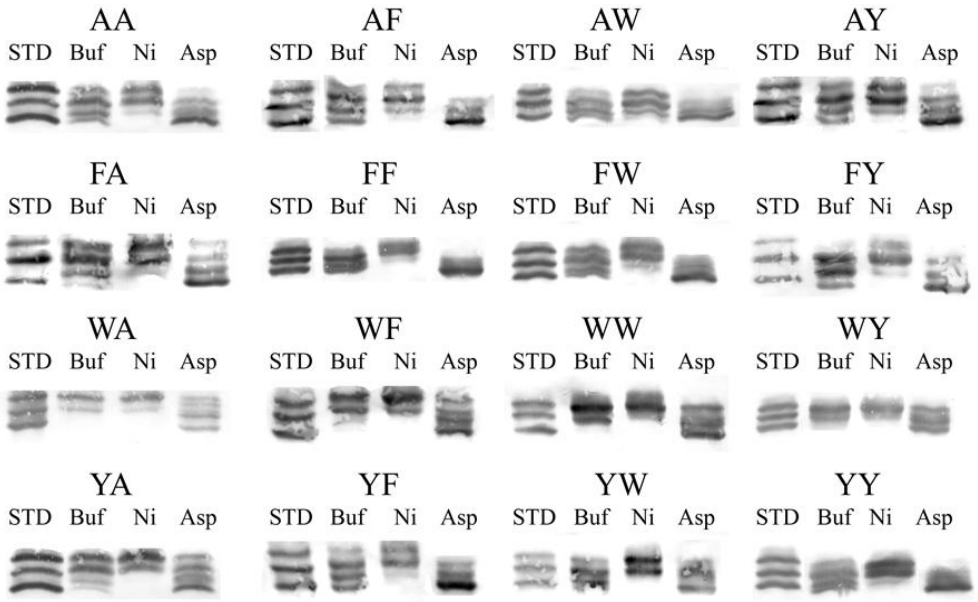

Figure 18. Steady-state patterns of covalent modification of Tar_{Ec} receptors. Proteins from VB13 (ΔT *cheR*$^+$*B*$^+$) cells expressing one of the Tar_{Ec} recoptors from pRD200 were analyzed. Cells were exposed to buffer only, 10 mM $NiSO_4$, or 100 mM aspartate (Asp). A mixture of equal amounts receptors representing the unmodified (EEEE), partly modified (QEQE) and fully modified (QQQQ) forms of Tar_{Ec} (STD) was run for each receptor variant. The rate of migration during SDS-PAGE is related to the extent of modification, with the more-highly modified forms migrating at a faster rate.

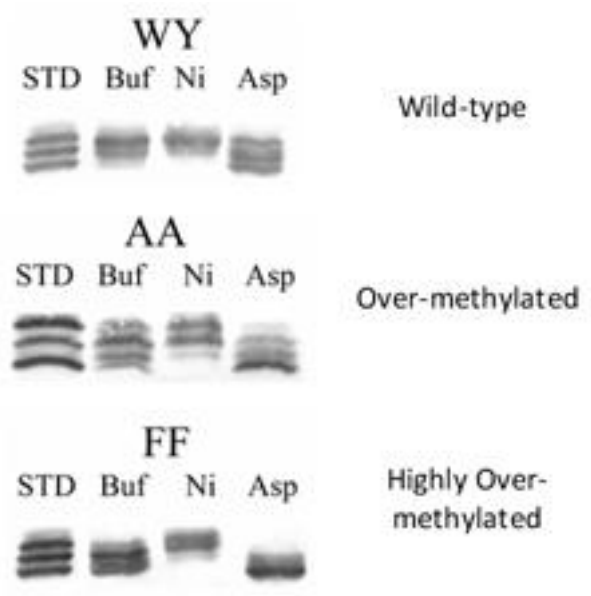

Figure 19. Examples of band-migration patterns for Tar_{Ec} variants from each category of covalent modification states. Tar_{Ec} variants were clustered into three groups depending on the degree of modification in the baseline signaling state and in the presence of the repellent Ni^{2+} and the attractant aspartate. The wild-type anchor (WY) is shown for the wild-type class. Tar_{Ec} with the AA anchor represents a moderate increase (over-methylated) in baseline and aspartate-induced modification states. Tar_{Ec} with the FF anchor represents a greater increase (highly over-methylated) in the baseline and aspartate-induced modification states.

The extent of adaptive methylation required to maintain baseline Tar_{Ec} signal output correlates with the rate of chemotaxis ring expansion in semi-solid (swim) agar

All 16 receptors were examined for their ability to support chemotaxis to aspartate and maltose in VB13 cells. The expansion rates of chemotaxis rings in semi-solid agar containing 100 μM aspartate or 100 μM maltose were calculated (**Figure 20**, **Table 3**). All receptors with Trp at position 209 were as good as wild-type Tar_{Ec} at supporting aspartate taxis, with expansion rates ranging from 1.49 mm/h for wild-type to 1.67 mm/h for the WF variant. None of the other variants supported ring expansion rates above 1.32 mm/h. The three slowest rates, ~ 0.8 mm/h, were shown by the AY, AF, and AW receptors. Even though the rate of migration between mutants varies significantly, all mutants produce migratory rings with a similar appearance (**Figure 21**).

The rates of ring expansion in maltose semi-sold agar generally correlated with those for aspartate, with the fastest rate of 0.7 mm/h supported by the WF variant and the slowest rates of 0.42-0.49 mm/h shown by the AY, AF, and AW variants. The ratios of aspartate to maltose ring expansion rates generally lay between 1.8 and 2.4 (**Table 3**), with the higher values associated with the receptors supporting the best aspartate taxis. However, the ratio for the WW receptor was 2.6, and the ratio for the WA receptor was 3.1, indicating that these receptors were selectively defective for maltose taxis.

Residue 210 contributes modestly to Tar_{Ec} function when residue 209 is Trp

To examine the contribution of residue 210 to signal output when position 209 is occupied by the favored Trp residue, we constructed a series of Tar_{Ec} variants different

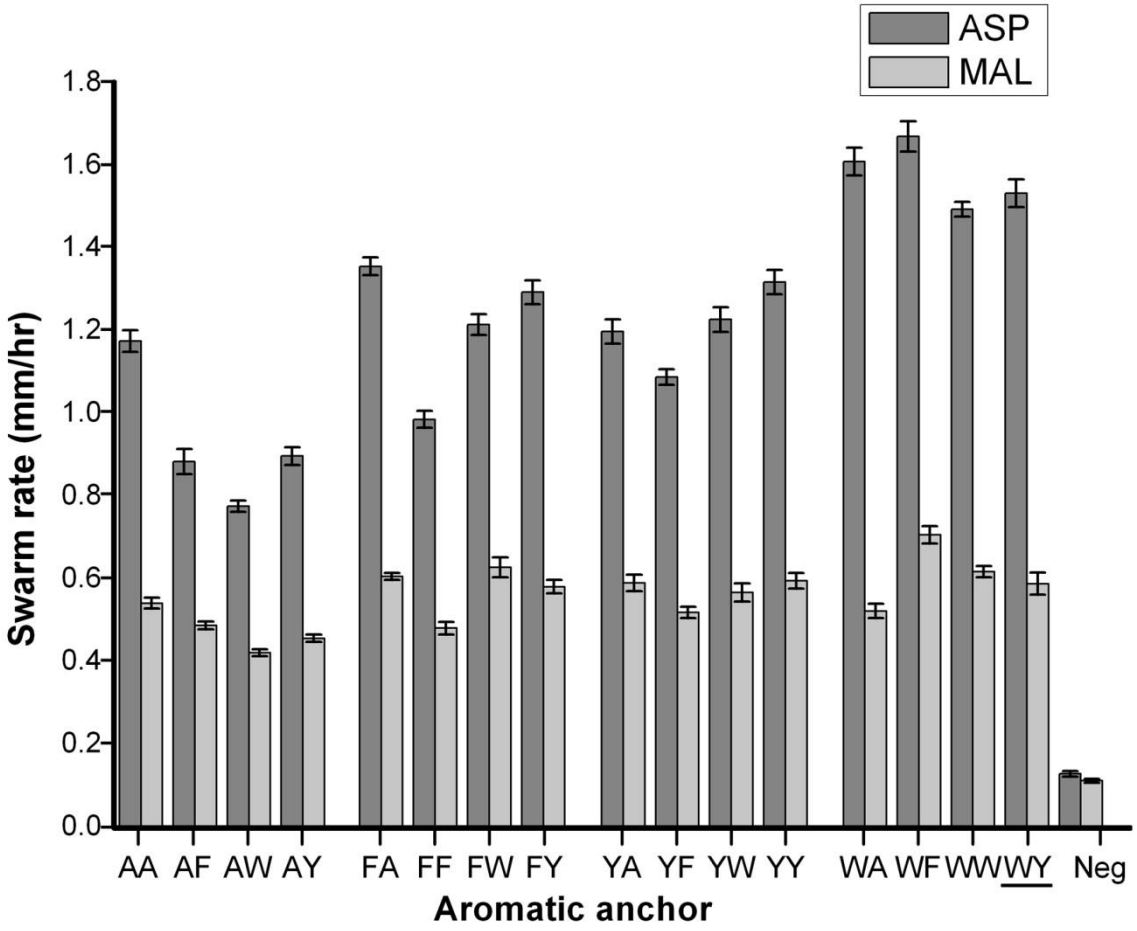

Figure 20. Chemotaxis ring formation in aspartate and maltose swim plates by cells expressing Tar_{Ec} variants containing different aromatic anchors. VB13 (ΔT *cheR*$^{+}$*B*$^{+}$) cells expressing wild-type Tar_{Ec} or different Tar_{Ec} variants from pRD200 (*68*) were inoculated into semi-solid agar containing aspartate or maltose. Plates were incubated at 30°C and measured after 8 hours, when migratory rings first became visible. The ring diameter was measured every 4 hours thereafter, and the migration rate was calculated in mm/hr. The error bars show the standard error of the mean for the expansion rates of ≥ 18 colonies. The wild-type anchor (WY) is underlined.

Receptor	AA	AF	AW	AY	FA	FF	FW	FY
Asp[a]	79±10.9	59±1.1	60±1.1	52±1.0	91±1.3	66±2.2	87±2.4	81±3.1
Mal[a]	88±20.1	79±1.5	74±1.4	68±1.3	98±1.4	78±2.6	94±2.6	102±3.9
Asp:Mal Ratio[b]	2.2±0.05	1.8±0.03	2.0±0.04	1.8±0.04	2.2±0.03	2.0±0.07	2.2±0.06	1.9±0.07
Receptor	WA	WF	WW	**WY**	YA	YF	YW	YY
Asp[a]	108±3.6	112±3.3	103±4.7	**100±2.2**	80±2.7	73±1.9	88±2.8	82±3.2
Mal[a]	114±2.8	114±3.4	93±4.3	**100±2.2**	95±3.3	84±2.2	96±3.1	92±3.5
Asp:Mal Ratio[b]	3.1±0.10	2.4±0.07	2.6±0.12	**2.4±0.05**	2.1±0.07	2.1±0.05	2.2±0.07	2.2±0.08

Table 3. Relative rates of migration of VB13 cells expressing the Tar_{Ec} variants in semi-solid (swim) agar containing aspartate or maltose.

[a]The means and standard error of the rate of migration for VB13 cells expressing various receptors were normalized to that of VB13 cells expressing wild-type (WY) Tar_{Ec}. The wild-type (WY) is underlined and values are indicated in bold. Error values for aspartate and maltose represent the propagated error when normalizing the data to the VB13 cells harboring pBR322 and expressing wild-type receptor.

[b]The Asp:Mal ratio is the rate of expansion of the aspartate chemotaxis ring divided by the rate of expansion for the maltose chemotaxis ring. The error values for the Asp:Mal ratio represent the propagated error from the previous calculations.

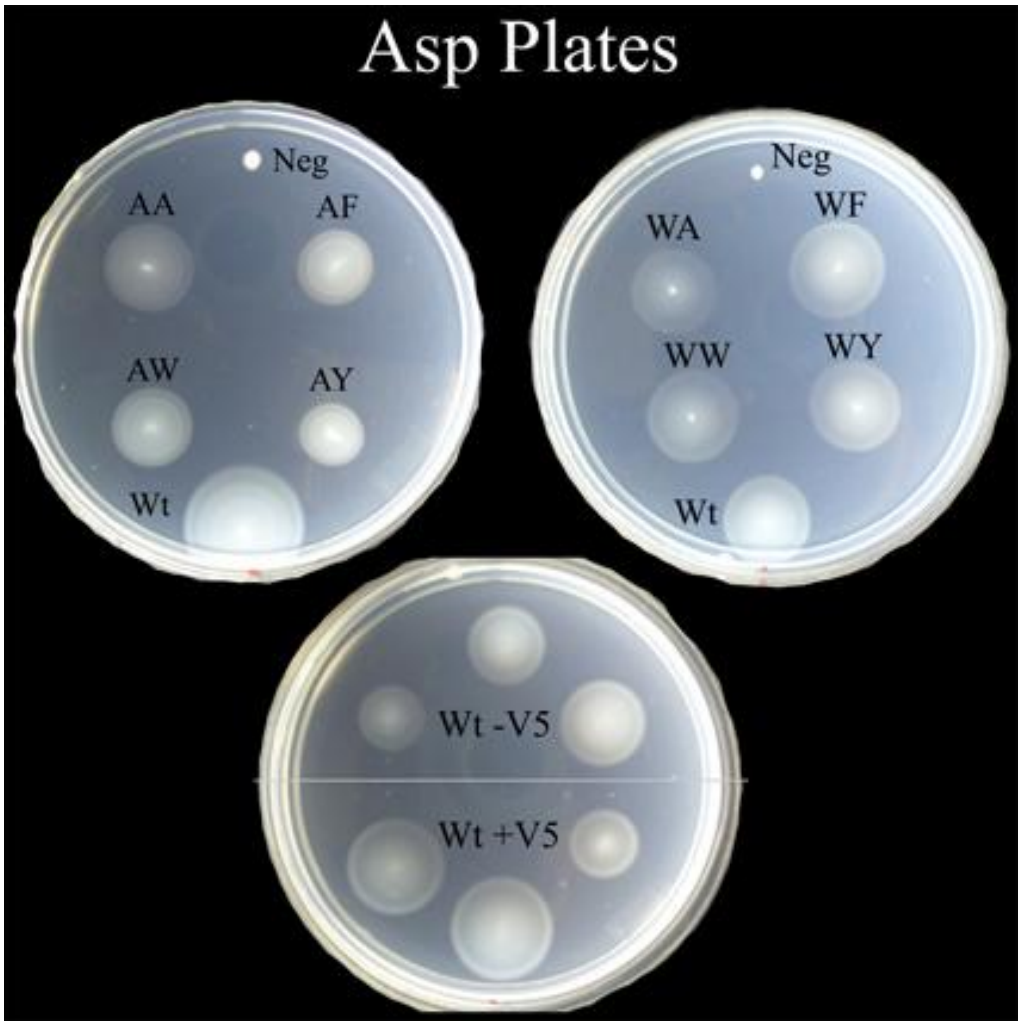

Figure 21. Images of swim plates containing VB13 cells expressing representative sets of different Tar$_{Ec}$ receptors after 12 hours on aspartate containing media. Similarities in the appearance of the migratory rings to aspartate strongly suggest that differences are due to ligand sensitivity and not metabolism of the aspartate or differences in overall cellular metabolic rate. It is important to note that each stab inoculum contains a different number of bacteria. Thus the size of the chemotactic ring after 12 h will vary for a given mutant, but the calculated expansion rates per hour will be very similar. These are the data given in **Tables 3** and **4**.

residue replacements at position 210 (**Figure 22; Table 4**). All of the receptors supported aspartate taxis, with ring expansion rates ranging from 1.3 mm/h for the WS variant to 1.5 mm/h for the WL and WV variants. However, larger differences were seen for maltose taxis. With the WL and WV receptors the expansion rates were similar to wild-type rate of 0.65 mm/h, and only slightly lower (0.6 mm/h) for WI variant. However, with the WE and WR receptors the expansion rates were only 0.45 mm/h, and only 0.36 for the WS variant. The ratios of the aspartate to maltose ring expansion rates ranged from 2.3 mm/h for cells expressing the WI receptor to 3.7 for cells expressing the WS receptor.

None of the WX receptors differed significantly from wild-type Tar_{Ec} in their baseline levels of covalent modification or in changes seen after addition of aspartate or $NiSO_4$ (**Figure 23**). We therefore anticipated that they would support essentially wild-type patterns of rotational bias and switching frequency. Analysis of tethered HCB436 cells expressing the different receptors confirmed this prediction (**Figure 24**). We conclude that, when Trp is present at position 209, the residue at position 210 has relatively little effect on receptor function unless it is charged (Glu or Arg) or uncharged but highly polar (Ser).

Discussion

E. coli chemoreceptors are membrane-spanning enzymes with multiple allosteric inputs (*136*), including ligand binding, covalent modification, and interaction with other receptors and Che proteins. The relatively small energetic contributions of these inputs

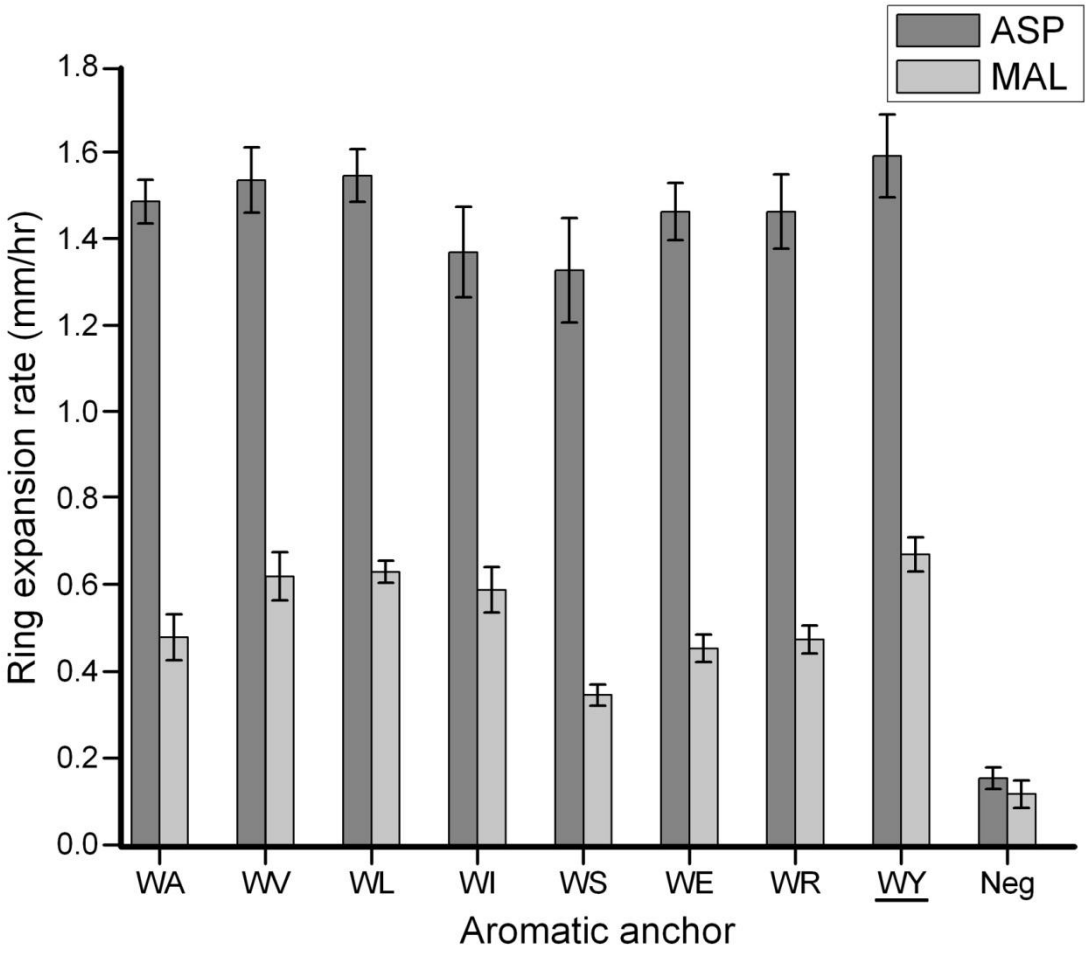

Figure 22. Chemotaxis ring formation in aspartate and maltose swim plates by cells expressing Tar_{Ec} with Trp-209 and various different residues at position 210. The measurement of ring expansion rates were performed as described in **Figure 3**. The error bars represent the standard deviation of the mean for the expansion rates of $\geq$ 6 colonies. The wild-type anchor (WY) is underlined.

	WA	WV	WL	WI	WS	WE	WR	WY
Asp[a]	93± 5.6	96± 5.8	97± 5.8	86± 5.2	83± 5.1	92± 5.5	92± 5.5	**100± 5.9**
Mal[a]	72± 4.2	92± 5.4	94± 5.5	88± 5.1	53± 3.1	68± 4.0	71± 4.1	**100± 5.8**
Asp:Mal Ratio[b]	3.1± 0.34	2.5± 0.22	2.4± 0.10	2.3± 0.2	3.7± 0.33	3.2± 0.23	3.1± 0.21	**2.4± 0.14**

Table 4. Relative rates of migration of VB13 cells expressing Tar_{Ec} WX aromatic-anchor variants in semi-solid (swim) agar containing aspartate or maltose.

[a]The means and standard deviations of the rate of migration for VB13 cells expressing various receptors were normalized to that of VB13 cells expressing wild-type (WY) Tar_{Ec}. The wild-type (WY) is underlined and values are indicated in bold. Error values for Aspartate and Maltose conditions represent the propagated error when normalizing the data to the VB13 cells harboring pBR322 and expressing wild-type receptor.

[b]The Asp:Mal ratio is the rate of expansion of the aspartate chemotaxis ring divided by the rate of expansion for the maltose chemotaxis ring. The error values for the Asp:Mal ratio represent the propagated error from the previous calculations.

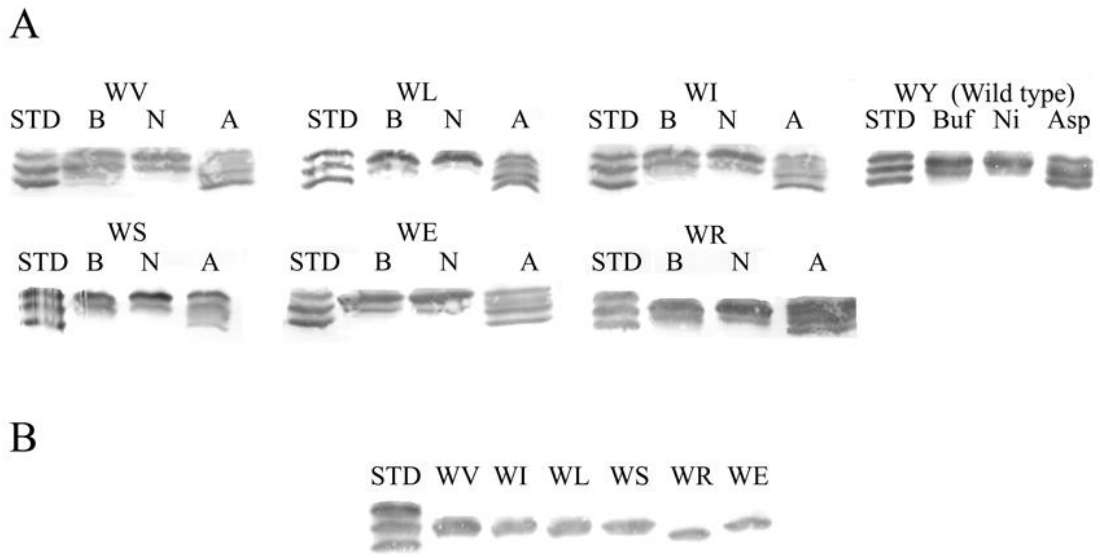

Figure 23. Steady-state patterns of covalent modification of the Tar_{Ec} WX series receptors with and without the *cheRB* adaptation system. (A) Lanes labeled B, N, and A were run with samples incubated in buffer, buffer plus 10 mM $NiSO_4$ and 100 mM asparate. The STD lanes contain the mix of EEEE, QEQE, and QQQQ standards. **(B)** Migration of proteins from HCB436 cells. Note that the WR sample migrates more rapidly, indicating that the slightly faster migration of the WR variant seen in panel A is due to an intrinsically altered migration rate of the WR protein rather than due to a difference in covalent modification level.

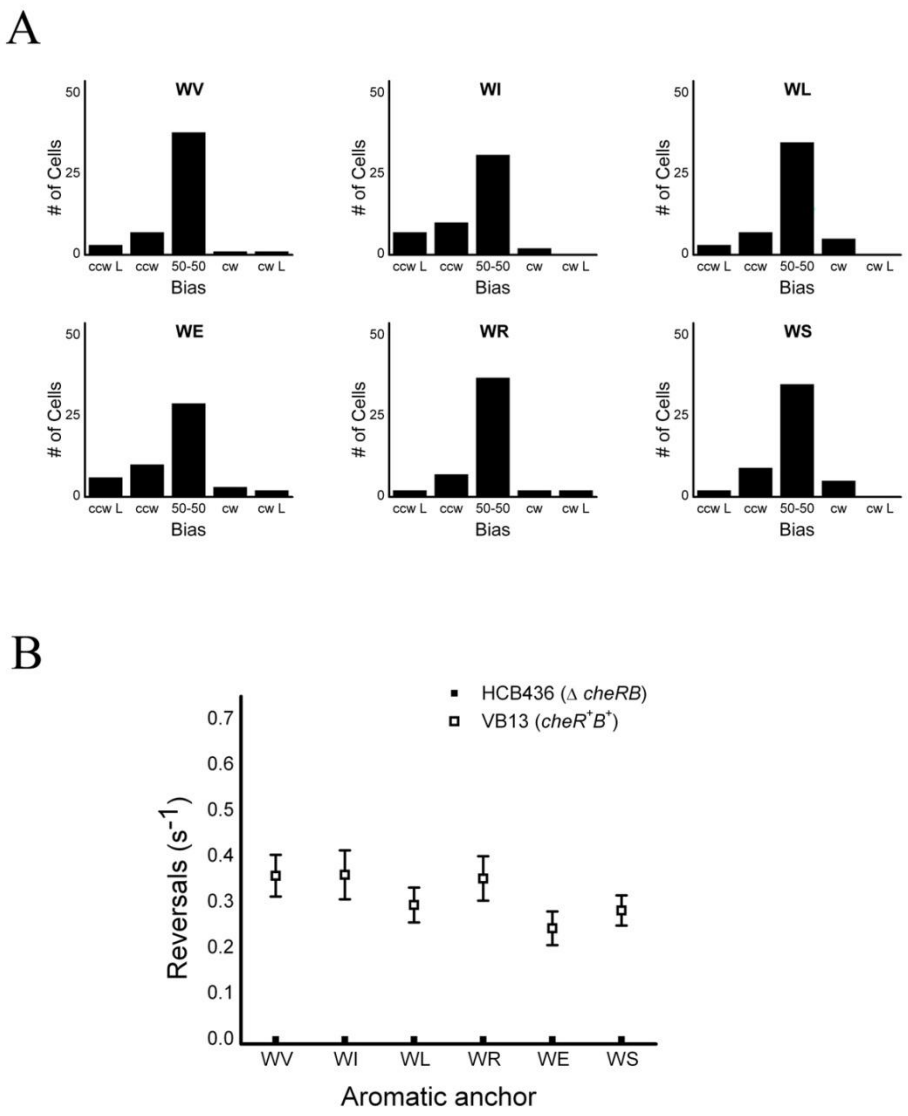

Figure 24. Rotational biases and reversal frequencies of the WX series of Tar$_{Ec}$ receptors. (A) Rotational biases of tethered cells of strain HB436 (Δ*cheRB*) expressing one of the indicated variants from pRD200. Scoring was as described in the legend to **Figure 1** except that only 50 cells per receptor variant were scored. (B) Mean reversal frequencies of tethered cells of strain HB436 (Δ*cheRB*) expressing one of the indicated variants from pRD200. Scoring was as described in the legend to **Figure 1** except that only 50 cells per receptor variant were scored. The error bars represent the standard error of the calculated mean.

strongly suggest that the receptors exist in metastable states and are poised to respond to small changes. The binding of a ligand to the periplasmic domain must be communicated through the cell membrane to the signal-processing HAMP domain via TM2. It is therefore clear that the TM2 of a particular receptor must evolve to undergo conformational changes that are driven by the binding energy of their respective ligands.

The dynamic-bundle model for function of the HAMP domain during chemoreceptor signaling (*137*, *138*) suggests that the stability of the HAMP domain is regulated by its attachment to TM2 via a five-residue linker, called the control cable (*57*, *138*). Previous experimental data (*67-69*) and a recent computer simulation (*55*) suggest that the aromatic anchor of TM2 is essential for normal transmembrane signaling. The work reported here indicates that one function of the aromatic anchor is to maintain a receptor in a baseline signaling state that allows both kinase-inhibiting (attractant) and kinase-stimulating (repellent) signals to be sensed with high sensitivity and a wide dynamic range. Although changes in the baseline signaling state can be compensated by increasing or decreasing the state of covalent modification, as appropriate, such adjustments displace the receptor from its properly poised baseline signaling state. The dynamic range of a receptor with an inappropriate aromatic anchor may be limited by the initially skewed state of covalent modification, and the mutant receptor may no longer be maximally responsive to the energy input provided by the binding of its particular ligand(s).

Our variant Tar_{Ec} receptors provide evidence of both types of disruption to receptor function. All receptors that lack Trp at position 209 have baseline signaling

states shifted toward a kinase-inhibiting, attractant-mimicking configuration (**Figure 15**). With all of these receptors, some level of CW rotation could be restored by an increased level of covalent modification (**Figure 16, Figure 17**), but these receptors are all defective, to varying degrees, in supporting aspartate and maltose taxis (**Figure 20**), Receptors with the highest baseline modification state were the most defective for chemotaxis.

A second, more subtle disruption is evidenced by receptors that have Trp at position 209 but lack an aromatic or aliphatic residue at position 210. The WA, WR, WE, and WS receptors all were able to mediate essentially normal aspartate taxis, and they showed wild-type patterns of covalent modification in the baseline state. However, these four receptors were all selectively defective for maltose taxis (**Figure 22**). We propose that this is because the energy supplied by interaction of the periplasmic domain of Tar_{Ec} with ligand-bound MBP is lower than the energy supplied by interaction with aspartate. This result is based on the stronger response of *E. coli* to aspartate than to maltose in capillary assays, the longer response times to addition of aspartate than to addition of maltose in tethered cell assays, and the ability of aspartate to completely block the response to maltose in certain competition assays (*33, 52*). In terms of a mechanical analogy, against whose overuse we have cautioned (*139*), the spring constant resisting the piston-like movement of helix 4 of TM2 is greater for the WA, WE, WR, and WS receptors.

Our current model for the function of the cytoplasmic aromatic anchor is illustrated in the diagram in **Figure 25**. In the wild-type receptor in the absence of

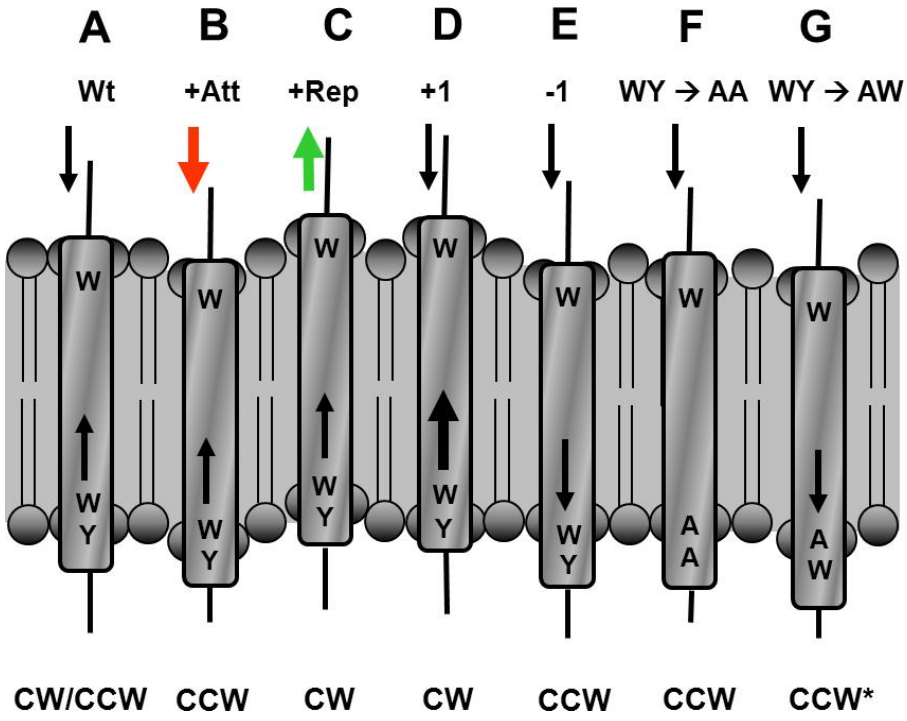

Figure 25. Model for the role of the cytoplasmic aromatic anchor of TM2 in transmembrane signaling. (A) In the wild-type (WT) receptor, a weak inward-directed force (thin downward arrow) exerted by the periplasmic domain is balanced by a weak outward-directed force (thin upward arrow) caused by the energetic cost of moving the WY tandem pair from the hydrophobic/polar interface at the cytoplasmic surface of the membrane. The receptor remains in a CW/CCW-balanced signaling state. (B) When an attractant binds to the periplasmic domain, the inward-directed force (red arrow) becomes greater, and TM2 is displaced inward, leading to CCW signaling. The membrane surfaces may also be slightly deformed. C) Upon binding of a repellent, an outward-directed force (green arrow) is exerted by the periplasmic domain, and TM2 is displaced outward, leading to CW signaling. Again, the membrane surfaces may be slightly deformed. D) When the WY tandem pair is shifted one position toward the C-terminus (+1), the upward restoring force imposed by the aromatic anchor increases (bold black upward arrow), and a CW signaling state is favored. E) When the WY tandem pair is shifted one position toward the N-terminus (-1), the inward force exerted by the periplasmic domain is augmented by an inward-directed force generated by the displaced aromatic anchor (lower thin downward arrow), leading to a CCW signaling state. F) When the cytoplasmic aromatic anchor is weakened by replacement of the WY tandem pair with AA, there is no resistance to the inward force exerted by the periplasmic domain, and the receptor is shifted toward a CCW signaling state. (G) When the WY tandem pair of the cytoplasmic aromatic anchor is replaced by AW, there is an additional inward-directed force (lower thin downward arrow) induced by the C-terminally shifted Trp residue, and the inward-directed force is augmented to lead to a more strongly CCW* signaling state.

ligand, a postulated inward-directed force on TM2 is balanced by a restoring force of the WY cytoplasmic anchor (**Figure 25A**), and the receptor is maintained in an alternating CW/CCW signaling state. The other WX anchors apparently exert a similar restoring force. When the attractant binds, the inward force imposed by the periplasmic domain increases, the balancing force of the cytoplasmic anchor is overcome, and TM2 is displaced inward (**Figure 25B**). The result is that the receptor is converted into a CCW signaling state. Binding of a repellent exerts an opposite, outward-directed force that results in CW signaling (**Figure 25C**). Moving the WY anchor one residue in the C-terminal direction (the +1 receptor(*69*)) generates a stronger outward-directed force that also leads to CW signaling (**Figure 25D**). Moving the WY anchor one residue in the N-terminal direction (the −1 receptor(*69*)) generates an inward-directed force that leads to CCW signaling (**Figure 25E**). When the aromatic anchor is removed (the AA receptor), the restoring force is eliminated and the inward-directed force imposed by the periplasmic domain dominates, leading to CCW signaling (**Figure 25F**). Finally, when Trp-209 is replaced with Ala and an aromatic residue is retained at position 210 (e.g., the AW receptor), the displaced aromatic anchor may interact additively with the inward-directed force exerted by the periplasmic domain to create an even stronger CCW (CCW*) signaling bias (**Figure 25G**). In all cases of CCW signaling bias, an increased level of covalent modification can restore the CW/CCW signaling state in a *che*R^+B^+ cell.The known TM2 sequences of MCPs in *E. coli* and two other enteric bacteria, *Salmonella enterica* and *Enterobacter aerogenes*, are given in **Table 2**. All of the MCPs that have a C-terminal pentapeptide CheR-binding motif (NWE$^S/_T$F) have Trp residues

at the hydrophobic–polar interfaces of the both the periplasmic and the cytoplasmic membrane surfaces. These receptors are the most important for determining the baseline signaling state of the receptor patch, and they are typically the most abundant of the chemoreceptors. It therefore seems reasonable that they are the ones for which the position of TM2 relative to the membrane would need to be most tightly regulated.

The remaining MCPs have a more variable TM2 composition, although they all have aromatic residues at the C-terminal end of the TM2 core region. The same is true of the TM2 core regions of the histidine protein kinases (HPKs) NarX, NarQ, PhoQ, and EnvZ, and of the Aer redox chemoreceptor, all of which also have a HAMP domain that follows closely after their TM2 helices. It may be that the precise positioning of TM2 is less critical for these proteins. For the lower-abundance MCPs and Aer, this could be because they exist in mixed patches with the high-abundance MCPs, which might dictate the signaling states of the mixed trimers of dimers (*7*). For histidine kinases that regulate gene expression on a time scale of minutes or hours, fine control of their activity on a short time scale may not be as important a consideration as it is for chemoreceptors that mediate responses on a scale of a few seconds.

Functional hybrids can be made between the sensing and signal-output domains of different chemoreceptors (Tsr-Tar and Tar-Tsr,(*25*)); Trg-Tsr,(*140*); Tap-Tar,(*62*); and between an HPK sensing domain and a chemoreceptor output domain (NarX-Tar; (*132, 141*)). Because all of these proteins mediate effective chemotaxis when they are present as the sole MCP in a cell, adaptive covalent modification must be able to accommodate whatever defects there may be in their function. Perhaps some of them

would not support normal CW/CCW rotation biases in Δ*cheRB* cells. It is reasonable to propose that the precise composition and placement of the cytoplasmic aromatic anchor of TM2 determine the baseline signaling state and the energy input required for transmembrane signaling. Thus, the aromatic anchor and the ligand-binding site should coevolve to provide optimal performance for each receptor type.

CHAPTER III

RESIDUES AT THE TM2-HAMP INTERFACE SET SIGNAL OUTPUT AND LIGAND SENSITIVITY OF THE *E.COLI* TAR CHEMORECEPTOR

Overview

I designed and performed most of the work described in this chapter. Dr. Roger R. Draheim constructed a number of the mutants used in the experiments, and Mr. Garrett Rueda and Mr. Raj Desai assisted with various experiments during the year they worked as undergraduates in the Manson laboratory.

Summary

Baseline signal output and communication between the periplasmic and cytoplasmic domains of the *E. coli* aspartate chemoreceptor Tar_{Ec} are both strongly influenced by residues at the C-terminus of transmembrane helix 2 (TM2). In particular, the cytoplasmic aromatic anchor, composed of residues Trp-209 and Tyr-210 in wild-type Tar_{Ec}, is important for determining the CheA kinase-stimulating activity of the receptor and its ability to respond to chemoeffector-induced stimuli. Here, we have studied the effect on Tar_{Ec} function of the six-residue sequence at positions 207-212. Moving various combinations of aromatic residues among these positions generates substantial changes in receptor activity. Trp has the largest effect on function, both in maintaining normal activity and in altering activity when it is moved. Tyr has less of an effect, and Phe has the least, but all three aromatic residues can alter signal output when

they are placed in novel positions. We also find that Gly-211 plays an important role in receptor function, perhaps because of the flexibility it introduces into the TM2-HAMP domain connector. The results suggest that the signaling properties of the transmembrane sensor kinases of two-component systems can be predicted by the nature of their TM2-HAMP connections. It may also be possible to modulate their activity in a controlled way by manipulating the amino acid sequences that comprise those connections.

Introduction

An *Escherichia coli* cell moves through a chemically homogenous environment by employing a three-dimensional random walk consisting of a series of smooth-swimming "runs" interspersed with brief "tumbles" that randomly reorient the bacterium. When flagella rotate counterclockwise (CCW), they coalesce into a bundle at one end of the cell and propel it in a smooth swim (*1*, *3*). When one or more flagella switch from CCW to clockwise (CW), the bundle is disrupted, resulting in a random reorientation of the bacterium that is called a tumble (*3*). Several transmembrane chemoreceptors, known as methyl-accepting chemotaxis proteins (MCPs), mediate behavioral responses to specific sets of compounds. These MCPs, along with the aerotaxis receptor (Aer_{Ec}), are members of a common chemotaxis circuit that couples detection of environmental compounds to modulation of the rotational bias of the flagellar motors. By decreasing the probability of CCW rotation, a cell can extend the duration of runs in a favorable direction, either up an attractant gradient or down a repellent gradient (*115*, *116*).

The aspartate chemoreceptor of *E. coli* (Tar_{Ec}) detects the presence of attractants both directly (aspartate) and indirectly (maltose). Aspartate binds at one of two rotationally symmetric binding sites in the periplasmic domain of the Tar_{Ec} homodimer. Maltose, in contrast, first associates with the periplasmic maltose-binding protein (MBP), causing MBP to adopt a conformation that facilitates interaction with Tar_{Ec} (*21, 31*). Maltose-bound MBP binds to the apex of the Tar periplasmic four-helix bundle (*28, 51*). Tar_{Ec} also mediates repellent taxis to Ni^{2+} and Co^{2+} (*39, 40*), which also bind directly to its periplasmic domain, as shown by isothermal calorimetry (ITC) (I. Kawagishi, personal communication). Attractant binding also induces covalent modification of the cognate MCP (*92*). Methyl groups are added by a methyltransferase, CheR, and removed by a methylesterase, CheB (*70, 142*). Increased methylation of eight specific glutamyl residues within the receptor homodimer stimulates the activity of the CheA kinase, whereas decreased methylation decreases CheA stimulation (*117*).

E. coli MCPs contain two transmembrane helices. Transmembrane helix 1 (TM1) is an N-terminal extension of helix 1 of the periplasmic domain, whereas transmembrane helix 2 (TM2) is a C-terminal extension of helix 4 of the periplasmic domain. TM2 communicates conformational changes induced by ligand binding to the cytoplasmic HAMP domain (histidine kinases, adenylyl cyclases, methyl-accepting chemotaxis proteins, and certain phosphatases) (*53*). The mechanism of signal transduction from the periplasmic domain to the HAMP domain is not fully understood, but several hypotheses have been advanced to explain the process (*27, 54, 57*). Whatever the signaling mechanism may be, the preponderance of evidence suggests that a small (~ 1–3 Å)

inward displacement of helix 4/TM2 roughly perpendicular to the plane of the membrane occurs upon binding of aspartate (*63*-*69*).

Substitutions of the aromatic residues Trp-209/Tyr-210 at the cytoplasmic end of TM2 of Tar_{Ec} with other aromatic or alanine residues result in a steady-state signal output consistent with an aspartate-bound conformation (*114*). Repositioning the Trp-209/Tyr-210 tandem up to several residues from its original position modulates Tar_{Ec} signal output (*69*). Here, we have extended that study by examining in detail how the amino acid sequence of residues 207 to 212 affects the signaling properties of Tar_{Ec} and its ability to mediate aspartate chemotaxis. The results identify the distributions of aromatic residues within this region that support normal receptor function and highlight the importance of residue Gly-211 in overall receptor performance.

Materials and methods

Bacterial strains and plasmids

Strains HCB436 (Δ*tsr7021* Δ*trg100* Δ(*tar-cheB)2234*) (*122*), RP3098 (Δ*(fhlD-flhB)4*) (*123*), and VB13 (Δ*tsr7021* Δ*tar-tap5201 trg*::Tn*10*) (*62*) are derived from the *E. coli* K-12 strain RP437 (*124*). Strain VB13 is deleted for all chemoreceptor genes other than *aer*, as is strain HCB436, which is also deleted for *cheRB*. All *in vivo* assays of receptor activity were conducted with these two strains. Strain RP3098 contains a deletion of the master regulator *flhDC* and therefore fails to produce any Che proteins. Plasmid pRD200 (*68*), derived from pMK113 (*28*), was used to express wild-type or mutant *tar* genes constitutively for all *in vivo* experiments. An in-frame coding sequence

for a seven-residue linker (GGSSAAG) (*128*) and a C-terminal V5 epitope tag (GKPIPNPLLGLDST) (*129*) was added to the 3' end of *tar*. Plasmid pRD300 (*68*) is a derivative of pBAD18 (*130*) that expresses *tar* with the same C-terminal linker and V5 epitope tag upon induction with L-arabinose. Strain RP3098 was used with pRD300 to produce standards for the *in vivo* methylation assay (*68*). Mutations in *tar* were introduced via site-directed mutagenesis (Stratagene).

Observation of tethered cells

HCB436 or VB13 cells containing plasmid pRD200 were grown overnight in tryptone broth (*131*) supplemented with 100 μg/mL ampicillin. Overnight cultures were then back-diluted 1:100 in tryptone broth and grown at 30°C with agitation until an OD_{600nm} of ~ 0.6. At this time, a 10-mL aliquot of cells was pelleted, and the cells were resuspended in 10 mL of tethering buffer (10 mM potassium phosphate [pH 7.0], 100 mM NaCl, 10 μM EDTA, 20 μM L-methionine, 20 mM sodium DL-lactate, and 100 μg/mL chloramphenicol). Flagella were sheared in a Waring blender (*132*) during eight repetitions of 7 s intervals of shearing at high speed interspersed with 13 s pauses to prevent overheating. Cells were collected by centrifugation, washed three times in tethering buffer, and mixed with an equal volume of a 1:200 dilution of anti-flagellar filament antibody. A 40-µL aliquot of this cell/antibody mix was added to the center of a glass coverslip. Coverslips were then incubated in a humidity chamber for 30 min at 30°C and affixed to a flow chamber (*133*); non-tethered cells were removed by flushing the chamber with chemotaxis buffer. Cells were observed under reverse phase contrast at

1000x magnification, using an Olympus BH-2 microscope. Rotating cells were digitally recorded, and at least 50 cells for each specific receptor were monitored visually during 20 s playback. Cells were assigned to one of five rotational categories as described previously (*114*), and the percentage CW rotation was determined by summing across the five classes using the weighting protocol established by Ames *et al*., 2002 (*7*): rotating exclusively CCW; rotating mostly CCW with occasional reversals (25%); reversing frequently with no clear bias (50%); rotating mostly CW with occasional reversals (75%); and rotating exclusively CW (100%). Reversal frequency was determined by tallying the number of reversals for each cell during video playback.

Determination of the methylation state of receptors in vivo

HCB436 or VB13 cells containing plasmid pRD200 were grown overnight at 30ºC in tryptone broth supplemented with 100 μg/mL ampicillin. Overnight cultures were then back-diluted 1:100 in tryptone broth without ampicillin and grown at 30°C to an OD600 nm of ~0.6. Cells were harvested by centrifugation, washed three times with 10 ml of 10 mM potassium phosphate buffer (pH 7.0) containing 0.1 mM EDTA, and resuspended in 5 ml of 10 mM potassium phosphate (pH 7.0) containing 0.1 mM EDTA, 10 mM sodium DL-lactate, and 100 µg/ml of chloramphenicol. One mL aliquots were transferred to 10-mL scintillation vials and incubated for 10 min at 32^{o}C, with agitation. Cells were then incubated for another 30 min after the addition of L-methionine to 100 µM. A 100 µL aliquot of 100 mM L-aspartate or 10 mM $NiSO_4$ solutions, or 100 µL of buffer as control, were added at this time, and the cells were incubated for an additional

20 min. Reactions were terminated by addition of 100 μL ice-cold 100% TCA, and the samples were then incubated on ice for 15 min. Denatured proteins were pelleted, washed with 1% TCA and acetone, and resuspended in 100 mL 2X SDS-loading buffer. A 15-μL aliquot of each sample was subjected to SDS-PAGE and immunoblotting with antibodies raised against the V5 epitope that were conjugated to alkaline phosphatase (Invitrogen). Standards were run as a mixture of Tar proteins containing equal proportions of V5-tagged versions of the EEEE, QEQE, and QQQQ forms of the Tar receptor produced from RP3098 cells containing pRD300. The Gln residues affect protein migration like methylated Glu residues, so that the standards migrate like the unmethylated, doubly methylated, and quadrupally methylated forms of the receptor, respectively.

Chemotactic swim-plate assays

Semi-solid motility agar contained 3.25 g/L Difco BactoAgar (Difco) in motility medium [10 mM potassium phosphate (pH 7.0), 1 mM $(NH_4)_2SO_4$, 1 mM $MgSO_4$, 1 mM $MgCl_2$, 1 mM glycerol, 90 mM NaCl] and was supplemented with 20 μg/mL of L-threonine, L-histidine, L-methionine, and L-leucine and 1 μg/mL thiamine. Aspartate and maltose were added to final concentrations of 100 μM. Plates were inoculated with toothpicks from isolated colonies of strain VB13 expressing one of the various Tar receptors from pRD200. Swarm plates were incubated at 30ºC. Once chemotaxis rings became visible (typically 8 h for aspartate and 12 h for maltose plates), their diameter was measured every 4 h.

Results

Generation of mutant receptors

The replacement of Trp-Tyr (WY) at positions 209 and 210 with Ala-Ala (AA) in Tar_{Ec} results in a CCW-locked signal output when the mutant receptor is expressed in the ΔT *cheRB*-deleted strain HCB436 (*114*). However, the AA receptor can support chemotaxis ring expansion of the ΔT *cheR*$^+$*B*$^+$ strain VB13 in semi-solid aspartate minimal agar at ~80% of the rate obtained with cells expressing the wild-type receptor. The AA receptor supports some chemotaxis because in the *cheR*$^+$*B*$^+$ strain adaptive methylation restores enough CW signal output to allow the run-tumble behavior required to carry out a biased random walk (*114*).

Because an Ala-Ala tandem generally has minimal positioning character with respect to the membrane (*143*), we consider the Tar_{Ec} AA receptor to represent the default behavior observed in the absence of a cytoplasmic aromatic anchor in TM2. The properties of the Tar_{Ec} AA receptor thus serve as a standard against which other mutant Tar_{Ec} receptors can be evaluated.

Our strategy was to create a library of mutants containing different combinations of single and tandem-double aromatic residues at positions 207-212 region of Tar_{Ec} (**Table 5**). Including the wild-type Tar_{Ec} receptor, 59 receptor variants were analyzed. A majority of the receptors were constructed for this study, but some previously published mutants were analyzed as well and are designated as such in the table. Each of the receptors is given a shorthand designation in the table. All of the Tar_{Ec} constructs carried a V5 epitope tag at their C-terminus; the tag has little effect on the output of the

CCW-locked <25% ring	CCW-locked <50% ring	CCW-locked <75% ring	CCW-locked >75% ring	CW-biased <25% ring	CW/CCW <50% ring	CW-biased <75% ring	CW/CCW >75% ring	
AWVAGIR (AW-2)	VALLAWR (AW+2)	AFVAGIR (AF-2)	VAFAGIR (AF-1)	VAWYLIR (AWYL)	VALLWAR (WA+2)	VAWYAIR (AWYA)	VALAFIR (AF+1)	VALFFIR (FF+1)
VWAAGIR (WA-1)	VAAYGIR **(AY*)**	VAAFGIR **(AF*)**	WAVAGIR (WA-2)	VAWYPIR (AWYP)	VALLAYR (AY+2)		VALLAFR (AF+2)	VALLFFR (FF+2)
AYVAGIR (AY-2)	VYYAGIR (YY-1)	VAAWGIR **(AW*)**	VAYAGIR (AY-1)	VAAWPIR (AAWP)	VALLWWR (WW+2)		VAWAGIR (AW-1)	VALWYIR **(WY+1*)**
WWVAGIR (WW-2)		FFVAGIR (FF-2)	VFFAGIR (FF-1)		VALLYYR (YY+2)		VALAWIR (AW+1)	VALWWIR (WW+1)
YYVAGIR (YY-2)		VAFFGIR **(FF*)**	VAFAGIR **(FA*)**		VALLWYR **(WY+2*)**		VALWAIR (WA+1)	VALYYIR (YY+1)
WYVAGIR **(WY-2*)**		VWWAGIR (WW-1)	VAFWGIR **(FW*)**				VALAYIR (AY+1)	**VAWYGIR (AWYG)**
		VAYFGIR **(YF*)**	VAFYGIR **(FY*)**				VAAWGIR (AAWG)	VGWYGIR (GWYG)
		VWYAGIR **(WY-1*)**	VAYWGIR **(YW*)**				VALWGIR (ALWG)	VAAWAIR (AAWA)
			VAAAGIR **(AA*)**				VAWxGIR **(Wx*)**	VAGWAIR (AGWA)
			VAFYGIR **(YY*)**					VAAWLIR (AAWL)

Table 5. Library of TM2 terminal region mutants. The amino acid sequence of the seven residue potentially altered by mutations made at the C-terminal region of TM2 and the start of the connector region between TM2 and the HAMP domain are listed. Abbreviations are given to all receptors and previously studied mutants are noted with bold lettering and an asterisk after their abbreviated name. The baseline receptor with tandem Ala residues (AA) is highlighted with a yellow background. The wild-type receptor is in bold lettering and underlined with an orange background. Mutant receptors with similar phenotypes, as seen in **Figure 26,** are grouped together with the same color highlighting.

receptor (*114*).

Plasmids expressing these Tar_{Ec} variants were expressed in cells of strains VB13 and HCB436. The receptors were modestly over-expressed, and all of them were present at approximately the same concentration. In aspartate semi-solid agar, the ring-expansion rate (RER) of a colony of strain VB13 expressing plasmid-encoded, V5-tagged wild-type Tar_{Ec} was similar to that of the wild-type strain RP437 (*114*). We thus set the RER of strain VB13 expressing wild-type (WY) Tar_{Ec} at 100% and expressed the RERs for all of the other receptors as a percentage of the wild-type RER. The data obtained with the different receptors in different assays are summarized in **Table 5, Figure 26,** and **Figure 27**. Histograms showing the actual distribution of rotational biases for each receptor are given in **Figures 28-30**.

Support of CW rotation in strain HCB436 (Δ*cheRB*)

Because strain HCB436 lacks both methyltransferase and methylesterase/deamidase activities, Tar_{Ec} produced in this strain remains in the QEQE modification state in which it is originally translated. This receptor behaves much like a half-methylated $E^{m}EE^{m}E$ receptor because the negative charge of two glutamyl residues is neutralized in each case.

Twenty-two out of the 59 receptors examined (58 mutants plus wild type) failed to support any significant level of CW flagellar rotation (≤2% CW rotation, as defined in Materials and Methods and Ames, 2002) when tethered HCB436 cells were observed (**Figure 26**). All of the remaining 37 receptors supported ≥30% CW rotation. The

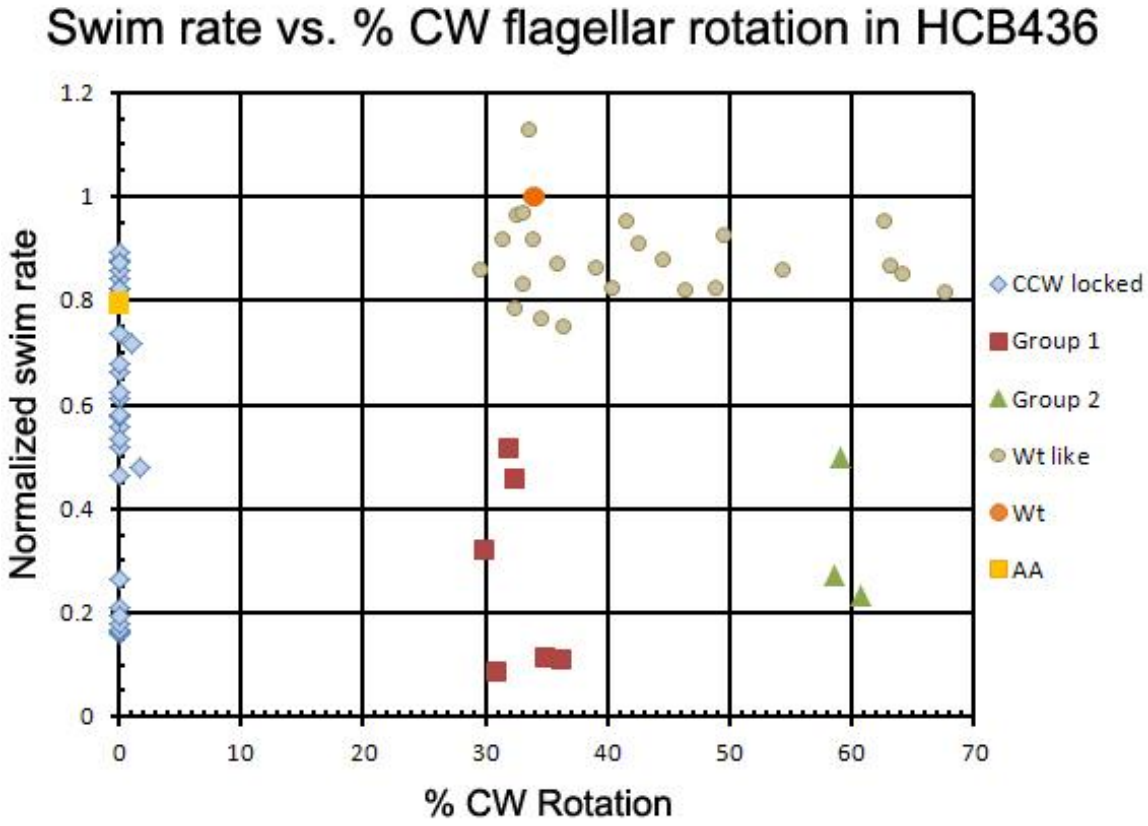

Figure 26. RER versus percentage CW flagellar rotation of HCB436 cells expressing Tar$_{Ec}$ wild-type or mutant variants of the region of TM2 near the cytoplasmic membrane interface. RER data were collected from VB13 (ΔT *cheR*$^+$*B*$^+$) cells expressing the wild-type or mutant Tar$_{Ec}$ variants from pRD200 (*68*). The average RER for each mutant was normalized to the wild-type average for each set of assays. Flagellar rotation was analyzed with tethered cells of HCB436 (ΔT Δ*cheRB*) cells expressing the wild-type or mutant Tar$_{Ec}$ variants from pRD200 (*68*). The percentage CW flagellar rotation was determined as described in Materials and Methods. The data for the wild-type (WY) receptor is indicated as an orange circle, the AA mutant is indicated as a yellow square, and the data for the other mutant receptors associated with similar phenotypes are indicated with the same symbols.

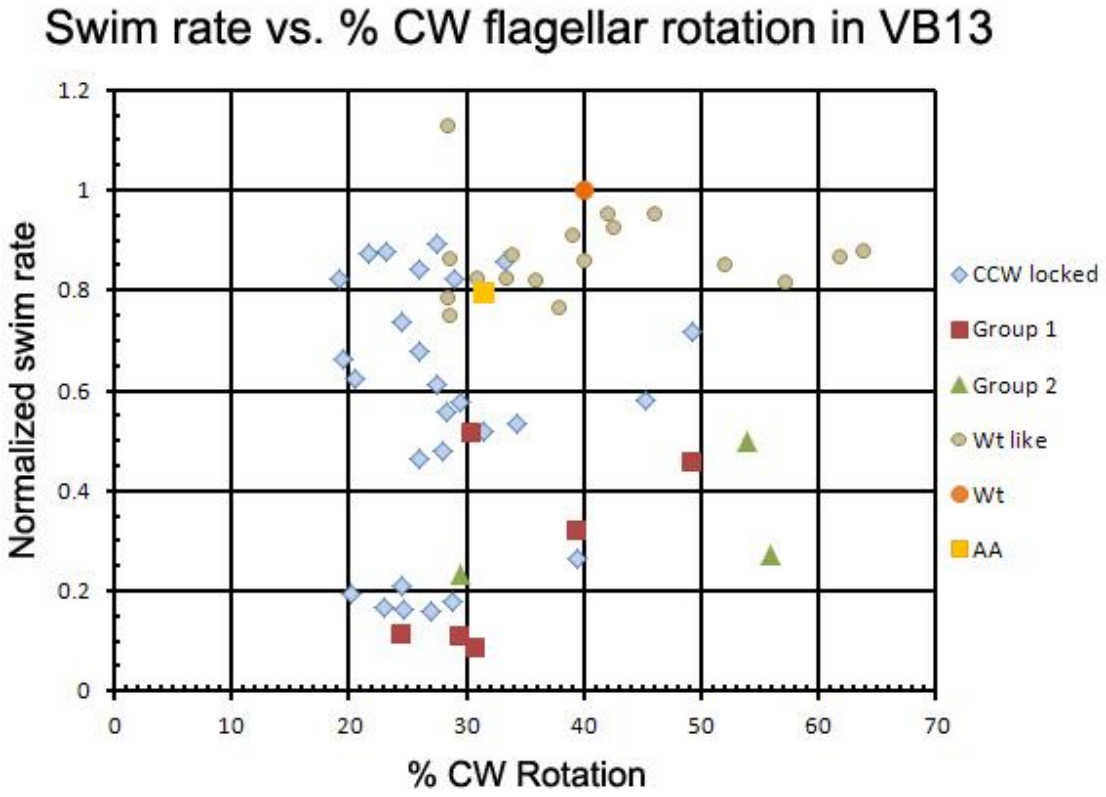

Figure 27. RER versus percentage CW flagellar rotation of VB13 cells expressing Tar_{Ec} wild-type or mutant variants of the region of TM2 near the cytoplasmic membrane interface. RER data were collected from VB13 (ΔT *cheR*$^+$*B*$^+$) cells expressing wild-type or mutant Tar_{Ec} variants from pRD200 (*68*). The average RER for each mutant was normalized to the wild-type average for each set of assays. Flagellar rotation was analyzed with tethered cells of VB13 (ΔT) cells expressing the wild-type or mutant Tar_{Ec} variants from pRD200 (*68*). The percentage CW flagellar rotation was determined as described in Materials and Methods. The symbols are as in **Figure 26**.

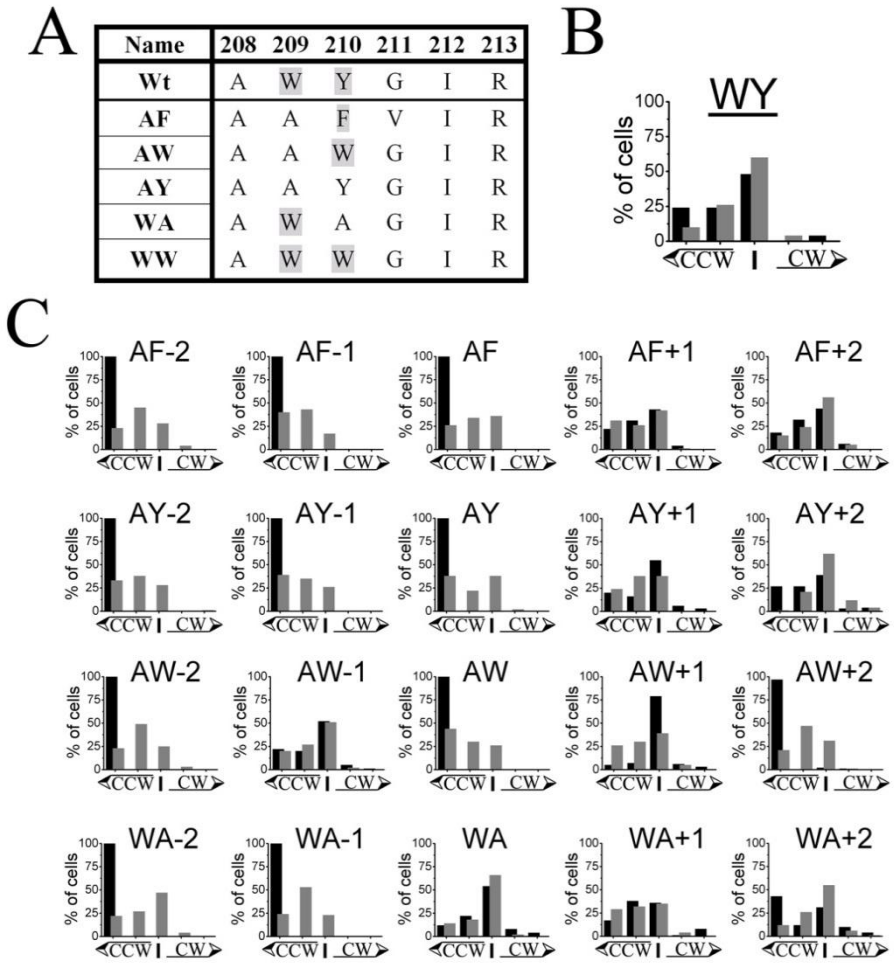

Figure 28. Flagellar rotational bias of cells expressing wild-type or mutant Tar$_{Ec}$ variants with a single aromatic residue in the cytoplasmic aromatic anchor. (A) Amino acid sequence of wild-type Tar$_{Ec}$ and select mutant variants. Aromatic residues are indicated with a shaded background. **(B)** VB13 (ΔT *cheR*$^{+}$*B*$^{+}$) or HCB436 (ΔT Δ*cheRB*) cells expressing the wild-type Tar$_{Ec}$ receptor from pRD200 (*68*) were tethered, observed for 20 sec, and assigned to one of five categories based on their apparent flagellar rotational bias. From left to right, these categories are designated: counterclockwise rotation with no switching (CCW only), counterclockwise-biased with frequent switching (CCW), frequent reversing with no apparent bias (CCW/CW), clockwise-biased with frequent switching (CW), and clockwise rotation with no switching (CW only). Results from VB13 cells are depicted as gray bars; results from HCB436 are depicted as black bars. Each histogram contains data from one hundred VB13 cells and one hundred HCB436 cells. **(C)** Flagellar rotational bias of mutant Tar$_{Ec}$ variants as described in part B.

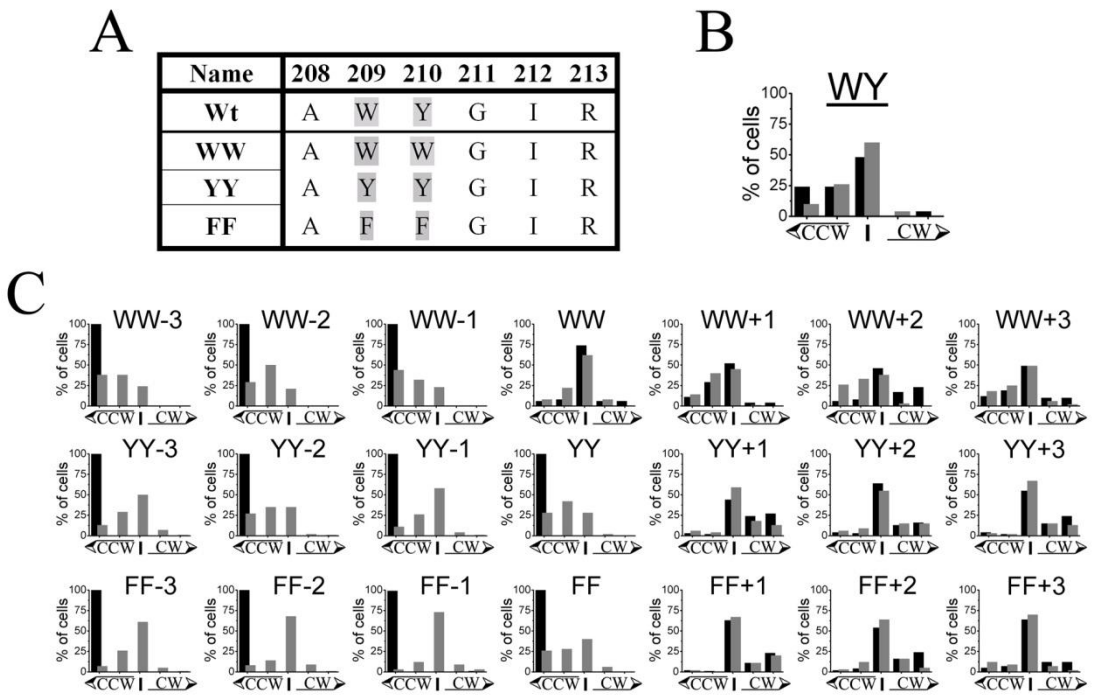

Name	208	209	210	211	212	213
Wt	A	W	Y	G	I	R
WW	A	W	W	G	I	R
YY	A	Y	Y	G	I	R
FF	A	F	F	G	I	R

Figure 29. Flagellar rotational bias of cells expressing wild-type or mutant Tar$_{Ec}$ variants with two aromatic residues in the cytoplasmic aromatic anchor. (A) Amino acid sequence of wild-type Tar$_{Ec}$ and select mutant variants. Aromatic residues are indicated with a shaded background. **(B)** Flagellar rotational bias of the Wild-type Tar$_{Ec}$ receptor as described in **Figure 28**. **(C)** Flagellar rotational bias of mutant Tar$_{Ec}$ variants as described in **Figure 28**.

A

Name	208	209	210	211	212	213
AWYG (Wt)	A	W	Y	G	I	R
ALWA	A	L	W	A	I	R
AAWG	A	A	W	G	I	R
AGWA	A	G	W	A	I	R
AAWA	A	A	W	A	I	R
AAWL	A	A	W	L	I	R
AAWP	A	A	W	P	I	R
AWYA	A	W	Y	A	I	R
AWYL	A	W	Y	L	I	R
AWYP	A	W	Y	P	I	R

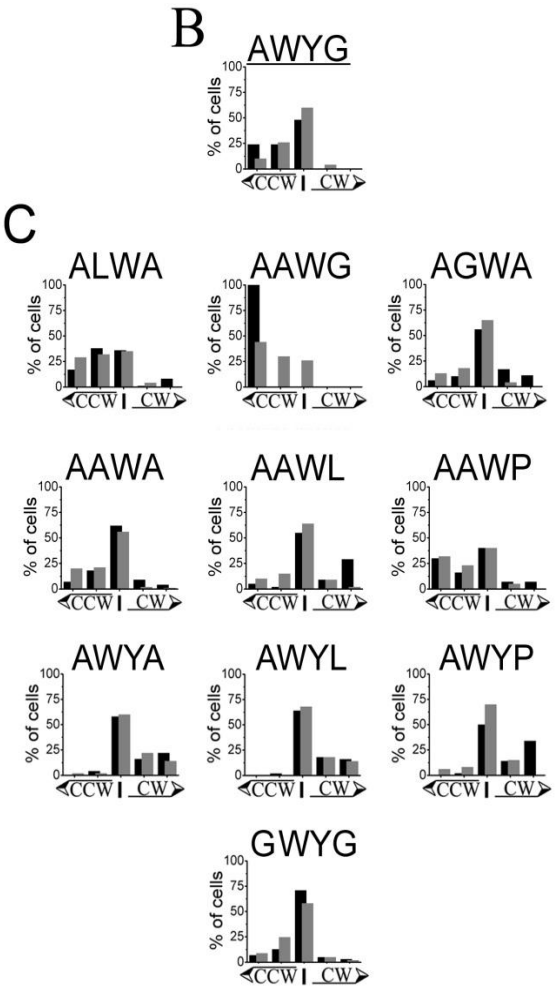

Figure 30. Flagellar rotational bias of cells expressing Tar_{Ec} variants substitutions at Trp-210, or substitutions at G211 in the cytoplasmic aromatic anchor. (A) Amino acid sequence of wild-type Tar_{Ec} and select mutant variants. Aromatic residues hare indicated with a shaded background. **(B)** Flagellar rotational bias of the wild-type Tar_{Ec} receptor as described in **Figure 28**. **(C)** Flagellar rotational bias of mutant Tar_{Ec} variants as described in **Figure 28**.

highest level of CW rotation was 74%. The wild-type (WY) receptor supported 34% CW rotation. Thus, there was a large gap between the signal output of "CCW -locked" receptors and the essentially wild-type or CW-biased receptors.

Support of CW rotation in strain VB13 (*cheR*$^+$*B*$^+$)

In strain VB13, the inherent signaling bias of mutant Tar$_{Ec}$ receptors can be offset by increasing or decreasing the level of covalent medication through the combined activities of CheR and CheB. The effectiveness of this mechanism is attested by the fact that all 53 examined in strain VB13 supported ≥20% CW rotation (**Figure 27**). (The rotational bias of some WX receptors, where X is any amino acid, were not determined in the *cheR*$^+$*B*$^+$ strain because they supported wild-type rotational biases in the Δ*cheRB* strain (*114*)). The wild-type (WY) receptor expressed in this strain supported 40% CW rotation, a slightly higher value than in strain HCB436. The highest level of CW rotation was 64%.

All of the receptors that produced CCW-locked behavior in strain HCB436 showed a significant level of CW signal output when adaptive methylation could occur. There was only a 10% decrease in the CW signal output of the receptors that were most CW-biased in strain when they were expressed in strain VB13. The distribution of CW percentages decreased over the ensemble of receptors from 0-74% in strain HCB436 to 20-64% in strain VB13 (**Figure 27**).

Ability of the mutant receptors to support aspartate chemotaxis

The chemotaxis ring formed by strain VB13 expressing wild-type Tar$_{Ec}$ expands

in minimal-aspartate semi-solid agar at a rate of 1.5 to 2.1 mm/hr at 30ºC (**Figure 31-33**). The variation is presumably due to slight differences in agar concentration or incubation temperature. Thus, for each set of measurements, the RER was set relative to an RER of 100% for wild-type Tar in the same experiment. The colony formed by the negative control, VB13 cells with the empty vector, expanded at only 0.1 mm/hr (~5% of the wild-type rate) under these conditions.

A number of the receptors supported aspartate taxis nearly as well or, in one case, better than the WY wild type. The highest RER (113%) was seen with the WF receptor. Overall, 26 of the 59 receptors (44%) supported RERs of ≥75%, and 37 out of 59 (63%) supported RERs of ≥50%. Of the 22 receptors that had CCW-locked signal output in strain HCB436, four (18%) supported RERs of ≥75%, and 13 (59%) supported RERs of ≥50%. These data demonstrate the effectiveness of adaptive methylation. They may also testify to the forgiving nature of the semi-solid agar assay, in which the chemotaxis ring is localized within a region in which there is a very sharp concentration gradient of aspartate at the edge of the expanding colony.

In the other half of the distribution, 16 of 59 receptors (27%) supported RERs of ≤50% and ten (17%) supported RERs of ≤25%. Of the 16, nine produced CCW-locked output in strain HCB436, three supported wild-type (30-49% CW) rotational biases, and five supported CW-biased rotation (≥50% CW). Of the bottom ten, six were CCW locked, one supported wild-type CW/CCW biases, and three had CW-biased signal output.

A striking feature of these data is that there is little correlation between the

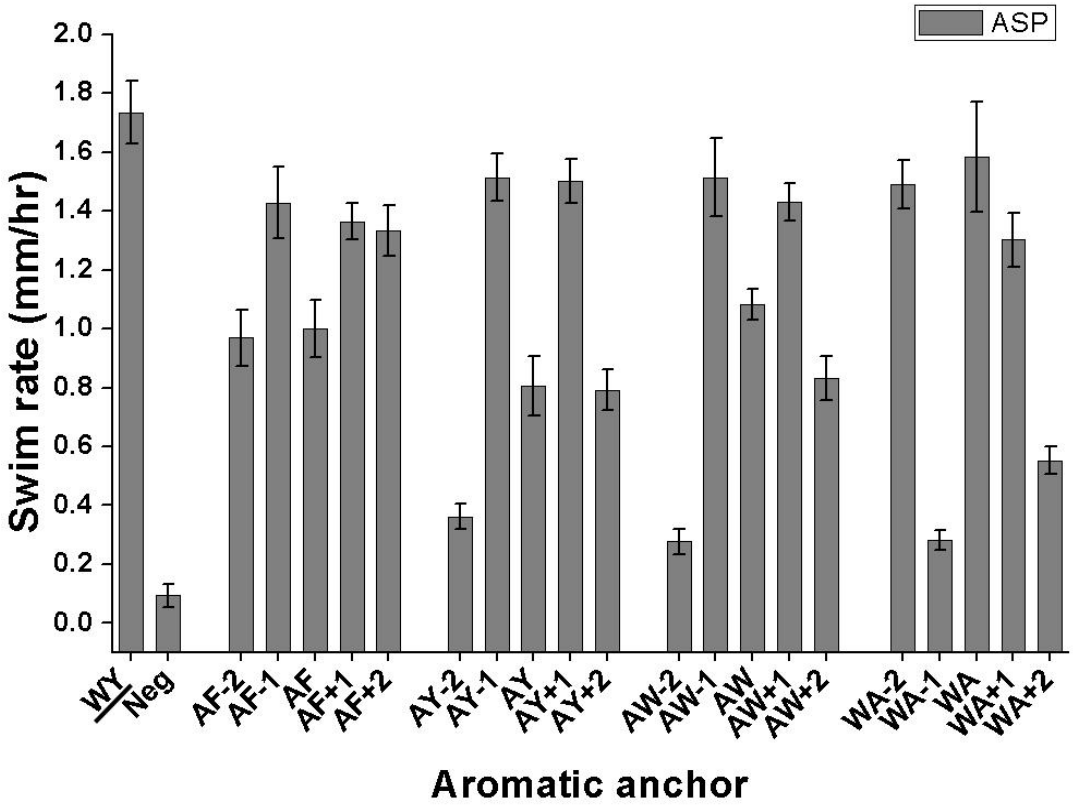

Figure 31. Chemotaxis ring formation in aspartate and maltose swim plates by cells expressing Tar$_{Ec}$ variants containing aromatic anchors with a single aromatic residue. VB13 (ΔT *cheR*$^+$*B*$^+$) cells expressing wild-type Tar$_{Ec}$ or different Tar$_{Ec}$ variants expressed from pRD200 (*68*) were inoculated into semi-solid agar containing aspartate. Plates were incubated at 30°C and measured after 8 h, when migratory rings first became visible. The ring diameter was measured every 4 hours thereafter, and the ring expansion rate (RER) was calculated in mm/hr. The error bars show the standard deviation of the mean for the RERs of $\geq$ 6 colonies. The wild-type anchor (WY) is underlined.

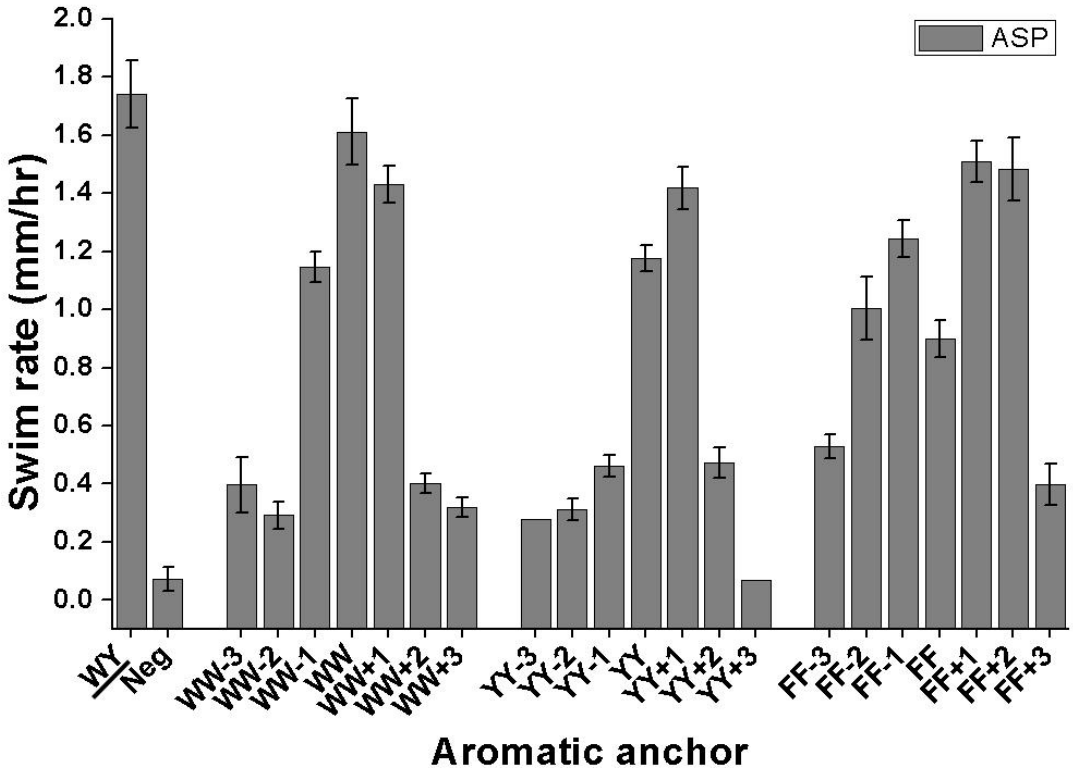

Figure 32. Chemotaxis ring formation in aspartate and maltose swim plates by cells expressing Tar_{Ec} variants containing aromatic anchors with two aromatic residues. VB13 (ΔT *cheR*$^+$*B*$^+$) cells expressing wild-type Tar_{Ec} or different Tar_{Ec} variants from pRD200 (*68*) were inoculated into semi-solid agar containing aspartate. Plates were incubated at 30°C and measured after 8 h, when migratory rings first became visible. The ring diameter was measured every 4 hours thereafter, and the RER was calculated in mm/hr. The error bars show the standard deviation of the mean for the expansion rates of ≥ 6 colonies. The wild-type anchor (WY) is underlined.

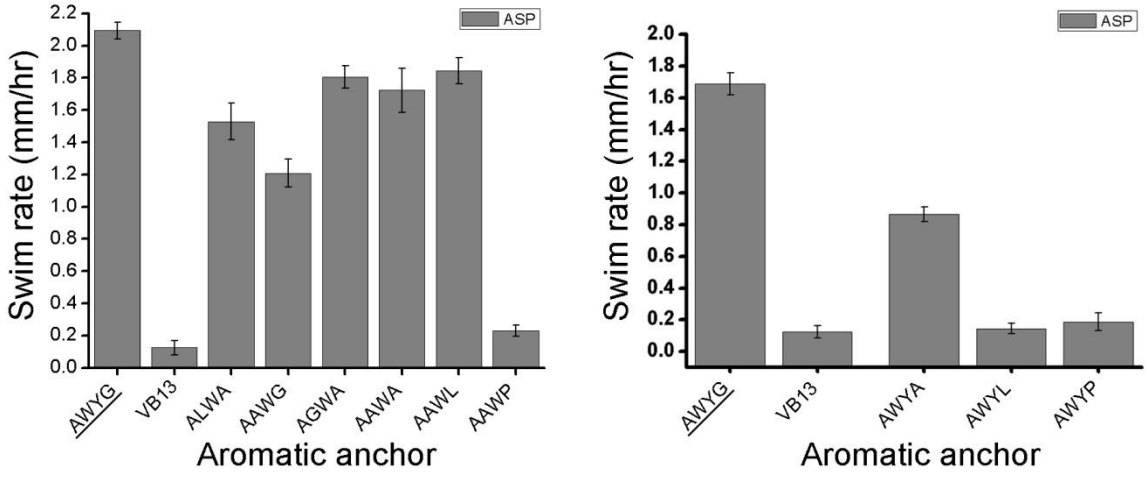

Figure 33. Chemotaxis ring formation in aspartate swim plates by cells expressing Tar_{Ec} variants containing a Trp-210 aromatic anchor or Gly-211 substitution. VB13 (ΔT *cheR*$^+$*B*$^+$) cells expressing wild-type Tar_{Ec} or different Tar_{Ec} variants from pRD200 (*68*) were inoculated into semi-solid agar containing aspartate. Plates were incubated at 30°C and measured after 8 h, when chemotaxis rings first became visible. The ring diameter was measured every 4 hours thereafter, and the migration rate was calculated in mm/hr. The error bars show the standard deviation of the mean for the expansion rates of ≥ 6 colonies. The wild-type anchor AWYG is underlined in each graph.

baseline signal output in the Δ*cheRB* strain and the ability to support aspartate chemotaxis in the *cheR*$^+$*B*$^+$ strain (**Figure 26**). The levels of CW rotation seen in the *cheR*$^+$*B*$^+$ strain also show no obvious correlation with the ability to support aspartate chemotaxis (**Figure 2**). The overall conclusion is that baseline CW signal output, a measure of the baseline intracellular CheY-P concentration, is a poor predictor of the ability to support aspartate chemotaxis.

Adaptive methylation determines whether a receptor can support aspartate chemotaxis

If receptor baseline signal output is not a good measure of receptor function in chemotaxis, what is? Presumably, it is the ability of the receptor to communicate ligand-induced conformational changes across the membrane. Although this can, in principle, be assayed directly with in vivo receptor-linked assays of CheA-kinase activity (Draheim, 2005), it is more conveniently assessed by determining whether a receptor is capable of changing its level of adaptive methylation in response to chemoeffectors.

The AAWP receptor, which produced essentially wild-type levels of CW rotation in both Δ*cheRB* and *cheR*$^+$*B*$^+$ cells (**Figures 26 and 27**), and the AWYL and AWYP receptors, which had a CW-biased signal output, were very defective for aspartate chemotaxis (RERs of ≤11%). All three of these receptors migrate as a single band in *cheR*$^+$*B*$^+$ cells both in the absence of chemoeffectors and after the addition of 100 mM aspartate or 10 mM $NiSO_4$ (**Figure 34**). This band corresponds to the QEQE modification state in which the receptors are originally made (**Figure 35**). The AWYA receptor, which also has a CW-biased signal output, supported 50% of the wild-type

Faithful rendition of gels seen so far

Currently working on publishable quality gels

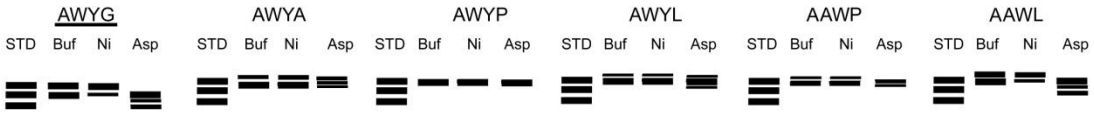

Figure 34. Steady-state patterns of covalent modification of the wild-type Tar_{Ec} receptors or Trp-210 receptors with Gly-211 substitutions in cells with an intact *cheRB* adaptation system. Proteins from VB13 (ΔT $cheR^{+}B^{+}$) cells expressing one of the Tar_{Ec} receptors from pRD200 were analyzed. Cells were exposed to buffer only, to 10 mM $NiSO_4$, or to 100 mM aspartate (Asp) for 20 min. A mixture of equal amounts receptors representing the unmodified (EEEE), partly modified (QEQE) and fully modified (QQQQ) forms of Tar_{Ec} (STD) was run for each receptor variant. The rate of migration during SDS-PAGE is related to the extent of modification, with the more-highly modified forms migrating at a faster rate. The wild-type (WY) is underlined.

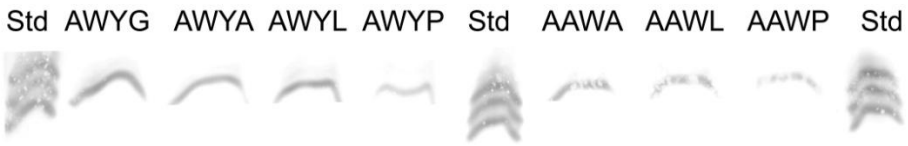

Figure 35. Steady-state patterns of covalent modification of the wild-type Tar_{Ec} receptors or Trp-210 receptors with Gly-211 substitutions in Δ*cheRB* cells. Proteins from HCB436 (ΔT Δ*cheRB*) cells expressing one of the Tar_{Ec} receptors from pRD200 were analyzed. Cells were exposed to buffer only for 20 min. A mixture of equal amounts receptors representing the unmodified (EEEE), partly modified (QEQE) and fully modified (QQQQ) forms of Tar_{Ec} (STD) was run for each receptor variant. The rate of migration during SDS-PAGE is related to the extent of modification, with the more-highly modified forms migrating at a faster rate. The wild-type (WY) is underlined.

RER in aspartate semi-solid agar, but it also did not change its state of covalent modification significantly in response to attractant or repellent (**Figure 34**).

The WW+2 receptor, which produced 61% CW rotation in the HCB436 strain, supported 30% CW rotation in strain VB13. This receptor was undermethylated in its baseline state in strain VB13 and showed only a small increase in methylation after addition of aspartate (**Figure 36**). The AW-2, WA-1, WW-2, WY-2, and YY-2 receptors, all of which have a CCW-locked signal output in strain HCB436, were heavily overmethylated in their baseline state in strain VB13 (**Figures 36 and 37**). As a result, they all support between 20% and 30% CW rotation in that strain. However, because of their high baseline level of methylation, they were able to increase methylation only slightly after addition of aspartate. Thus, they have a limited dynamic range in their attractant responses and, as a result, impaired performance in aspartate chemotaxis.

Discussion

The dynamic bundle model of signaling (*137, 138*) suggests that the stability of the HAMP domain is regulated by its attachment to TM2 via the control cable (*57, 138*). Previous experimental data (*67-69*) and recent computer simulations (*55*) suggest that the aromatic anchor at the cytoplasmic end of TM2 is essential for maintenance of normal signal output from Tar_{Ec}. The work presented here builds upon previous results that demonstrate the importance of the residue composition of the aromatic anchor of Tar_{Ec} (*114*) and the position of the aromatic anchor (*69*).

We examined in aggregate 59 receptors with different amino acid sequences

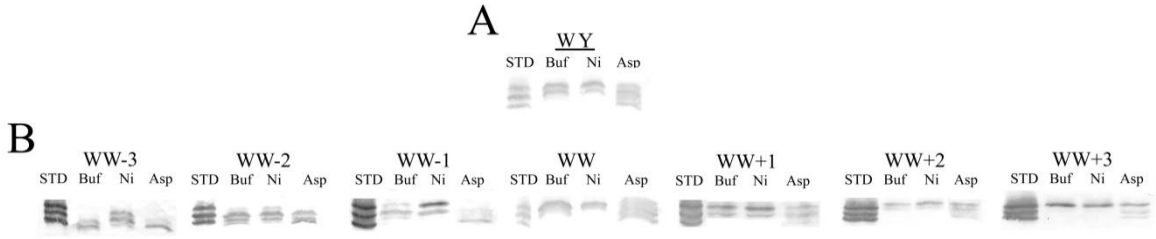

Figure 36. Steady-state patterns of covalent modification of the Tar_{Ec} receptors with a tandem Trp aromatic anchor in cells with an intact *cheRB* adaptation system. Proteins from VB13 (ΔT $cheR^{+}B^{+}$) cells expressing one of the Tar_{Ec} receptors from pRD200 were analyzed. Cells were exposed to buffer only, to 10 mM $NiSO_4$, or to 100 mM aspartate (Asp) for 20 min. A mixture of equal amounts receptors representing the unmodified (EEEE), partly modified (QEQE) and fully modified (QQQQ) forms of Tar_{Ec} (STD) was run for each receptor variant. The rate of migration during SDS-PAGE is related to the extent of modification, with the more-highly modified forms migrating at a faster rate. The wild-type (WY) is underlined.

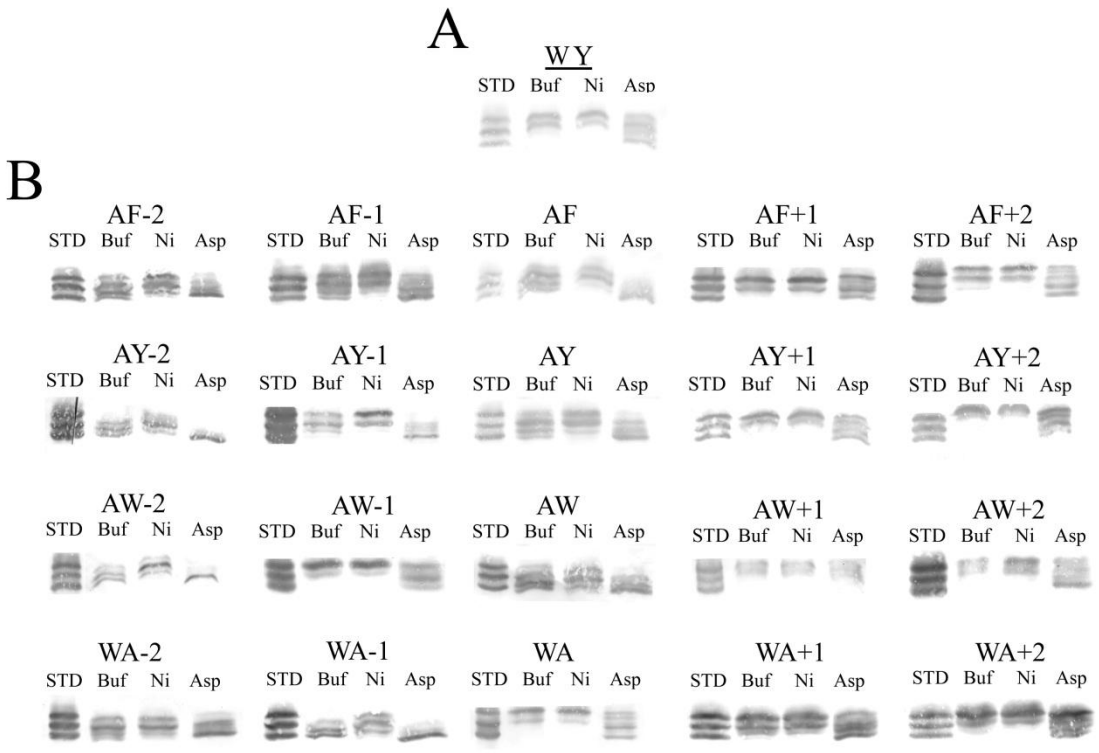

Figure 37. Steady-state patterns of covalent modification of the Tar_{Ec} receptors with a single aromatic residue in the aromatic anchor in cells with the *cheRB* adaptation system. Proteins from VB13 (ΔT $cheR^{+}B^{+}$) cells expressing one of the Tar_{Ec} receptors from pRD200 were analyzed. Conditions were as described in the legend to **Figure 36**.

comprising residues 207-212 of Tar_{Ec}. Twenty of these receptors have been described previously (*68, 69, 114*); the remainder were constructed specifically for this study. To make sense of the large amount of data that were generated, it is useful to consider the different phenotypes that were observed and then attempt to make some generalizations about the properties of the TM2/HAMP connection.

CCW-locked receptors

A total of 22 of the mutant receptors had a CCW-locked signal output (<2% CW rotation) in strain HCB436 (Δ*cheRB*; **Figure 26** and **Table 5**). All of these receptors were overmethylated in strain VB13 ($cheR^+B^+$) relative to the wild-type receptor, although the extent of overmethylation varied (**Figures 34, 36, 37**). The increased level of methylation allowed all of the mutant receptors to produce a significant CW signal output in strain VB13 (**Figures 27, 38-40** and **Table 5**), but the different receptors varied enormously in their ability to support aspartate chemotaxis in semi-solid agar. The six most defective receptors (chemotaxis ring diameters ≤25% of the wild type) all had either Trp or Tyr, the two amphipathic aromatic amino acids, as residue 208 and had no aromatic residue after position 208. The residue at position 207 seems to have little effect, as cells expressing the WA-2 receptor supported an RER of 85%. The AA receptor, which has no aromatic residue in positions 207 to 212, had an RER of 80%.

It is striking that having any residue other than Trp at position 209, any aromatic residue at position 210, and Gly at position 211 leads to CCW-locked signal output in Δ*cheRB* HCB436 cells, even though an intact adaptation system in strain VB13 can

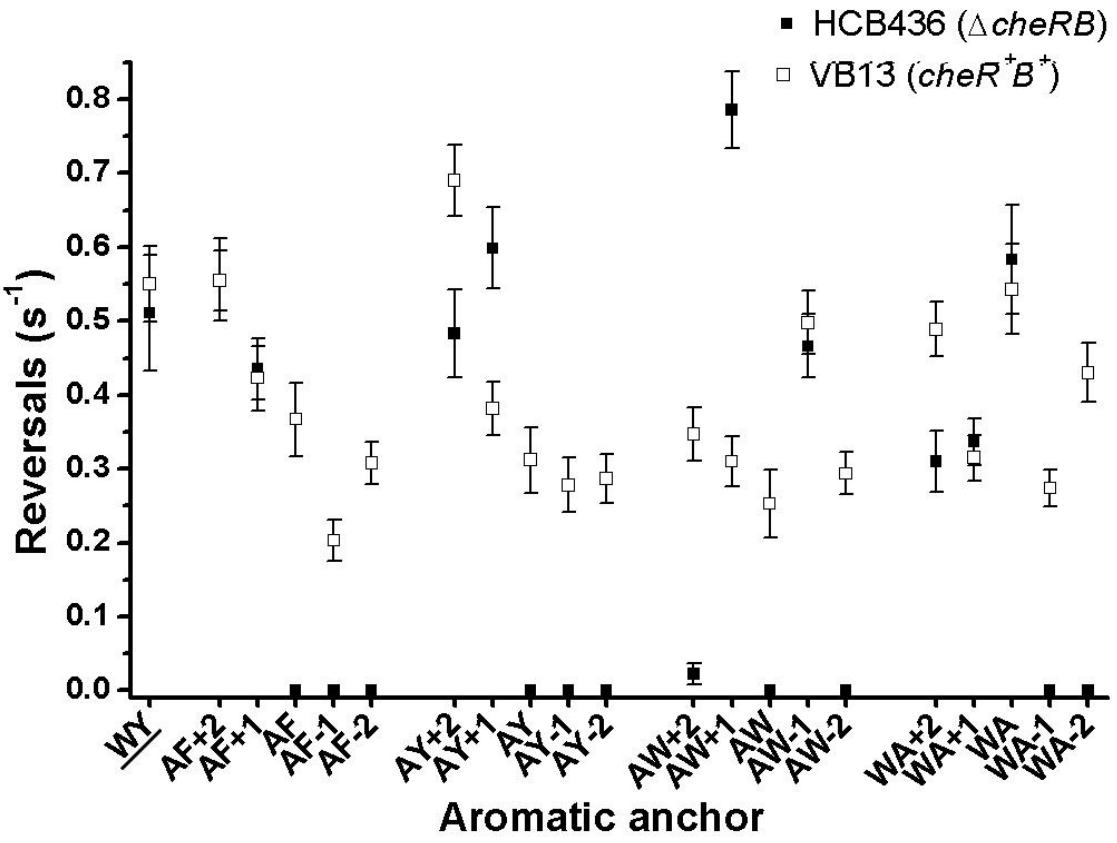

Figure 38. Mean Reversal Frequency (MRF) of tethered cells expressing Tar_{Ec} receptors with wild-type or mutant aromatic anchors. The number of flagellar reversals were tabulated from the tethered VB13 (ΔT *cheR*$^+$*B*$^+$) or HCB436 (ΔT Δ*cheRB*) cells whose rotational bias is shown in **Figures 26 and 27**. Each data point represents the mean number of reversals for one hundred cells examined for 20 sec. The error bars represent the standard error of the mean. The wild-type (WY) aromatic anchor found in Tar_{Ec} is underlined.

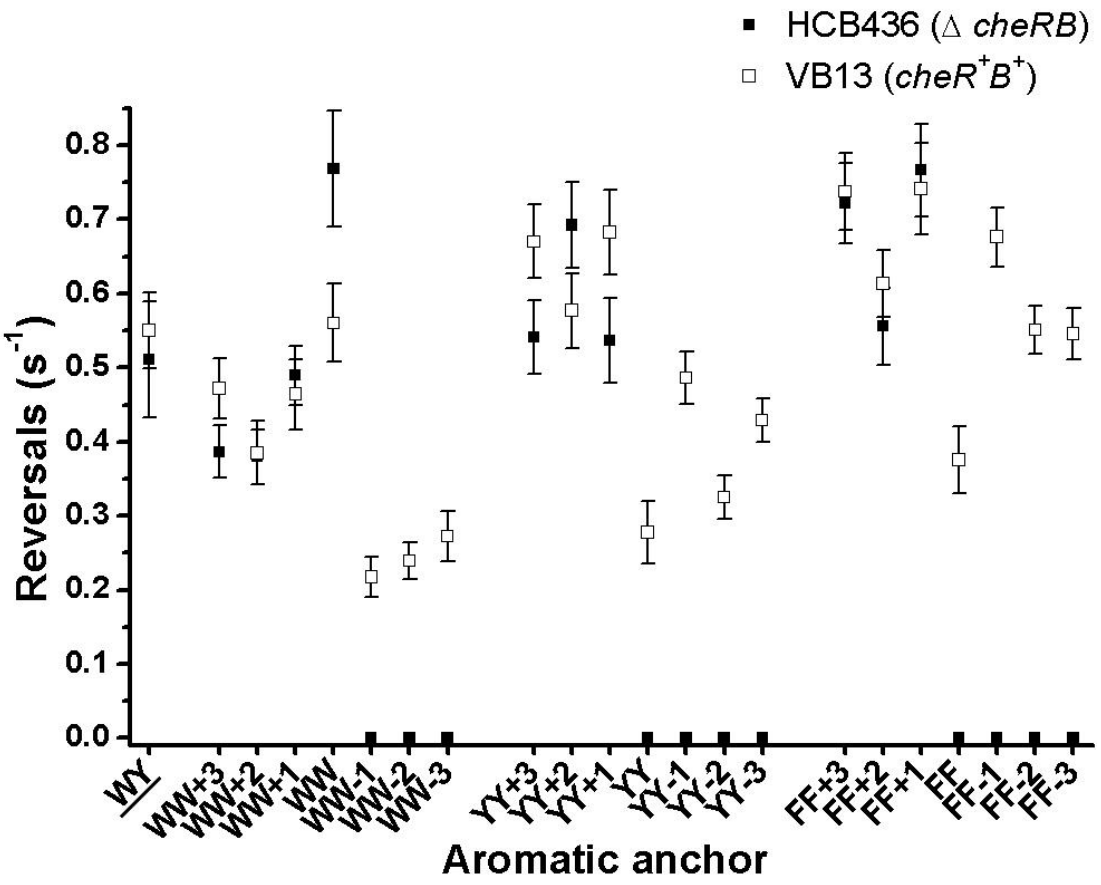

Figure 39. Mean Reversal Frequency (MRF) of tethered cells expressing Tar_{Ec} receptors with wild-type or mutants with anchors containing two aromatic residues. The number of flagellar reversals were tabulated from the tethered VB13 (ΔT *cheR*$^+$*B*$^+$) or HCB436 (ΔT Δ*cheRB*) cells as in **Figure 38**. The wild-type (WY) aromatic anchor found in Tar_{Ec} is underlined.

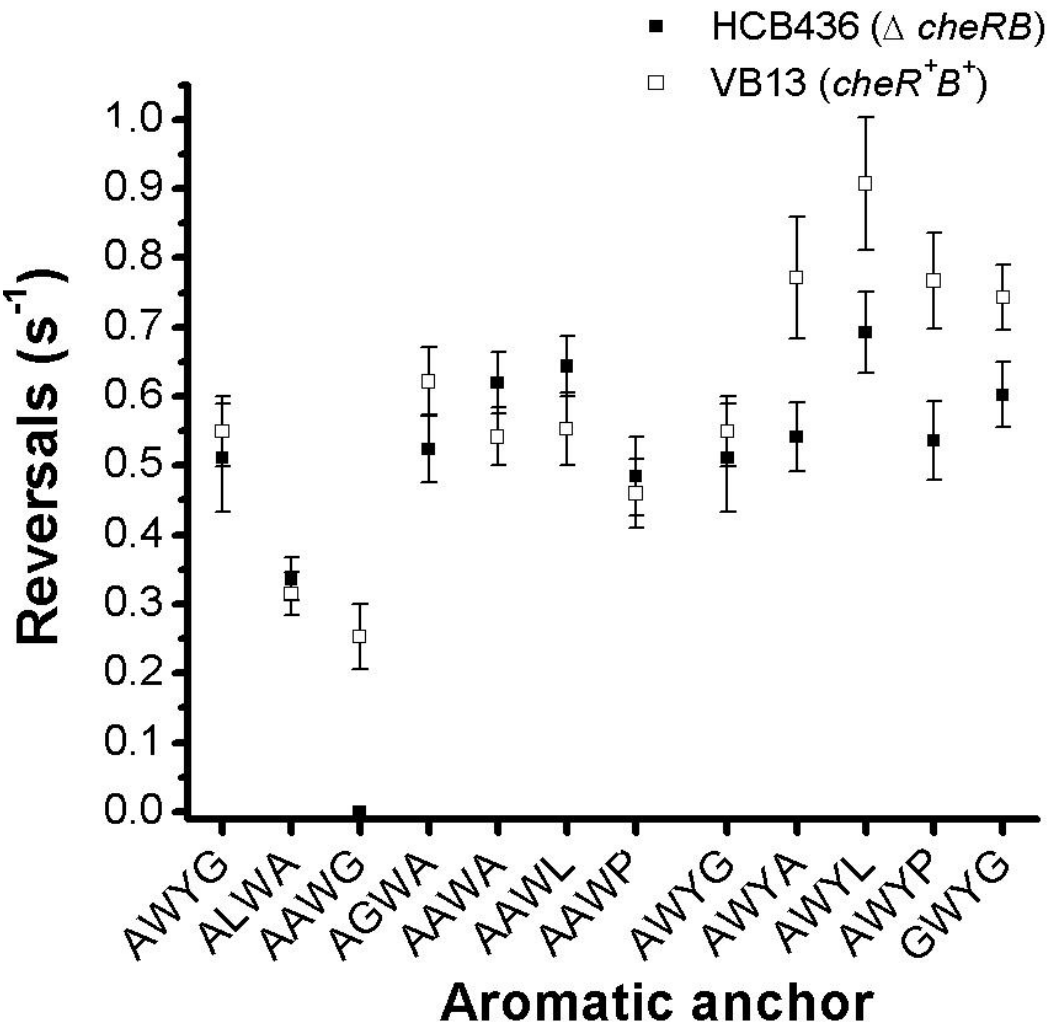

Figure 40. Mean Reversal Frequency (MRF) of tethered cells expressing Tar_{Ec} variants containing a Trp-210 aromatic anchor. The number of flagellar reversals were tabulated from the tethered VB13 (ΔT *cheR*$^+$*B*$^+$) or HCB436 (ΔT Δ*cheRB*) cells whose rotational bias is shown in **Figure 26 and 27**. Each data point represents the mean number as in **Figure 38**. The wild-type (WY) aromatic anchor found in Tar_{Ec} is underlined.

restore CW signaling and reasonably good aspartate taxis to many of these strains (**Figures 38-40**). The only CCW-locked receptor without Gly as residue 211 was AW+2, which has Ala at position 211 and Trp at position 212. Trp-212 may be displaced so far from the hydrophobic/hydrophilic membrane interface that it can no longer interact with the membrane interface. It still must have some influence in orienting TM2 in an attractant mimicking position, however, because the AF+2 and AY+2 receptors both support normal levels of CW rotation in HCB435 cells.

CW-biased receptors

The strongly CW-biased receptors (>50% CW signal output in strain HCB436) represent a rather mixed bag, both with respect to the sequence of residues 207-212 and their ability to support aspartate chemotaxis. Two of the CW-biased receptors, with the sequences AWYL and AWYP at residues 208-211, were among the most defective of any of the mutant receptors in aspartate chemotaxis (9% and 11% of the wild-type ring RERs, respectively). Both of these receptors shared the property of being unable to carry out adaptive covalent modification (**Figure 34**) as well as having almost identical CW/CCW signal outputs in the *cheR*$^+$*B*$^+$ and Δ*cheRB* strains (**Table 5**). The AWYA receptor was somewhat better at supporting aspartate chemotaxis (an RER of 50%), but it shared the property of showing a negligible change from the initial QEQE modification state under any conditions when expressed in strain VB13 (**Figure 34**).

The WW+2 receptor was also quite defective in mediating aspartate chemotaxis, but it showed a different response to the adaptation system. Demethylation/deamidation

could compensate for its intrinsically CW-biased signal output in Δ*cheRB* cells (**Figure 34**); it was apparently a defect in increasing the level of methylation enough in response to addition of aspartate that limited the dynamic range of the chemotaxis response. The remaining receptors with CW-biased signal output ranged from poor (the YY+2 receptor, with an RER of 27%) to almost normal (the WY+1 receptor, with an RER of 95%) in supporting aspartate chemotaxis.

A receptor with normal baseline output but extremely defective chemotaxis

Most of the receptors that supported 30-50% CW rotation in Δ*cheRB* cells also had RERs of ≥75%. Exceptions were the WA+2 and AY+2 receptors, with RERs of 32% and 46%, respectively, and most notably the AAWP receptor, which had an RER of 11% (**Table 5**). Like the AWYL, AWYP, and AWYA receptors, the AAWP receptor seemed to be stuck in the QEQE state under all conditions. Perhaps some distortion of the TM2-HAMP connection in these receptors is transferred to the adaptation domain in such a way that the receptor becomes a poor substrate for the adaptation enzymes.

Which TM2-HAMP connector sequences support good aspartate chemotaxis?

Of the 59 Tar_{Ec} receptors tested, 26 supported RERs of ≥75% (**Table 5**). Of these, in the Δ*cheRB* strain four led to CCW-locked signal output, six led to CW-biased signal output, and 16 led to wild-type signal output. One mutant (the WF receptor) actually had a higher RER (~113%) than wild type, and 4 others had RERs of > 90%.

If we define "wild-type" behavior to be 30-50% CW rotation in Δ*cheRB* cells and an RER of ≥75%, 16 receptors fall into this category. Of these, nine have a Trp residue at position 209 and a Gly residue at position 211. The residue at position 210 seems to make relatively little difference (Table 1) if it is flanked by Trp and Gly, at least in the behaviors we have tested. The remaining seven receptors all lack Gly-211, having it replaced with Ala in the AF+1, WA+1, and AAWA, receptors, with Leu in the AAWL receptor, and with an aromatic residue in the AF+1, AW+1 and AY+1 receptors.

The importance of position 211

The importance of Trp-209 was established in previous studies (*68, 114*). The role of Gly-211 in receptor function in Tar_{Ec} was not anticipated. A recent study (*57*) demonstrated that the equivalent Gly-213 residue in the closely related chemoreceptor *E. coli* Tsr (Tsr_{Ec}) could be replaced with any amino acid other than Tyr without having a significant effect on serine chemotaxis. Even the Tyr replacement still allowed some level of serine taxis. Here, we found that the replacement of Gly-211 with Ala, and to an even greater extent with Leu and Pro, in the AWYA, AWYL, and AWYP receptors seriously disrupted aspartate chemotaxis and led to a CW signaling bias. Whether this is because Tsr_{Ec} has a Phe rather than a Tyr preceding the Gly residue or for some other reason is not known.

The situation is complicated further by the observation that receptors with the sequences ALWA, AAWA, and AAWL at residues 208-211 function relatively normally, as do some receptors in which Gly-211 is replaced by an aromatic residue.

Thus, Gly-211 is not crucial in every sequence context. The AAWP receptor represents a special case; it is almost totally defective in aspartate chemotaxis, but it supports a normal CW/CCW signal output in both HCB436 and VB13 cells. It would seem that Pro is especially disruptive at position 211, perhaps because it has the most extreme effect in constraining the flexibility of the TM2-HAMP connector.

A model for aromatic anchor function

Our previous model (*114*) proposed that an innate force imposed by the periplasmic domain and directed toward the cytoplasm caused by is counterbalanced by the Trp residue positioned at the cytoplasmic interface. This model of signal transduction through TM2 does not take into account the importance of the residue Gly-211. Past observations of changes in signal output (*68, 69, 114*) can be explained as a majority of functional mutants replace the residue Gly-211. **Figure 41** takes the possible role of Gly-211 as a critical transition point in signal transduction into account. In our model, Gly-211 acts as a flexible joint that alters the helical character of the connector cable that links TM2 to AS1 of the HAMP domain (**Figure 41A**). The substitution of other residues, such as Ala, at position 211 decreases the flexibility of the connector cable and leads to an increase in kinase stimulation and a reduction in responsiveness to attractant stimuli (**Figure 41B**). The G211L and G211P substitutions leave the signaling domain in its default CW-signaling state (**Figure 41C**), perhaps by increasing the helix rigidity.

In the Trp-210 mutants, the Trp residue is not in its optimal position and pulls TM2 toward the periplasm. These mutants have a slight decrease in their baseline

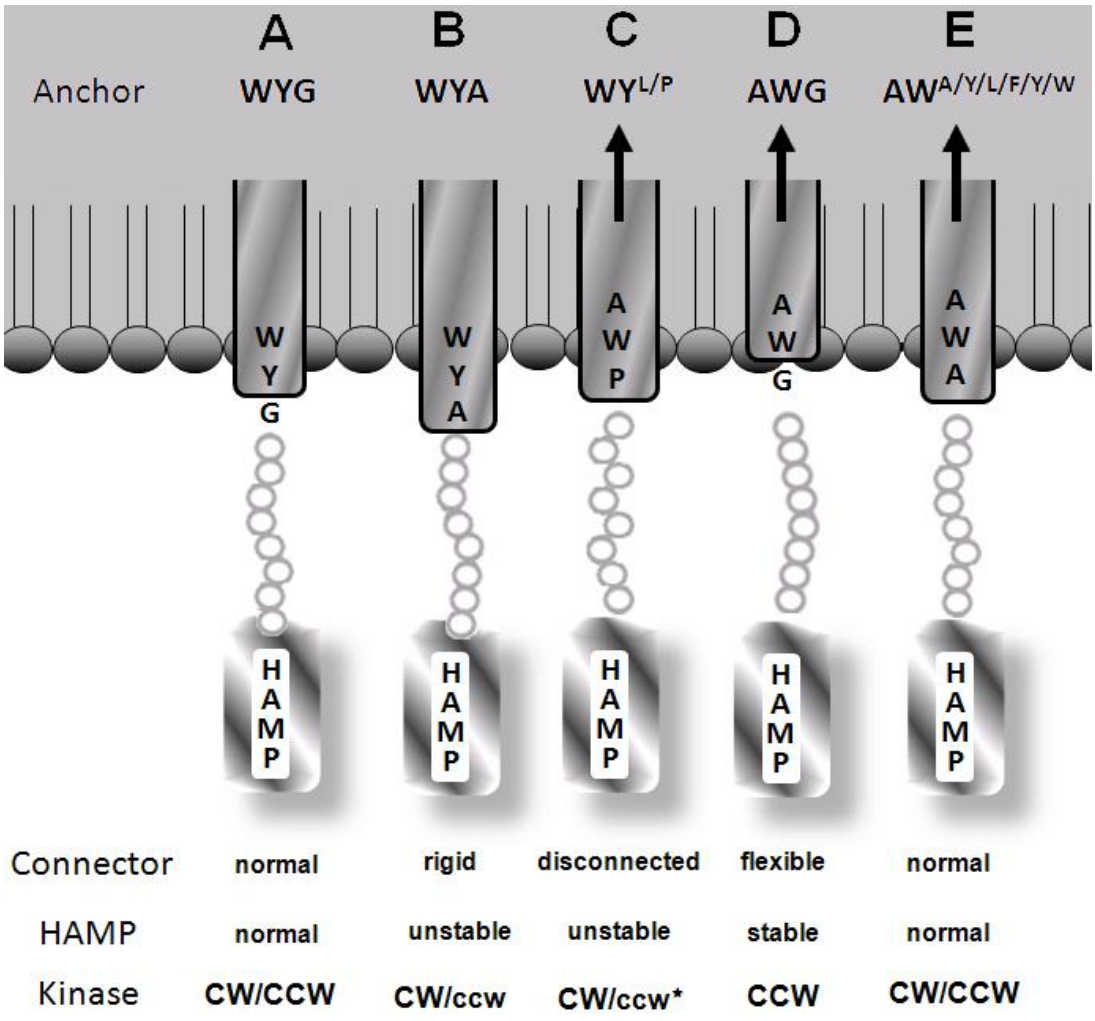

Figure 41. Model of signal transduction through TM2 with wild-type and mutant aromatic anchors. **(A)** The glycine at position 211 acts as a flexible joint altering the helical character of the alpha helix of TM2 between TM2 and the connector cable that links TM2 to AS1 of the HAMP domain **(B)** The G211A mutation decreases the flexibility of the connector cable leading to an increase in kinase activity and a reduction in attractant stimuli **(C)** Mutations such as G211L or G211P eliminate response to attractant and leave the signal output domain at its default CW state. **(D)** In Trp-210 mutants, the Trp residue is not in its optimal position and exerts a force on TM2 pulling it towards the periplasm (black arrow). In Trp-210 with G-211, the TM2 helix ends prematurely, leading to an altered tension on the control cable that disrupts its helicity and leads to increased flexibility and a CCW-locked phenotype in cells lacking adaptive methylation. **(E)** Substitutions of Gly-211 in a mutant with a Trp-210 anchor extend TM2, thereby increasing the rigidity of the connector helix and restoring wild-type function.

methylation level. In Trp-210/G-211 receptor, the TM2 helix ends prematurely, leading to an altered tension on the control cable and disruption of its normal helicity, perhaps leading to increased flexibility and a CCW-locked phenotype in cells lacking adaptive methylation (**Figure 41D**). Substitutions of Gly-211 in a mutant with Trp-210 extend TM2 and thus increase the rigidity of the connector helix. This change restores wild-type baseline signaling and allows the adaptive system to function properly (**Figure 41E**).

Even though the Tar_{Ec} and Tsr_{Ec} receptors are quite similar, they apparently have somewhat different mechanisms of transmembrane signal transduction. It seems likely that each receptor has evolved to optimize its signal function with respect to its relative abundance and its range of chemoeffector ligands. Thus, any attempts to extrapolate data obtained with one receptor to another must be done with caution and with empirical tests of the generality of conclusions.

Implications for transmembrane signaling in two-component sensor kinases

Many bacterial transmembrane histidine protein kinases (HPKs) have aromatic residues at the cytoplasmic end of TM2 (*68*). **Table 6** lists all HPKs in which a functional HAMP domain has been proven to exist through *in vivo* or *in vitro* assays. Our previous studies and the current work suggest that a large number of different configurations of the cytoplasmic aromatic anchor are compatible with function. What is striking is that the residue composition and position of the aromatic anchor can bias signaling either toward the off (kinase-inhibiting) or on (kinase-stimulating) state. In chemoreceptors, these biases can, to a large extent, be offset by the adaptation system

and appear as strong phenotypes only in an adaptation-deficient Δ*cheRB* strain. Sensor kinases, which generally lack adaptation capability and mediate chronic rather than rapidly changing chemical signals, may be particularly sensitive to the exact configuration of their aromatic anchors.

If the statement in the last sentence of the preceding paragraph is true, it may be possible to predict the baseline and ligand-stimulated signaling states of HPKs of unknown function based on the information presented here. It may also be possible to tune the sensitivities, and even the baseline on or off states, of HPKs by manipulation of their aromatic anchors and the precise sequence contexts in which those anchors exist. It is notable that only the Tar and Tsr receptors show the motif of two aromatic residues followed by a Gly residue and that even in Tsr the Gly residue seems not be essential. We hope that the results reported here will find general application in the study of transmembrane signaling by a wide variety of bacterial membrane-spanning receptors.

Gene	Ligands	-2	-1	1	2	3	4	5	6	7	8	9	10	11	12	13	14	15	16	17	18	19	+1	+2	+3	+4	+5	+6	+7	+8	+9
Tar	Asp/Mal	A	Q	W	Q	L	A	V	I	A	L	V	V	V	L	I	L	L	V	A	W	Y	G	I	R	R	M	L	L	T	P
Tsr	Ser/AI-2	A	M	W	I	L	V	G	V	M	I	V	V	L	A	V	I	F	A	V	W	F	G	I	K	A	S	L	V	A	P
Trg	Rib/Gal	G	G	M	F	M	I	G	A	F	V	L	A	L	V	M	T	L	I	T	F	M	V	L	R	R	I	V	I	R	P
Tap	Pep/Pyr	A	L	V	F	I	S	M	I	I	V	A	A	I	Y	I	S	S	A	L	W	W	T	R	K	M	I	V	Q	-	P
PhoQ	Mg^{2+}	W	S	W	F	I	Y	V	L	S	A	N	L	L	L	V	I	P	L	L	W	V	A	A	W	W	S	L	R	-	P
CpxA	Misfold prot.	D	R	P	L	L	L	L	I	V	T	M	L	V	S	T	P	L	L	L	W	L	A	W	S	L	A	K	-	-	P
EnvZ	Str/MzrA	F	S	P	L	F	R	Y	T	L	A	I	M	L	L	A	I	G	G	A	W	L	F	I	R	I	Q	N	R	-	P
NarQ	NO_3 NO_2	M	L	L	V	V	A	I	S	L	A	G	G	I	G	I	F	T	L	V	F	F	T	L	R	R	I	R	H	Q	V
NarX	NO_3 NO_2	L	V	H	R	V	M	A	V	F	M	A	L	L	L	V	F	T	I	I	W	L	R	A	R	L	L	Q	-	-	P
TorS	TAMO	Q	Y	S	L	L	L	L	G	M	V	S	L	C	A	L	I	L	I	L	W	R	V	V	Y	R	S	V	T	R	P
QseC	AI-2	I	V	A	G	Q	L	I	P	W	L	V	A	L	P	I	M	L	I	I	M	M	V	L	L	G	R	E	L	A	P
CusS	Cu	L	M	N	K	L	I	M	T	A	S	V	I	S	I	L	I	V	F	I	V	L	L	A	V	H	K	G	H	A	P
QseE	Unknown	G	Q	Y	F	G	W	Q	S	L	V	L	F	L	V	S	L	V	M	V	L	L	F	T	R	M	I	I	G	-	P
BarA	Unknown	I	F	I	S	S	V	M	M	L	F	C	I	G	I	A	L	I	F	G	W	R	L	M	R	D	V	T	G	-	P
BaeS*	Unknown	R	Q	T	S	W	L	I	V	A	L	A	T	L	L	A	A	L	A	T	F	L	L	A	R	G	L	L	A	-	P
BasS*	Unknown	V	A	S	L	I	V	P	G	V	F	M	V	S	L	T	L	F	I	C	Y	Q	A	V	R	R	I	T	R	-	P
CreC	Unknown	L	W	A	S	A	I	L	L	G	I	A	L	V	I	G	A	G	M	V	W	W	I	N	R	S	I	A	R	L	T
EvgS*	Unknown	E	Q	F	Y	I	V	T	T	L	S	V	L	L	V	G	S	S	L	L	W	G	F	Y	L	L	R	S	V	R	R
NtrB*	Unknown	R	I	I	I	V	L	T	A	G	L	L	I	S	L	L	L	I	V	L	F	S	R	R	L	S	A	N	I	D	I
RstB*	Unknown	L	D	I	A	L	I	A	F	I	A	I	S	L	A	F	P	V	F	I	W	M	R	P	H	W	Q	D	M	L	K
YedV*	Unknown	E	Q	Y	K	I	N	S	I	I	I	C	I	V	A	I	V	L	C	S	V	L	S	P	L	L	I	R	T	G	L

Table 6. Alignment of all known functional *E. coli* two component system receptors that contain only a HAMP domain. Functional two component system receptors that contain a HAMP domain and/or PAS domain were excluded from this alignment. The conserved Pro residue at the N-terminus of the first amphipathic helix (AS1) of the linker region provided the reference point for the alignment. Common motifs such as aromatic residues at the C-terminal region of TM2, and basic residues in the linker are seen among most receptors. N-terminal aromatic residues are present in most receptors but are not as strictly conserved. Genes expressing receptors with known ligands are indicated with the ligand abbreviated or if the ligand of the receptor is not known it is listed as unknown. Receptors without an asterisk have been shown to function *in vivo*, while receptors with an asterisk have only been shown to function *in vitro*. Aromatic residues near the membrane interface regions are indicated with white text with a black background while all Pro residues in the alignment area shown are indicated as black text on a grey background. The figure shows the hypothetical buried TM2 region indicated as residue 1 to residue 18 and is enclosed in a boxed. Ligand abbreviations are aspartate (Asp), maltose (Mal), Serine (Ser), autoinducer 2 (AI-2), ribose (Rib), galactose (Gal), dipeptides (Pep), pyrimidines (Pyr), magnesium ions (Mg^{2+}), osmotic stress (str), the protein MzrA (MzrA), nitrate (NO_3^-), Nitrite (NO_2^-), trimethylamine-N-oxide (TMAO), and copper ions (Cu).

CHAPTER IV

CONTRIBUTION OF THE PERIPLASMIC TRYPTOPHAN AROMATIC ANCHOR TO THE OUTPUT OF THE ASPARTATE/MALTOSE CHEMORECEPTOR TAR OF *ESCHERICHIA COLI*

Overview

The importance of aromatic residue composition in transmembrane helix 2 (TM2) of the Tar chemoreceptor at the membrane interface at the cytoplasmic side of the lipid bilayer was studied in the previous two chapters. However, there is also a Trp residue in TM2 at the periplasmic side of the ligand bilayer. The role of this aromatic residue in propagating a signal or maintaining TM2 in the correct position has not been well characterized. This chapter covers experiments that were conducted to obtain some understanding of the importance of this aromatic residue and the effects of a limited series of substitutions at this position.

Results

Position of the periplasmic Trp residue(s) has minor effect of the output of the receptor

Changes in the position of the periplasmic Trp residue had little effect on the swim rate except at the +2 offset, for which there was a greater than 50% reduction in chemotactic ring migration rate and at the -3 position, where there was an ~50% reduction in migration rate (**Figure 42**). Analysis of tethered cells revealed wild-type patterns if the Trp residue was moved only one residue from its wild-type position. Any additional increase in the displacement caused the cells to become locked in a CCW bias

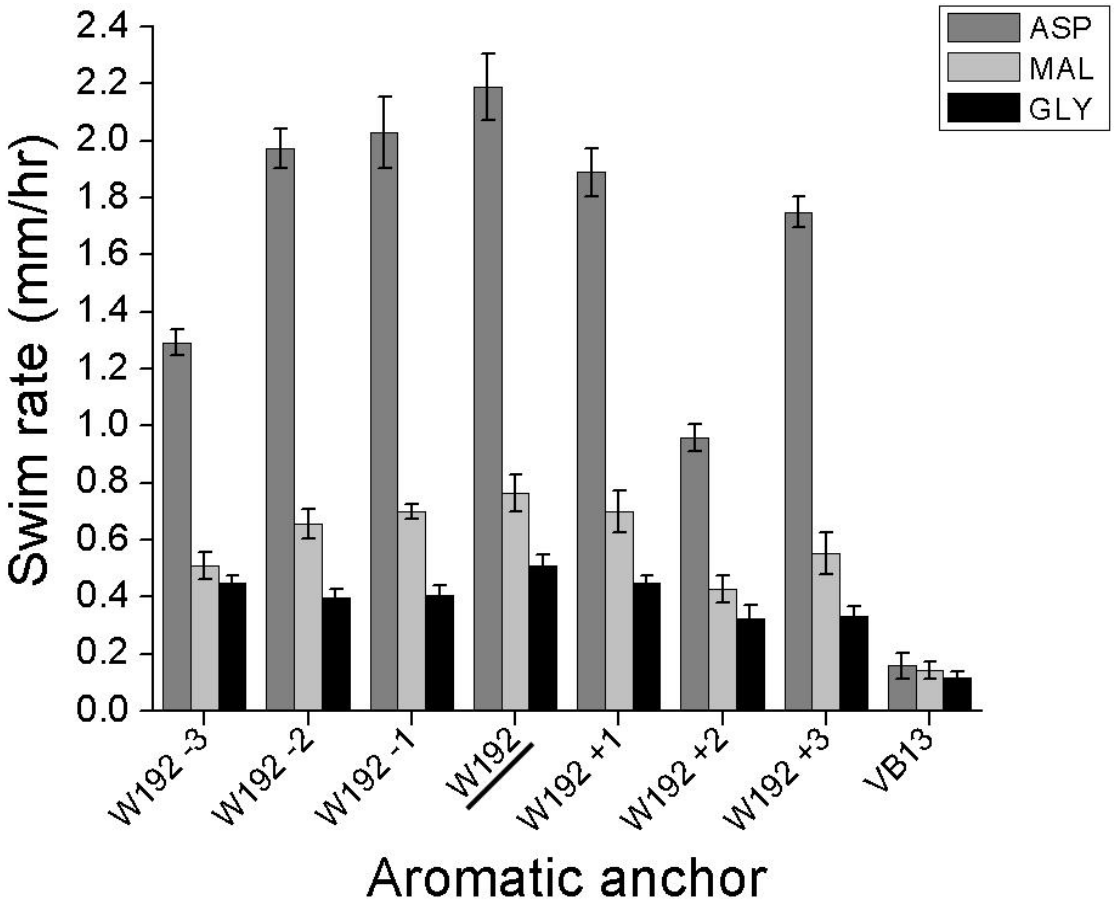

Figure 42. Chemotaxis ring formation in aspartate, maltose, and glycerol swim plates by cells expressing Tar_{Ec} with W192 shifted to different positions. VB13 (ΔT *cheR*$^+$*B*$^+$) cells expressing wild-type Tar_{Ec} or different Tar_{Ec} variants from pRD200 (*68*) were inoculated into semi-solid agar containing aspartate, maltose, or glycerol. Plates were incubated at 30°C and measured after 8 hours, when migratory rings first became visible. The ring diameter was measured every 4 hours thereafter, and the migration rate was calculated in mm/hr. The error bars show the standard deviation of the mean for the expansion rates of ≥ 6 colonies. The wild-type anchor (W192) is underlined.

when they lacked the adaptation system, except for the +3 shift, for which a majority of the cells were locked CCW but retained some CW rotation (**Figure 43**). The mean reversal frequencies (MRFs) of mutants with a single-residue displacement like that of the wild-type. As the distance of displacement from the wild-type position increases, the MRF decreased (**Figure 44**).

Substitution of each Gln residue flanking the periplasmic Trp residue with a Trp residue produces a tandem Trp-Trp anchor. Each substitution was carried out in a receptor with a wild-type cytoplasmic anchor (Trp-209 Tyr-210) and in a receptor with an Ala-Ala substitution at these two positions. Analysis of swim plates indicated that Tar with a Trp-Trp periplasmic anchor and a wild-type cytoplasmic anchor responds to attractants like wild-type Tar. Receptors with wither the 191-192 or 192-193 Trp-Trp periplasmic anchor and an Ala-Ala cytoplasmic anchor showed a greater than 50% reduction in chemotactic ring migration rate with aspartate (**Figure 45**). These mutants have a similar swarm rate as the Ala-Ala cytoplasmic tandem receptor with a wild-type Trp-192 (**Figure 20**). Both 191-192 and 192-193 Trp-Trp periplasmic anchor with Ala-Ala cytoplasmic anchor had a locked CCW phenotype in cells lacking adapative methylation (data not shown).

Removal of the periplasmic Trp leads to an increase in CCW output of the receptor

Two mutant cytoplasmic anchors, Ala-Ala and Ala-Trp, were studied in combination with the W192A substitution to determine how Trp-192 affects signal output. The rate of chemotactic ring migration in semi-solid agar was approximately the

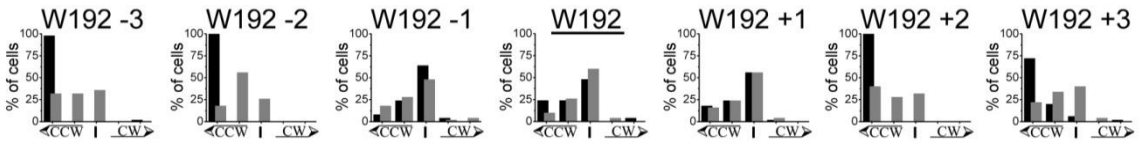

Figure 43. Flagellar rotational bias of cells expressing Tar_{Ec} with W192 shifted to different positions. VB13 (ΔT cheR+B+) or HCB436 (ΔT ΔcheRB) cells expressing the wild-type or mutant TarEc variants from pRD200 (47), posessing a C-terminal epitope V5 tag were tethered, observed for 20 sec and assigned to one of five categories based on their apparent flagellar rotational bias. From left to right, these categories are designated: counterclockwise rotation with no switching (CCW only), counterclockwise-biased with frequent switching (CCW), frequent reversing with no apparent bias (CCW/CW), clockwise-biased with frequent switching (CW) and clockwise rotation with no switching (CW only). Results from VB13 cells are depicted as grey bars in the foreground while results from HCB436 are depicted as black bars in the background. Each histogram contains the classification of fifty VB13 and fifty HCB436 cells expressing each TarEc variant. The wild-type aromatic anchor found in Tar_{Ec} is underlined.

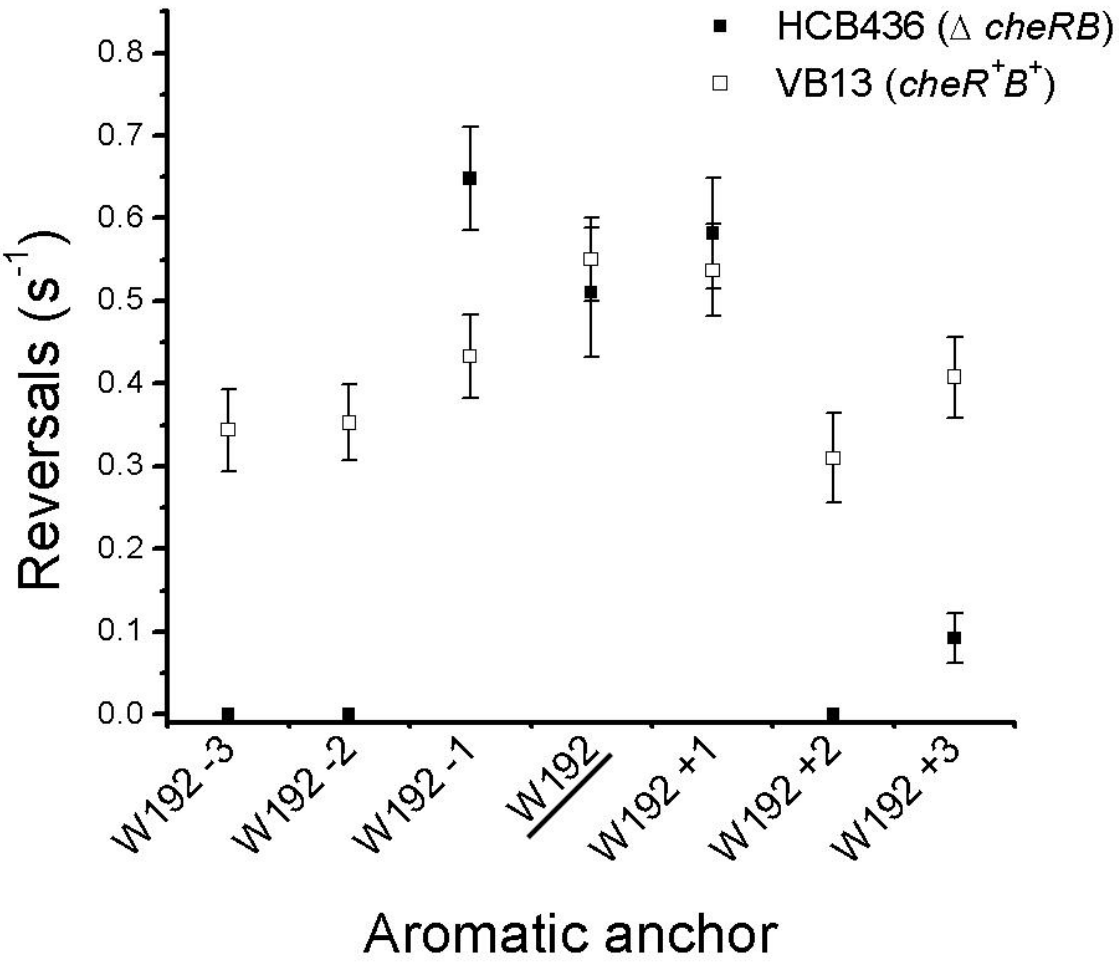

Figure 44. Mean Reversal Frequency (MRF) of flagella in cells expressing Tar_{Ec} with W192 shifted to different positions. The number of flagellar reversals were tabulated from the tethered VB13 (ΔT $cheR^+B^+$) or HCB436 (ΔT ΔcheRB) cells whose rotational bias is shown in **Figure 43**. Each data point represents the mean number of reversals for fifty cells, and the error bars represent the standard error of that mean. The wild-type aromatic anchor found in Tar_{Ec} is underlined.

A

Name	190	191	192	193	194 - 208	209	210	211
Wt	A	Q	W	Q	LAVIALVVVLILLVA	W	Y	G
191 AA	A	W	W	Q	LAVIALVVVLILLVA	A	A	G
191 WY	A	W	W	Q	LAVIALVVVLILLVA	W	Y	G
193 AA	A	Q	W	W	LAVIALVVVLILLVA	A	A	G
193 WY	A	Q	W	W	LAVIALVVVLILLVA	W	Y	G

B

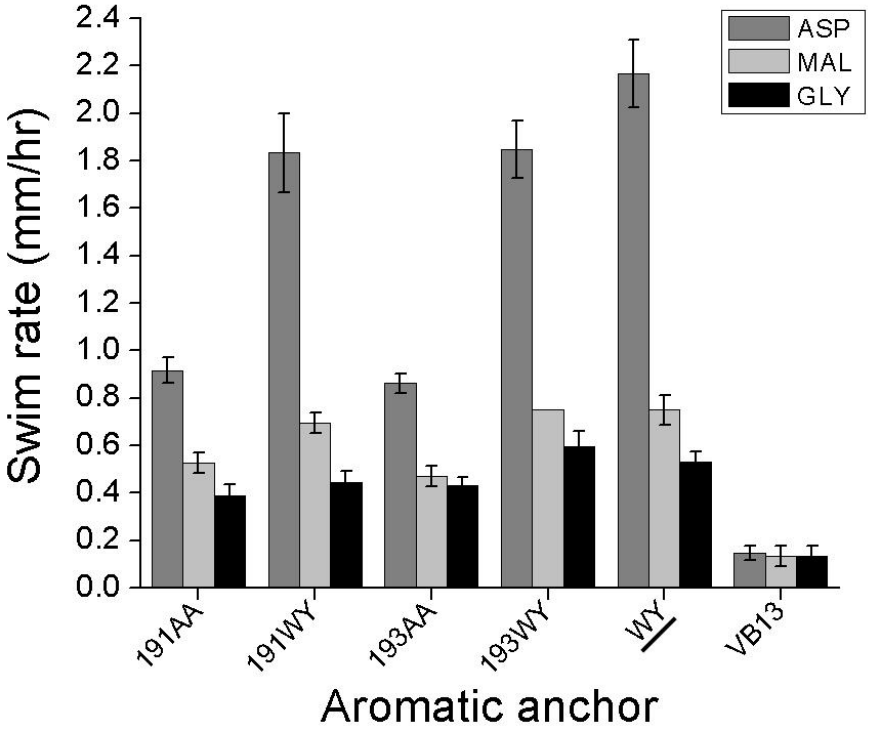

Figure 45. Chemotaxis ring formation in aspartate, maltose, and glycerol swim plates by cells expressing Tar_{Ec} variants containing two Trp residues in the periplasmic anchor. (A) Table of TM2 and nearby residues with mutations of the periplasmic and cytoplasmic aromatic anchors. Aromatic residues have a grey background. Wt designates the wild-type sequence. **(B)** VB13 (ΔT *cheR*$^+$*B*$^+$) cells expressing wild-type Tar_{Ec} or different Tar_{Ec} variants from pRD200 (*68*) were inoculated into semi-solid agar containing aspartate, maltose, or glycerol. Plates were incubated at 30°C and measured after 8 hours, when migratory rings first became visible. The ring diameter was measured every 4 hours thereafter, and the migration rate was calculated in mm/hr. The error bars show the standard error of the mean for the expansion rates of ≥ 6 colonies. The wild-type anchor (WY) is underlined.

same for cells expressing Tar with the W912A substitution and the wild-type WY cytoplasmic anchor as for wild-type Tar. However, the expansion rate increased for cells expressing Tar with the W192A substitution and either the AA or AW tandem pair at position 209-210 (**Figure 46**). There was an increased CCW bias in all W192A mutants, regardless of the residues at positions 209-210 in cells with an intact adaptive methylation system (**Figure 47**). In cells lacking adaptative methylation, the W192A change did not compensate for the CCW-locked phenotype of Tar with the AA and AW configurations at residues 209-210. Cells with Trp-192 had an increased reversal rate compared to cells with the W192A substitution (**Figure 48**). The methylation states of most receptors were consistent with their rotational bias, but there appears to an increase in the methylation state of receptors in W192A Tar mutants, an effect that is most clearly seen in the W192A mutant with a Ala-Ala cytoplasmic tandem (**Figure 49**).

Discussion

As seen in **Table 6**, many two-component systems have two or more (total) aromatic residues in their TM2 helices, and these residues are usually located near the hydrophobic/hydrophilic interface regions of the membrane-spanning helix. Some of these proteins have only a single aromatic residue at one or both ends of TM2 or lack one altogether at the periplasmic interface. The question addressed here was whether the single Trp residue at the periplasmic interface is necessary and sufficient to maintain Tar_{Ec} in a wild-type signaling state. Previous work has shown that changing Trp-192 to

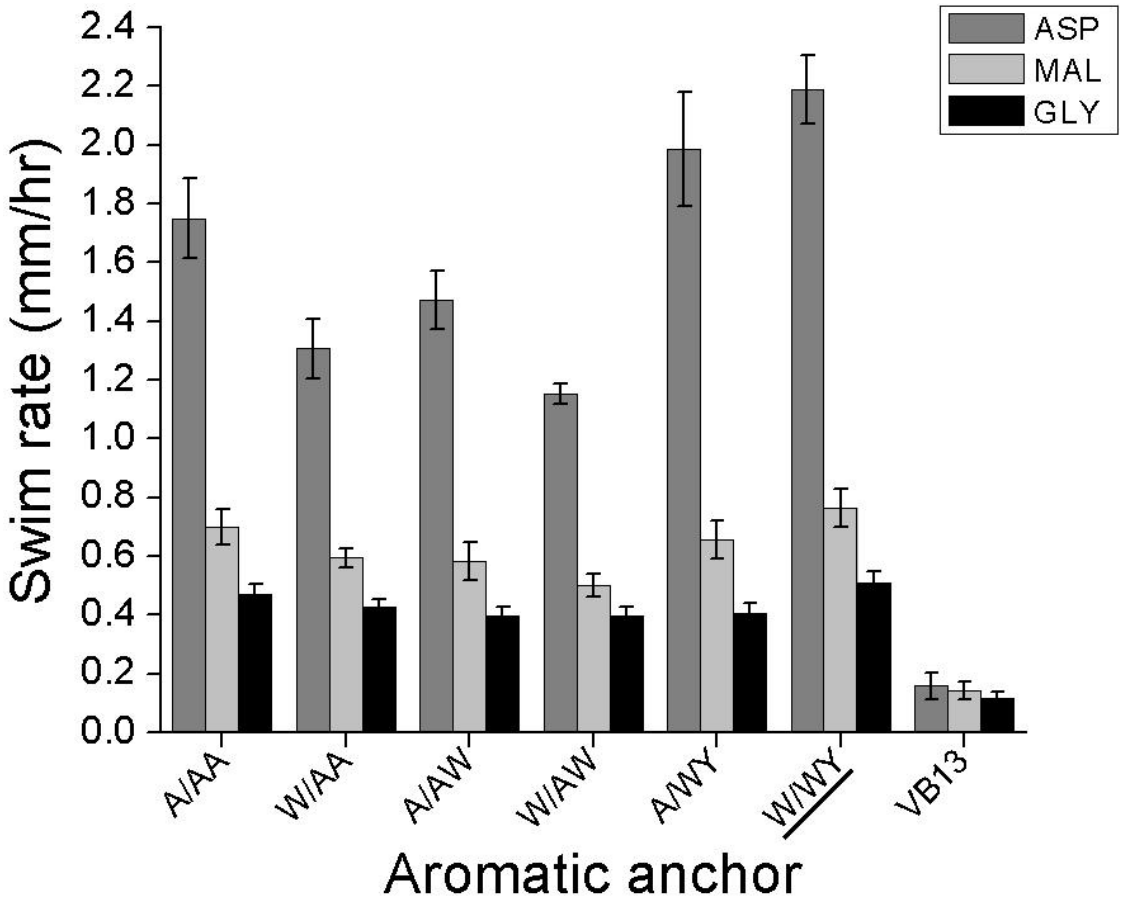

Figure 46. Chemotaxis ring formation in aspartate, maltose, and glycerol swim plates by cells expressing Tar_{Ec} variants containing different periplasmic / cytoplasmic aromatic anchors flanking the second transmembrane region. VB13 (ΔT *cheR*$^+$*B*$^+$) cells expressing wild-type Tar_{Ec} or different Tar_{Ec} variants from pRD200 (*68*) were inoculated into semi-solid agar containing aspartate, maltose, or glycerol. Plates were incubated at 30°C and measured after 8 hours, when migratory rings first became visible. The ring diameter was measured every 4 hours thereafter, and the migration rate was calculated in mm/hr. The error bars show the standard error of the mean for the expansion rates of $\geq$ 6 colonies. The wild-type anchor (W/WY) is underlined.

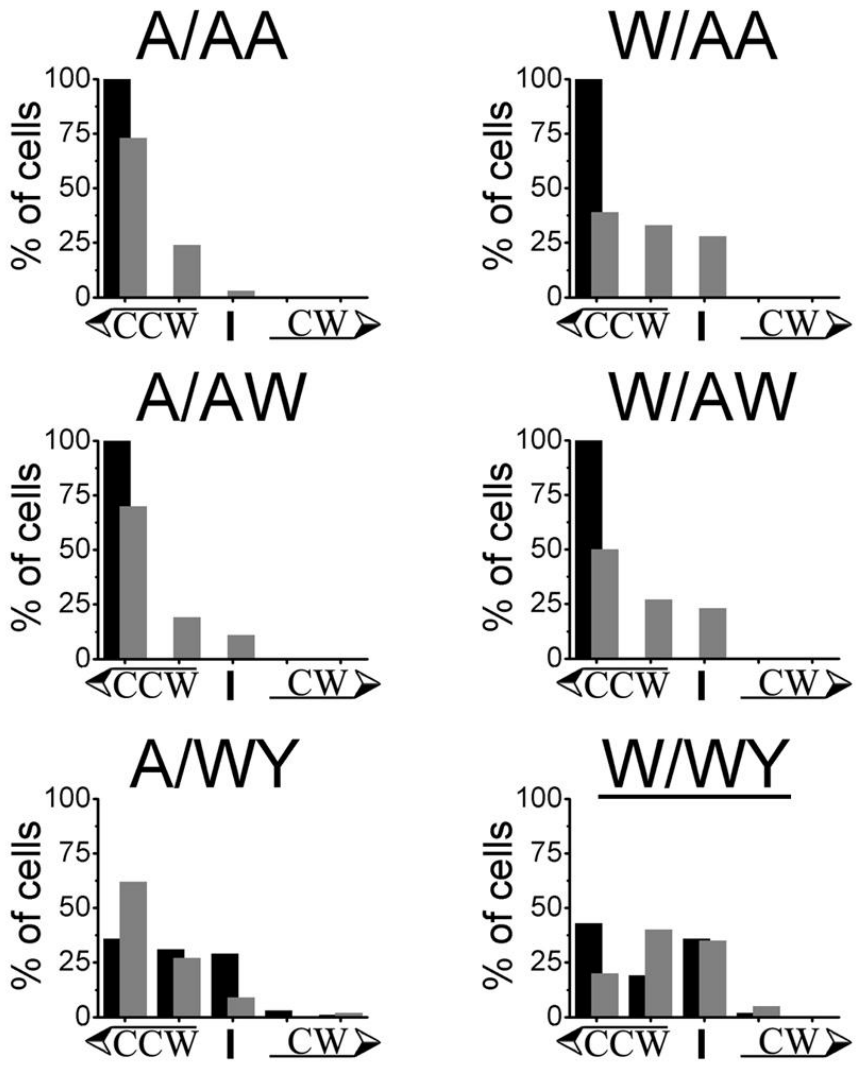

Figure 47. Flagellar rotational bias of cells expressing TarEc with W192 and aromatic anchor mutations. VB13 (ΔT cheR$^+$B$^+$) or HCB436 (ΔT ΔcheRB) cells expressing the wild-type or mutant TarEc variants from pRD200 (47), posessing a C-terminal epitope V5 tag were tethered, observed for 20 sec and assigned to one of five categories based on their apparent flagellar rotational bias. From left to right, these categories are designated: counterclockwise rotation with no switching (CCW only), counterclockwise-biased with frequent switching (CCW), frequent reversing with no apparent bias (CCW/CW), clockwise-biased with frequent switching (CW) and clockwise rotation with no switching (CW only). Results from VB13 cells are depicted as grey bars in the foreground while results from HCB436 are depicted as black bars in the background. Each histogram contains the classification of one hundred VB13 and one hundred HCB436 cells expressing each Tar_{Ec} variant. The wild-type aromatic anchor (W/WY) found in Tar_{Ec} is underlined.

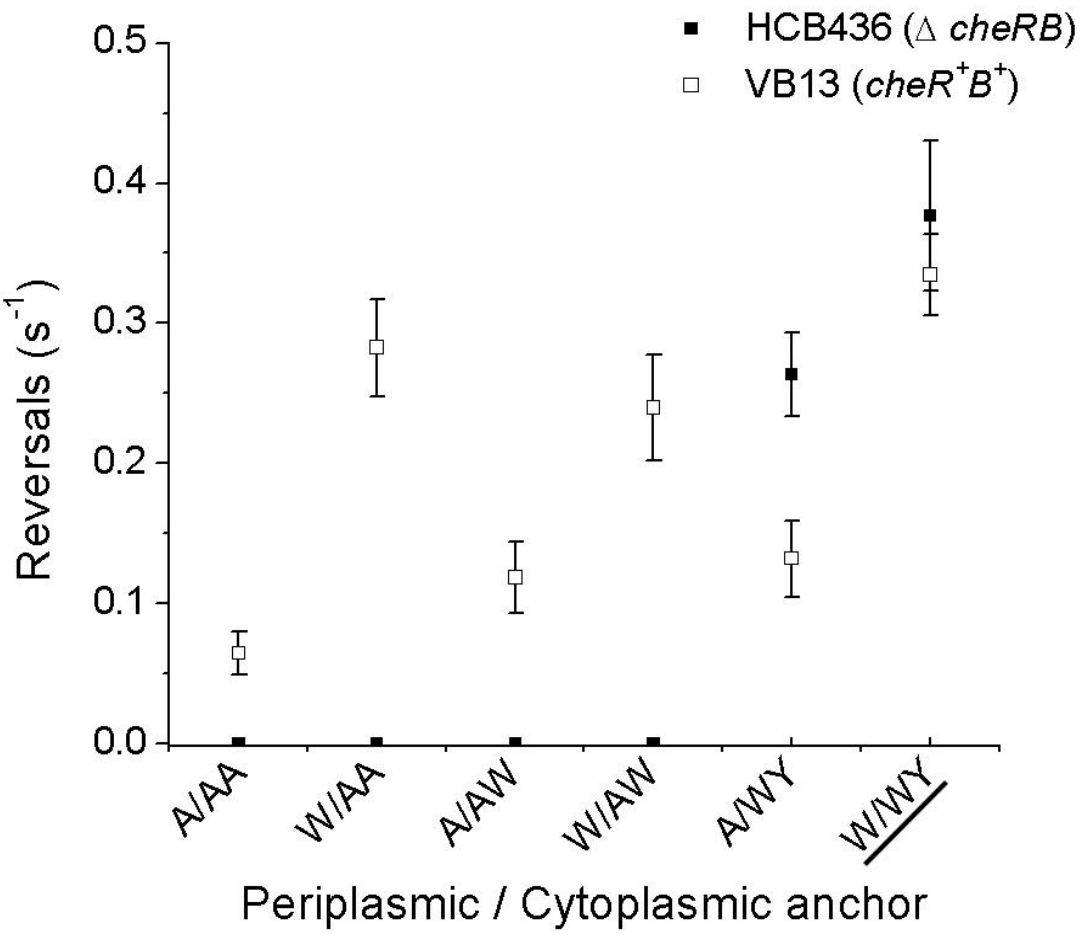

Figure 48. Mean Reversal Frequency (MRF) of flagella in cells expressing Tar_{Ec} with periplasmic / cytoplasmic aromatic anchor mutations. The number of flagellar reversals were tabulated from the tethered VB13 (ΔT $cheR^+B^+$) or HCB436 (ΔT ΔcheRB) cells whose rotational bias is shown in **Figure 46**. Each data point represents the mean number of reversals for one hundred cells, and the error bars represent the standard error of that mean. The wild-type aromatic anchor (W/WY) found in Tar_{Ec} is underlined.

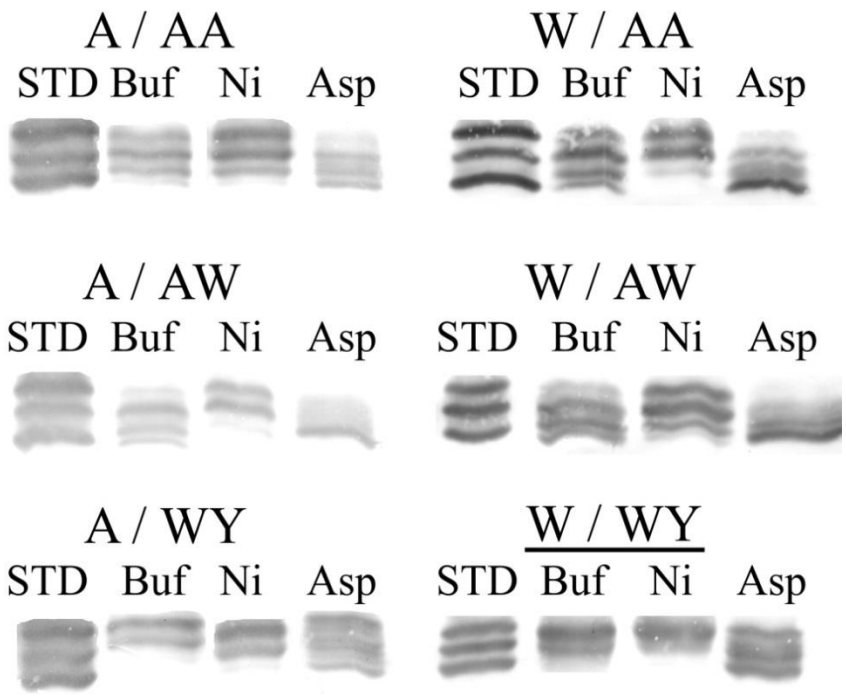

Figure 49. Steady-state patterns of covalent modification of the Tar_{Ec} receptor with mutations in the periplasmic/cytoplasmic anchor(s). Lanes labeled B, N, and A were run with samples incubated in buffer, buffer plus 10 mM $NiSO_4$ and 100 mM asparate. The STD lanes contain the mix of EEEE, QEQE, and QQQQ standards. The wild-type aromatic anchor (W/WY) found in Tar_{Ec} is underlined.

Ala had little effect on the kinase output of the Tar_{Ec} receptor (47). However, the wild-type cytoplasmic anchor may mitigate any effects the W192A substitution caused. Because changes in the position of the cytoplasmic Trp residue of TM2 affect receptor output, it seemed logical to use the same method to scan for changes in receptor output by altering the position of the Trp residue in the periplasmic anchor. Changes in the position of the Trp-192 residue by a single position had little effect on chemotaxis ring migration, rotational bias, or MRF (**Figure 42-44**). A normal distribution of bias was seen in cells expressing the W191, W192 (wt), and W193 receptors. With one exception, any further shifts in generated a CCW-locked phenotype in Δ*cheRB* cells that lack adaptation. The sole exception is W192+3 (W195), for which a majority of the cells were CCW locked and the cells that were not locked were CCW biased (**Figure 43**). Any further shift towards the C-terminus (plus direction) would likely yield a rotational bias more like wild-type Tar, as the Trp residue would be buried in the hydrophobic core of the transmembrane region and be unable to interact with the interface region to displace TM2 from its normal position. The ± 1-position range over which displacements of the Trp residue are tolerated corresponds to the normal range of motion of the receptor; the +1 shift mimics the attractant-bound conformation and the -1 shift-mimics the repellent-bound conformation.

To extend our test of our hypothesis, the Gln residues flanking the Trp-192 were substituted with a Trp residue. The substitution at position 191 created a tandem Trp-191 Trp-192 pair, whereas the substitution at position 193, created a Trp-192 Trp-193 tandem pair (**Figure 45**). There is no significant deviation in the rate of chemotactic ring

expansion for cells expressing Tar with either tandem Trp periplasmic anchor and the WY cytoplasmic anchor compared to cells expressing wild-type Tar. However, for cells expressing receptors with tandem Ala-Ala residues at the cytoplasmic membrane interface, the chemotaxis ring expansion rate with either the Trp-191 Trp-192 or the Trp-192-Trp 193 configuration was only 50% of cells expressing wild-type Tar (**Figure 45**). These swarm rates are similar to the wild-type W192 in an Ala-Ala cytoplasmic tandem (**Figure 20**). Therefore, neither tandem Trp configuration has the ability to restore wild-type receptor output likely due to the altered position of the C-terminal end of TM2 due to the tandem Ala-Ala substitution.

Further investigations into the relationship between the cytoplasmic and periplasmic aromatic anchors were conducted by pairing several cytoplasmic anchors with a receptor containing the W192A substitution. The cytoplasmic anchors chosen were WY (wild-type), AA, and AW. The AW pair should mimic the attractant-bound state of Tar. As seen previously (*68*), the W192A substitution combined with a wild-type cytoplasmic anchor (A/WY) had little effect on the rate of chemotaxis ring expansion. When the W192A substitution was paired with AA or AW at residues 209-210, the rate of chemotaxis ring expansion increased slightly relative to the rate seen when residue 192 was Trp (**Figure 46**). The tethered cell data indicate that CCW bias increases with the W192A substitution, whether WY, AA, or AW occupy positions 209-210. Additionally, cells expressing Tar with AA or AW at positions 209-210 remain CCW locked whether Trp or Ala is present as residue 192 (**Figure 47**). Adaptation-competent cells expressing receptors containing the W192A substitution have $\geq$ 50% reduction in

MRF when AA or AW occupy positions 209-210 but a ~60% increase in MRF when WY occupy positions 201-210 (**Figure 48**). Taken together, these experiments indicate that the composition of the cytoplasmic anchor has a greater role in determining signal output than the periplasmic anchor. However, in the absence of a cytoplasmic aromatic anchor, tandem Trp residues at the periplasmic membrane interface can apparently have a large effect on receptor function. These data then suggest that receptors with only a periplasmic anchor could possibly be tuned (**Table 6**).

The model presented in Chapter 2 and reference (*114*) suggested that an innate downward-directed force exerted on TM2 either from the periplasmic domain or from the periplasmic aromatic anchor. Here, it was seen that when the cytoplasmic aromatic anchor is eliminated, as in the 201-210 AA receptor, that the W192A substitution actually accentuates the CCW bias (**Figure 47, Figure 48**). This effect can also be seen in the increased methylation of the A/AA receptor compared to the W/AA receptor (**Figure 49**). This result suggests that the Trp-192 residue also resists the downward force exerted by the periplasmic domain to some extent. This leads to a more refined model seen in **Figure 41** where changes at the cytoplasmic anchor effects the output of the receptor through the extension of TM2 exposed to the hydrophobic environment of the cytosol before the Gly residue allows for a change in helicity between TM2 and the connector region between TM2 and AS1 of the HAMP domain.

CHAPTER V

RESEARCH CONCLUSIONS AND FUTURE DIRECTIONS

Research Conclusions

The work accomplished within this dissertation has reiterated that the composition of the cytoplasmic aromatic anchor is critical for proper receptor function as receptors lacking a Trp at the wild-type position do not have CW output in a strain lacking the adaptation system. Analysis of the signaling properties of mutants with aromatic and non-aromatic substitutions in the cytoplasmic anchor indicated that an intrinsic and persistent force acts upon TM2 that is directed towards the cytoplasm.

Single and double residue containing aromatic anchors were repositioned in TM2 to determine if altering the position of an anchor could restore a more wild-type like function to a deficient aromatic anchor. Results confirmed that repositioning an aromatic anchor can restore a more wild-type like output for a receptor. Additional, it was shown that the residues Gly-211immediately after the aromatic anchor of Tar plays a critical role in signal transduction by allowing flexibility or a change in helicity of the connector region between TM2 and the HAMP domain. Repositioned anchors can function similar to wild-type when the Gly-211 residue is altered as well. In repositioned anchors with a Trp residue at position 210, any substitution tested other than glycine at position 211 is able to activate the CheA kinase in a strain lacking the adaptation system. The G211P substitution stimulates normal levels of CheA activation but does not respond to ligand suggesting that this substitution locks the receptor in state that can stimulate CheA to produce either a kinase on or a kinase off state.

An additional subset of mutants was generated to study the role of the periplasmic Trp in signal transduction and to determine whether the force pushing towards the cytoplasmic originates from the periplasm or from the periplasmic Trp residue. From a series of Ala substitutions it was determined that that the periplasmic Trp residue helps to counteract the displacement force as motor output is increasingly CCW biased when either or both aromatic anchor residues are replaced by Ala. Thus the persistent force acting upon TM2 is originating from periplasm.

Future research and possible applications

One question remaining from this study is why there is a distribution of CW/CCW switching in Tar_{Ec} chemoreceptors when the adaptation system is present. That is, why is adaptive methylation apparently incomplete? In wild-type cells in which CheR and CheB of the adaptation system are absent, Tar_{Ec} is produced in the half methylated (QEQE) form. For cells of this type the expression of a majority of the mutant receptors have flagellar motors that remain in a CCW locked state. When the adaptation system is present, these cells regain the ability to switch their flagellar motors, as their receptors are modified to a higher methylation state. However, these cells take significantly longer to regain a normal (i.e., wild-type) CW/CCW bias as they would after stimulation with saturating levels of aspartate.

The QEQE forms of the receptors presumably are associated with a locked CCW phenotype because they lack enough covalent modification to restore the receptor to its wild-type equilibrium signaling state. In wild-type cells, a population of methylated

receptors exists along with a distribution of flagellar bias. It is my hypothesis that cells with a locked CCW phenotype have a lower degree of methylation, whereas cells with receptors with a higher level of methylation spend progressively more time in CW rotation.

A experiment to test this theory would be to express the different mutant receptors in the QEEE (singly modified), QEQE (doubly modified), QQQE (triply modified), and QQQQ (quadruply modified) forms and to observe how the rotational bias of the cells correlates with the modification state. A potential issue to be addressed with this experiment is whether methylation has a different effect than amidation.

A related question is whether a receptor patch may need receptors with multiple modification states to function properly. Cooperativity between receptors has been well characterized, although the exact mechanism(s) of cooperativity between receptors is not known. Cooperativity could arise from differences in the methylation states of individual receptors in the patch. Having a single modification state could disrupt cooperativity, causing a decreased response to ligand. In the experiments performed thus far, the subpopulations of the various methylated forms of the mutant receptors may not give an optimal baseline signal level.

Signal output from a given methylation state can be determined by utilizing the receptor's property of asymmetric signaling within the receptor dimer. Mutations in the aspartate-binding pocket can be that prevent signaling from a homodimer but allow for signaling to occur when two mutant monomers with defects in different halves of the binding site combine to make a heterodimer. This experimental approach is similar to

the work done by Gardina *et al*., 1998, because we can study receptors with any mutation at the aspartate-binding site combined with any level of covalent modification. Thus we can determine the effect of a single methylations state on receptor output and by varying the ratios of receptors with different methylation states we can attempt to quantify the effect of mixed methylation states on receptor output. Data from previous research (*68, 69, 114*) can be used as a baseline to allow the accurate study of these receptors with various methylation states. This approach can be used *in vivo* or *in vitro* as there are multiple assays that can determine changes in the signal output of a chemoreceptor. Additionally, a majority of mutants necessary for this project have already been created by myself or others. Though the scope of the project is significant involving many variables and controls, a majority of the groundwork has been completed.

An important question that was a major point in my original research proposal was to determine if there is a "spring constant" in for transmembrane signaling by chemoreceptors. The term "spring constant" is used to describe the energy required to displace the aromatic anchor from its energy-minimum equilibrium position at the hydrophobic/hydrophilic interface of the membrane. Altering the composition and position of the aromatic anchor should lead to differences in this spring constant. If an anchor has a higher preference for a hydrophilic environment it may be displaced more easily toward the cytoplasm, as the energy needed to displace the TM region into the cytoplasm would be reduced. Thus, weaker attractants could have an increased effect on receptor output, thereby increasing sensitivity toward a ligand. However, in this

particular example the "spring constant" might be increased for a repellent, which is thought to pull TM2 into the membrane. If so, the effect on receptor output for attracts and repellents might be inverted. Conversely, a more-hydrophobic anchor might be harder to displace into the cytoplasm and have a higher "spring constant" for an attractant and a lower one for a repellent. The existence of a "spring constant" that responds in this way would provide additional evidence for a piston motion in TM2 that is tuned to the energy required for physiological ligands of a receptor to displace the cytoplasmic anchor in either direction.

A direct physical technique for detecting changes in the spring constant would be to use Isothermal titration calorimetry (ITC). Comparison between the ITC data and the results from chemotaxis assays could provide a critical test of the spring constant idea. The experiments outlined should be straightforward and relatively easy to complete, as there is a library of mutants already available. The major hurdle would be to make membrane preps of each mutant receptor. A selective screen of several candidate mutants would take less than a month and should indicate whether this line of research is worth pursuing.

Potential uses of the concepts explored in this dissertation could involve designing chimeric receptors. One such chimera that has already been studied expensively is Nart, which joins the periplasmic, transmembrane, and HAMP linker domains of NarX with the cytoplasmic adaptation and signaling domains of Tar (*132, 141*). Nart and other chimeric receptors were created without regard for the effects that the adaptation system might have on the baseline output of the chimeric receptor. The analysis of mutants from

my research has shown that the aromatic residues within TM2 are important in signal output,

As the mechanism of signal transduction likely co-evolved with the type of ligand(s) that a receptor detects to produce an ideal output for the system. Similarly, individual the HAMP domains are likely optimized by evolution to work with specific ligands and a particular aromatic anchor. The presence of adaptive methylation in chemoreceptors probably renders them more versatile with regard to ligand compared to a receptor that lacks an adaptation system. The two component system of bacterial chemotaxis relies on input from one or more receptors and it is possible that the mechanism of signal transduction differs between receptors for this system.

Different two component systems may require alternate methods of signal transduction in their respective receptors. Most two component systems do not reply upon multiple receptors for their input and for on-off signals of the type mediated by many sensors of two-component signaling systems, the aromatic anchor might have rather different constraints that it does in a chemoreceptor. The precise properties of the aromatic anchor, particularly on the cytoplasmic face of the membrane, might therefore be particularly important in designing or tuning the sensitivity of transmembrane sensors.

Determining the base signal output and the effects of altering an aromatic anchor's composition on signal output is needed to characterize a receptor. If we assume receptors that signal though a piston displacement behave similarly to the signal transduction mechanism of Tar_{Ec} then it is possible to determine the signaling mechanism of an

unknown receptor with a few select mutations. If the output of the unknown receptor changes in a similar fashion to Tar_{Ec} then it has a piston displacement, otherwise the displacement type is not a piston mechanism. This methodology of receptor classification relates signal output to a mechanical mechanism but depends upon two general assumptions which are (1) The same model of transduction will behave similarly in difference receptors, and (2) Other mechanisms of signal transduction can be determined by substitutions in the aromatic anchor. If these conditions are true, then determining the model of signal transduction for a particular receptor can be accomplished with minimal work.

The goal of the work presented in this dissertation was to increase our understanding of transmembrane signaling in two-component systems by utilizing Tar_{Ec} as a model. Clearly, the model is over-simplified in that not all receptors signal through the same mechanism, and not everything that applies to one two-component system can be successfully extrapolated to another. Signal transduction pathways are complex, and many different changes in a receptor can significantly alter kinase output. The focus of my research has been on the TM2 region, and in particular how the aromatic residues flanking TM2 affect the receptor output. I believe the research presented here helps to validate the efforts for previous researchers and provides new insights that can be used to understand the role of aromatic anchors in maintaining receptor equilibrium. Many questions remain unresolved, and I have endeavored to propose multiple experimental strategies to study the many elements involved in the proper function of a receptor. Although much of the low hanging fruit has been harvested, many questions remain to

be answered. It is my hope that the research I have conducted, the questions that I have raised, and the future experiments I have described will assist others with their research to characterize signal transduction in the chemotaxis field or within other model systems.

REFERENCES

1. Welch, M., Oosawa, K., Aizawa, S., Eisenbach, M. (1993) Phosphorylation-dependent binding of a signal molecule to the flagellar switch of bacteria., *Proc. Natl. Acad. Sci. U.S.A. 90*, 8787-8791.

2. Berg, H. C. (2000) Motile behavior of bacteria., *Phys. Today 53*, 24-29.
3. Silverman, M., Simon, M. (1974) Flagellar rotation and the mechanism of bacterial motility., *Nature 249*, 73-74.

4. Berg, H. C., Turner, L. (1995) Cells of *Escherichia coli* swim either end forward., *Proc. Natl. Acad. Sci. U.S.A. 92*, 477-479.

5. Li, G., Weis, R.M. (2000) Covalent modification regulates ligand binding to receptor complexes in the chemosensory system of *Escherichia coli*., *Cell (Cambridge, MA, U. S.) 100*, 357-365.

6. Sourjik, V., Berg, H.C. (2002) Receptor sensitivity in bacterial chemotaxis., *Proc. Natl. Acad. Sci. U.S.A. 99*, 123-127.

7. Ames, P., Studdert, C.A., Reiser, R.H., Parkinson, J.S. (2002) Collaborative signaling by mixed chemoreceptor teams in *Escherichia coli*., *Proc. Natl. Acad. Sci. U.S.A. 99*, 7060-7065.

8. Springer, M. S., Goy, M.F., Adler, J. (1977) Sensory transduction in *Escherichia coli*: two complementary pathways of information processing that involve methylated proteins., *Proc. Natl. Acad. Sci. U.S.A. 74*, 3312-3316.

9. Maeda, K., Imae, Y. (1979) Thermosensory transduction in *Escherichia coli*: inhibition of the thermoresponse by L-serine., *Proc. Natl. Acad. Sci. U.S.A. 76*, 91-95.

10. Hazelbauer, G. L. (1988) The bacterial chemosensory system., *J. Microbiology 34*, 466-474.

11. Wang, E. A., Koshland, D.E. Jr. (1980) Receptor structure in the bacterial sensing system., *Proc. Natl. Acad. Sci. U.S.A. 77*, 7157-7161.

12. Stewart, R. C., Dahlquist, F.W. (1987) Molecular components of bacterial chemotaxis., *Chem. Rev. 87*, 997-1025.

13. Bibikov, S. I., Biran, R., Rudd, K.E., Parkinson, J.S. (1997) A signal transducer for aerotaxis in *Escherichia coli*., *J. Bacteriol. 179*, 4075-4079.

14. Li, M., Hazelbauer, G.L. (2004) Cellular stoichiometry of the components of the chemotaxis signaling complex., *J. Bacteriol. 186*, 3687-3694.

15. Butler, S. M., Camilli, A. (2005) Going against the grain: chemotaxis and infection in *Vibrio cholerae*., *Nat. Rev. Microbiol. 3*, 611-620.

16. Liu, X., Parales, R.E. (2008) Chemotaxis of *Escherichia coli* to Pyrimidines: a New Role for the Signal Transducer Tap., *J. Biol. Chem. 190*, 972-979.

17. Hegde, M., Englert D.L., Schrock, S., Cohn, W.B., Vogt, C., Wood, T.K., Manson, M.D., Jayaraman, A. (2011) Chemotaxis to the Quorum-Sensing Signal AI-2 Requires the Tsr Chemoreceptor and the Periplasmic LsrB AI-2-Binding Protein., *193 3*, 768-773.

18. Adler, J., Templeton, B. (1967) The effect of environmental conditions on the motility of *Escherichia coli*., *J. Gen. Microbiol. 46*, 175-184.

19. Lin, L. N., Li, J., Brandts, J.F., Weis, R.M. (1994) The serine receptor of bacterial chemotaxis exhibits half-site saturation for serine binding., *Biochemistry 33*, 6564-6570.

20. Adler, J. (1973) A method for measuring chemotaxis and use of the method to determine optimum conditions for chemotaxis by *Escherichia coli*., *J. Gen. Microbiol. 74*, 77-91.

21. Hazelbauer, G. L. (1975) The binding of maltose to 'virgin' maltose-binding protein is biphasic., *J. Bacteriol. 122*, 206-214.

22. Ordal, G. W., Adler, J. (1974) Properties of mutants in galactose taxis and transport., *J. Bacteriol. 117*, 517-526.

23. Kondoh, H., Ball, C.B., Adler J. (1979) Identification of a methyl-accepting chemotaxis protein for the ribose and galactose chemoreceptors of *Escherichia coli*., *Proc. Natl. Acad. Sci. U.S.A. 76*, 260-264.

24. Clarke, S., Koshland, D.E. Jr. (1979) Membrane receptors for aspartate and serine in bacterial chemotaxis., *J. Biol. Chem. 254*, 9695-9702.

25. Krikos, A., Conley, M.P., Boyd, A., Berg, H.C., Simon, M.I. (1985) Chimeric sensory transducers of *Escherichia coli*., *Proc. Natl. Acad. Sci. U.S.A. 82*, 1326-1330.

26. Mowbray, S. L., Koshland, D.E. Jr. (1990) Mutations in the aspartate receptor which affects aspartate binding., *J. Biol. Chem. 265*, 15638-15643.

27. Milburn, M. V., Privé, G.G., Milligan, D.L., Scott, W.G., Yeh, J., Jancarik, J., Koshland, D.E. Jr., Kim, S.H. (1991) Three-dimensional structures of the ligand-binding domain of the bacterial aspartate receptor with and without a ligand., *Science 254*, 1342-1347.

28. Gardina, P., Conway, C., Kossman, M., Manson, M. (1992) Aspartate and maltose-binding protein interact with adjacent sites in the Tar chemotactic signal transducer of *Escherichia coli*., *J. Bacteriol. 174*, 1528-1536.

29. Yeh, J. I., Biemann, H.P., Prive, G.G., Pandit, J., Koshland, D.E., Jr., Kim, S.H. (1996) High-resolution structures of the ligand binding domain of the wild-type bacterial aspartate receptor., *J. Mol. Biol. 262*, 186-201.

30. Hazelbauer, G. L. (1975) Maltose chemoreceptor of *Escherichia coli*., *J. Bacteriol. 122*, 206-214.

31. Spurlino, J. C., Lu, G.Y., Quiocho, F.A. (1991) The 2.3A resolution structure of the maltose- or maltodextrin-binding protein, a primary receptor of bacterial active transport and chemotaxis., *J. Biol. Chem. 266*, 5202-5219.

32. Zhang, Y., Mannering, D.E., Davidson, A.L., Yao, N., Manson, M.D. (1996) Maltose-binding protein containing an interdomain disulfide bridge confers a dominant-negative phenotype for transport and chemotaxis., *J. Biol. Chem. 271*, 17881-17889.

33. Manson, M. D., Kossmann, M. (1986) Mutations in Tar suppress defects in maltose chemotaxis caused by specific malE mutations., *J. Bacteriol. 165*, 34-40.

34. Zhang, Y., Conway, C., Rosato, M., Suh, Y., Manson, M.D. (1992) Maltose chemotaxis involves residues in the N-terminal and C-terminal domains on the same face of maltose-binding protein., *J. Biol. Chem. 267*, 22813-22820.

35. Koiwai, O., Hayashi, H. (1979) Studies on bacterial chemotaxis. IV. Interaction of maltose receptor with a membranebound chemosensing component., *J. Biochem. 86*, 27-34.

36. Brass, J. M., Manson, M.D. (1984) Reconstitution of maltose chemotaxis in *Escherichia coli* by addition of maltose-binding protein to calcium-treated cells of maltose regulon mutants., *J. Bacteriol. 157*, 881-890.

37. Mesibov., R., Adler, J. (1972) Chemotaxis toward amino acids in *Escherichia coli*., *J. Bacteriol. 112*, 315-326.

38. Mizuno, T., Imae, Y. (1984) Conditional inversion of the thermoresponse in *Escherichia coli*., *J. Bacteriol. 159*, 360-367.

39. Tso, W. W., Adler, J. (1978) Negative chemotaxis in *Escherichia coli*., *J. Bacteriol. 118*, 560-576.

40. Englert, D. L., Adase, C.A., Jayaraman, A., Manson, M.D. (2010) Repellent taxis in response to nickel ion requires neither Ni2+ transport nor the periplasmic NikA binding protein., *J. Bacteriol. 192*, 2633-2637.

41. Sperandio, V., Torres, A.G., Kaper, J.B. (2002) Quorum sensing *Escherichia coli* regulators B and C (QseBC): a novel two-component regulatory system involved in the regulation of flagella and motility by quorum sensing in *E. coli*., *Mol. Microbiol. 43*, 809-821.

42. Miller, S. T., Xavier, K.B., Campagna, S.R., Taga, M.E., Semmelhack, M.F., Bassler, B.L., Hughson, F.M. (2004) *Salmonella typhimurium* recognizes a chemically distinct form of the bacterial quorum-sensing signal AI-2., *Mol. Cell. 15*, 667-687.

43. Aksamit, R. R., Koshland, D.E. Jr. (1974) Identification of the ribose binding protein as the receptor for ribose chemotaxis in *Salmonella typhimurium*., *Biochemistry 13*, 4473-4478.

44. Nara, T., Lee, L., Imae, I. (1991) Thermosensing ability of Trg and Tap chemoreceptors in *Escherichia coli*., *J. Bacteriol. 173*, 1120-1124.

45. Hazelbauer, G. L., Adler, J. (1971) Role of the galactose binding protein in chemotaxis of *Escherichia coli* toward galactose., *Nat. (London) New Biol. 230*, 101-104.

46. Manson, M. D., Blank, V., Brade, G., Higgins, C.F. (1986) Peptide chemotaxis in *E. coli* involves the Tap signal transducer and the dipeptide permease., *Nature 321*, 253-256.

47. Abouhamad, W. N., Manson, M., Gibson, M.M., Higgins, C.F. (1991) Peptide transport and chemotaxis in *Escherichia coli* and *Salmonella typhimurium*: characterization of the dipeptide permease (Dpp) and the dipeptide-binding protein., *Mol. Microbiol. 5*, 1035-1047.

48. Rebbapragada, A., Johnson, M.S., Harding, G.P., Zuccarelli, A.J., Fletcher, H.M., Zhulin, I.B., Taylor, B.L. (1997) The Aer protein and the serine chemoreceptor Tsr independently sense intracellular energy levels and transduce oxygen, redox, and energy signals for *Escherichia coli* behavior., *Proc. Natl. Acad. Sci. U.S.A. 94*, 10541-10546.

49. Nishiyama, S. I., Ohno, S., Ohta, N., Inoue, Y., Fukuoka, H., Ishijima, A., Kawagishi, I. (2010) Thermosensing function of the *Escherichia coli* redox sensor Aer., *J. Bacteriol. 192*, 1740-1743.

50. Bowie, J. U. (1995) The Three-Dimensional Structure of the Aspartate Receptor from *Escherichia coli*., *Acta Cryst. D*, 145-154.

51. Gardina, P. J., Bormans, A.F., Hawkins, M.A., Meeker, J.W., Manson, M.D. (1997) Maltose-binding protein interacts simultaneously and asymmetrically with both subunits of the Tar chemoreceptor., *Mol. Microbiol. 23*, 1181–1191.

52. Gardina, P. J., Bormans, A.F., Manson, M.D. (1998) A mechanism for simultaneous sensing of aspartate and maltose by the Tar chemoreceptor of *Escherichia coli*., *Mol. Microbiol. 29*, 1147-1154.

53. Aravind, L., Ponting, C.P. (1999) The cytoplasmic helical linker domain of receptor histidine kinase and methyl-accepting proteins is common to many prokaryotic signalling proteins., *FEMS Microbiol. Lett. 176*, 111-116.

54. Hulko, M., Berndt, F., Gruber, M., Linder, J.U., Truffault, V., Schultz, A., Martin, J., Schultz, J.E., Lupas, A.N., Coles, M. (2006) The HAMP domain structure implies helix rotation in transmembrane signaling., *Cell (Cambridge, MA, U. S.) 126*, 929-940.

55. Park, H., Im, W., Seok, C. (2011) Transmembrane signaling of chemotaxis receptor tar: insights from molecular dynamics simulation studies., *Biophys. J. 100*, 2955-2963.

56. Swain, K. E., Gonzalez, M.A., Falke, J.J. (2009) Engineered socket study of signaling through a four-helix bundle: evidence for a yin-yang mechanism in the kinase control module of the aspartate receptor., *Biochemistry 48*, 9266-9277.

57. Kitanovic, S., Ames, P., Parkinson, J.S. (2011) Mutational Analysis of the Control Cable That Mediates Transmembrane Signaling in the *Escherichia coli* Serine Chemoreceptor., *J. Bacteriol. 193*, 5062-5072.

58. Ames, P., Yu, Y.A., Parkinson, J.S. (1996) Methylation segments are not required for chemotactic signalling by cytoplasmic fragments of Tsr, the methyl-accepting serine chemoreceptor of *Escherichia coli*., *Mol. Microbiol. 19*, 737-746.

59. Alexander, R. P., Zhulin, I.B. (2006) Evolutionary genomics reveals conserved structural determinants of signaling and adaptation in microbial chemoreceptors., *Proc. Natl. Acad. Sci. U.S.A. 104*, 2885-2890.

60. Liu, J. D., Parkinson, J.S. (1991) Genetic evidence for interaction between the CheW and Tsr proteins during chemoreceptor signaling by *Escherichia coli*., *J. Bacteriol. 173*, 4941-4951.

61. Kim, K. K., Yokota, H., Kim, S-H. (1999) Four-helical-bundle structure of the cytoplasmic domain of a serine chemotaxis receptor., *Nature 400*, 787-792.

62. Weerasuriya, S., Schneider, B., Manson, M.D. (1998) Chimeric chemoreceptors in *Escherichia coli*: signaling properties of Tar-Tap and Tap-Tar hybrids., *J. Bacteriol. 180*, 914-920.

63. Chervitz, S. A., Falke, J.J. (1995) Lock on/off disulfides identify the transmembrane signaling helix of the aspartate receptor., *J. Biol. Chem. 270*, 24043-24053.

64. Hughson, A. G., Hazelbauer, G.L. (1996) Detecting the conformational change of transmembrane signaling in a bacterial chemoreceptor by measuring effects on disulfide cross-linking *in vivo*., *Proc. Natl. Acad. Sci. U.S.A. 93*, 11546-11551.

65. Ottemann, K. M., Xiao, W., Shin, Y.K., Koshland, D.E. Jr. (1999) A piston model for transmembrane signaling of the aspartate receptor., *Science 285*, 1751-1754.

66. Isaac, B., Gallagher, G.J., Balazs, Y.S., and Thompson, L.K. (2002) Site-directed rotational resonance solid-state NMR distance measurements probe structure and mechanism in the transmembrane domain of the serine bacterial chemoreceptor., *Biochemistry 41*, 3025-3036.

67. Miller, A. S., Falke, J.J. (2004) Side chains at the membrane-water interface modulate the signaling state of a transmembrane receptor., *Biochemistry 43*, 1763-1770.

68. Draheim, R. R., Bormans, A.F., Lai, R.-Z., and Manson, M.D. (2005) Tryptophan residues flanking the second transmembrane helix (TM2) set the signaling state of the Tar chemoreceptor., *Biochemistry 44*, 1268-1277.

69. Draheim, R. R., Bormans, A.F., Lai. R.-Z., Manson, M.D. (2006) Tuning a Bacterial Chemoreceptor with Protein-Membrane Interactions., *Biochemistry 45*, 14655-14664.

70. Stock, J. B., Koshland, D.E. Jr. (1978) A protein methylesterase involved in bacterial sensing., *Proc. Natl. Acad. Sci. U.S.A. 75*, 3659-3663.

71. Springer, W. R., Koshland, D.E. Jr. (1977) Identification of a protein methyltransferase as the cheR gene product in the bacterial sensing system., *Proc. Natl. Acad. Sci. U.S.A. 74*, 533-537.

72. Maddock, J. R., and Shapiro, L. (1993) Polar location of the chemoreceptor complex in the *Escherichia coli* cell., *Science 259*, 1717-1723.

73. Levit, M. N., Grebe, T.W., Stock, J.B. (2002) Organization of the receptor-kinase signaling array that regulates *Escherichia coli* chemotaxis., *J. Biol. Chem. 277*, 36748-36754.

74. Garzón, A., Parkinson, J.S. (1996) Chemotactic signaling by the P1 phosphorylation domain liberated from the CheA histidine kinase of *Escherichia coli*., *J. Bacteriol. 178*, 6752-6758.

75. Hess, J. F., Oosawa, K., Matsumura, P., Simon, M.I. (1987) Protein phosphorylation is involved in bacterial chemotaxis., *Proc. Natl. Acad. Sci. U.S.A. 84*, 7609-7613.

76. Hess, J. F., Bourret, R.B., Simon, M. I. (1988) Histidine phosphorylation and phosphoryl group transfer in bacterial chemotaxis., *Nature 336*, 139-143.

77. Hess, J. F., Oosawa, K., Kaplan, N., Simon, M.I. (1988) Phosphorylation of Three Proteins in the Signaling Pathway of Bacterial Chemotaxis., *Cell (Cambridge, MA, U. S.) 53*, 79-87.

78. Bourret, R. B., Hess, J.F., Simon, M.I. (1990) Conserved aspartate residues and phosphorylation in signal transduction by the chemotaxis protein CheY., *Proc. Natl. Acad. Sci. U.S.A. 87*, 41-45.

79. Roman, S. J., Meyers, M., Volz, K., Matsumura, P. (1992) A chemotactic signaling surface on CheY defined by suppressors of flagellar switch mutations., *J. Bacteriol. 174*, 6247-6255.

80. Barak, R., Eisenbach, M. (1992) Correlation between phosphorylation of the chemotaxis protein CheY and its activity at the flagellar motor., *Biochemistry 31*, 1821-1826.

81. Oosawa, K., Hess, J.F., Simon, M.I. (1988) Mutants Defective in Bacterial Chemotaxis Show Modified Protein Phosphorylation., *Cell (Cambridge, MA, U. S.) 53*, 89-96.

82. Kehry, M. R., Bond, M.W., Hunkapiller, M.W., Dahlquist, F.W. (1983) Enzymatic deamidation of methyl-accepting chemotaxis proteins in *Escherichia*

coli catalyzed by the cheB gene product., *Proc. Natl. Acad. Sci. U.S.A. 80*, 3599-3603.

83. Terwilliger, T. C., Bogonez, E., Wang, E.A., Koshland, D.E. Jr. (1983) Sites of methyl esterification on the aspartate receptor involved in bacterial chemotaxis., *J. Biol. Chem. 258*, 9608-9611.

84. Kehry, M. R., Doak, T.G., Dahlquist, F.W. (1984) Stimulus-induced changes in methylesterase activity during chemotaxis in *Escherichia coli*., *J. Biol. Chem. 259*, 11828-11835.

85. Barnakov, A. N., Barnakova, L.A., Hazelbauer, G.L. (1999) Efficient adaptational demethylation of chemoreceptors requires the same enzyme-docking site as efficient methylation., *Proc. Natl. Acad. Sci. U.S.A. 96*, 10667-10672.

86. Le Moual, H. Q., T. Koshland, D.E. Jr. (1997) Methylation of the *Escherichia coli* chemotaxis receptors: intra- and interdimer mechanisms., *Biochemistry 36*, 13441-13448.

87. Muppirala, U. K., Desensi, S., Lybrand, T.P., Hazelbauer, G.L. and Li, Z. (2009) Molecular Modeling of Flexible Arm-Mediated Interactions between Bacterial Chemoreceptors and their Modification Enzyme., *Protein Science 18*, 1702-1714.

88. Li, J. L., G., Weis, R.M. (1997) The serine chemoreceptor from *Escherichia coli* is methylated through an inter-dimer process., *Biochemistry 36*, 11851-11857.

89. Levin, M. D., Shimizu, T.S., Bray, D. (2002) Binding and diffusion of CheR molecules within a cluster of membrane receptors., *Biophys. J. 82*, 1809-1817.

90. Li, M., Hazelbauer, G.L. (2005) Adaptational assistance in clusters of bacterial chemoreceptors., *Mol. Microbiol. 56*, 1617-1626.

91. Lai, R. Z., Manson, J.M., Bormans, A.F., Draheim, R.R., Nguyen, N.T., Manson, M.D. (2005) Cooperative signaling among bacterial chemoreceptors., *Biochemistry 44*, 14298-14307.

92. Hazelbauer, G. L., Falke, J.J., Parkinson, J.S. (2008) Bacterial chemoreceptors: high-performance signaling in networked arrays., *Trends Biochem. Sci. 33*, 9-19.

93. Studdert, C. A., Parkinson, J.S. (2004) Crosslinking snapshots of bacterial chemoreceptor squads., *Proc. Natl. Acad. Sci. U.S.A. 101*, 2117-2122.

94. Li, M., Hazelbauer, G.L. (2011) Core unit of chemotaxis signaling complexes., *Proc. Natl. Acad. Sci. U.S.A. 108*, 9390-9395.

95. Briegel, A., Li, X., Bilwes, A.M., Hughes, K.T., Jensen, G.J., Crane, B.R. (2012) Bacterial chemoreceptor arrays are hexagonally packed trimers of receptor dimers networked by rings of kinase and coupling proteins., *Proc. Natl. Acad. Sci. U.S.A. 109*, 3766-3771.

96. Segall, J. E., Block, S.M., Berg, H.C. (1986) Temporal comparisons in bacterial chemotaxis., *Proc. Natl. Acad. Sci. U.S.A. 83*, 8987-8991.

97. Sourjik, V., Berg, H.C. (2004) Functional interactions between receptors in bacterial chemotaxis., *Nature 428*, 437-441.

98. Khursigara, C. M., Lan, G., Neumann, S., Wu, X., Ravindran, S., Borgnia, M.J., Sourjik, V., Milne, J., Tu, Y., Subramaniam, S. (2011) Lateral density of receptor arrays in the membraneplane influences sensitivity of the *E. coli* chemotaxis response., *EMBO 30*, 1719-1729.

99. McAndrew, R. S., Ellis, E.A, Manson, M.D., Holzenburg, A. (2004) TEM Analysis of Chemoreceptor Arrays in Native Membranes of *E. coli*., *Microsc. Microanal. 10*, 416-417.

100. Weis, R. M., Hirai, T., Chalah, A., Kessel, M., Peters, P.J., Subramaniam, S. (2003) Electron microscopic analysis of membrane assemblies formed by the bacterial chemotaxis receptor Tsr., *J. Bacteriol. 185*, 3636-3643.

101. Zhang, P., Khursigara, C.M., Hartnell, L.M, Subramaniam, S. (2007) Direct visualization of *Escherichia coli* chemotaxisreceptor arrays using cryo-electron microscopy., *Proc. Natl. Acad. Sci. U.S.A. 104*, 3777-3781.

102. Khursigara, C. M., Wu, W., Zhang, P., Lefman, J., Subramaniam, S. (2008) Role of HAMP domains in chemotaxis signalingby bacterial chemoreceptors., *Proc. Natl. Acad. Sci. U.S.A. 105*, 16555-16560.

103. Briegel, A., Ortega, D.R., Tocheva, E.L., Wuichet, K., Li, Z., Chen, S., Müller, A., Lancu, C.V., Murphy, G.E., Dobro, M.J., Zhulin, I.B., Jensen, G.J. (2009) Universal architecture of bacterial chemoreceptor arrays., *Proc. Natl. Acad. Sci. U.S.A. 106*, 17181-17186.

104. Liu J., H., B., Morado, D.R., Jani, S., Manson, M.D., Margolin, W. (2012) Molecular architecture of chemoreceptor arrays revealed by cryoelectron tomography of *Escherichia coli* minicells., *Proc. Natl. Acad. Sci. U.S.A. 109*, 1481-1488.

105. Hall, B. A., Armitage, J.P., Sansom, M.S. (2011) Transmembrane helix dynamics of bacterial chemoreceptors supports a piston model of signalling., *PLoS Comput. Biol. 7*.

106. White, S. H., Wimley, W.C. (1999) Membrane protein folding and stability: physical principles., *Annu. Rev. Biophys. Biomol. Struct. 28*, 319-365.

107. de Planque, M. R., Killian, J.A. (2003) Protein-lipid interactions studied with designed transmembrane peptides: role of hydrophobic matching and interfacial anchoring., *Mol. Membr. Biol. 20*, 271-284.

108. Wimley, W. C., White, S.H. (1992) Partitioning of tryptophan sidechain analogs between water and cyclohexane., *Biochemistry 31*, 12813-12818.

109. Wimley, W. C., White, S.H. (1993) Membranepartitioning: distinguishing bilayereffects from the hydrophobic effect., *Biochemistry 32*, 6307-6312.

110. Yau, W. M., Wimley, W.C., Gawrisch, K., White, S.H. (1998) The preference of tryptophan for membrane interfaces., *Biochemistry 37*, 14713-14718.

111. Nilsson, I., Saaf, A., Whitley, P., Gafvelin, G., Waller, C., and von Heijne, G. (1998) Proline-induced disruption of a transmembrane alpha-helix in its natural environment., *J. Mol. Biol. 284*, 1165-1175.

112. Braun, P., von Heijne, G. (1999) The aromatic residues Trp and Phe have different effects on the positioning of a transmembrane helix in the microsomal membrane., *Biochemistry 38*, 9778-9782.

113. Killian, J. A., Salemink, I., de Planque, M.R., Lindblom, G., Koeppe, R.E., 2nd, and Greathouse, D.V. (1996) Induction of nonbilayer structures in diacylphosphatidylcholine model membranes by transmembrane alpha-helical peptides: importance of hydrophobic mismatch and proposed role of tryptophans., *Biochemistry 35*, 1037-1045.

114. Adase, C. A., Draheim, R.R., Manson, M.D. (2012) The Residue Composition of the Aromatic Anchor of the Second Transmembrane Helix Determines the Signaling Properties of the Aspartate/Maltose Chemoreceptor Tar of *Escherichia coli*., *Biochemistry 51*, 1925-1932.

115. Berg, H. C., Brown, D.A. (1972) Chemotaxis in *Escherichia coli* analysed by three-dimensional tracking., *Nature 239*, 500-504.

116. Macnab R.M. and Koshland, D. E. J. (1972) The Gradient-Sensing Mechanism in Bacterial Chemotaxis., *Proc. Natl. Acad. Sci. U.S.A. 69*, 2509-2512.

117. Bornhorst, J. A., Falke, J.J. (2000) Attractant regulation of the aspartate receptor-kinase complex: limited cooperative interactions between receptors and effects of the receptor modification state., *Biochemistry 39*, 9486-9493.

118. Sevvana, M., Vijayan, V., Zweckstetter, M., Reinelt, S., Madden, D.R., Herbst-Irmer, R., Sheldrick, G.M., Bott, M., Griesinger, C., Becker, S. (2008) A ligand-induced switch in the periplasmic domain of sensor histidine kinase CitA., *J. Mol. Biol. 377*, 512-523.

119. Cheung, J., Le-Khac, M., Hendrickson, W.A. (2009) Crystal structure of a histidine kinase sensor domain with similarity to periplasmic binding proteins., *Proteins 77*, 235-241.

120. Moore, J. O., Hendrickson, W.A. (2009) Structural analysis of sensor domains from the TMAO-responsive histidine kinase receptor TorS., *Structure 17*, 1195-1204.

121. Zhang, Z., Hendrickson, W.A. (2010) Structural characterization of the predominant family of histidine kinase sensor domains., *J. Mol. Biol. 400*, 335-353.

122. Wolfe, A. J., Berg, H.C. (1989) Migration of bacteria in semisolid agar., *Proc. Natl. Acad. Sci. U.S.A. 86*, 6973-6977.

123. Smith, R. A., Parkinson, J.S. (1980) Overlapping genes at the cheA locus of *Escherichia coli*., *Proc. Natl. Acad. Sci. U.S.A. 77*, 5370-5374.

124. Parkinson, J. S. (1978) Complementation analysis and deletion mapping of *Escherichia coli* mutants defective in chemotaxis., *J. Bacteriol. 135*, 45-53.

125. Dahl, M. K., Boos, W., Manson, M.D. (1989) Evolution of chemotactic-signal transducers in enteric bacteria., *J. Bacteriol. 171*, 2361-2371.

126. Utsumi, R., Brissette, R.E., Rampersaud, A., Forst, S.A., Oosawa, K., Inouye, M. (1989) Activation of bacterial porin gene expression by a chimeric signal transducer in response to aspartate., *Science 245*, 1246-1249.

127. Baumgartner, J. W., Kim, C., Brissette, R.E., Inouye, M., Park, C., Hazelbauer, G.L. (1994) Transmembrane signalling by a hybrid protein: communication from the domain of chemoreceptor Trg that recognizes sugar-binding proteins to the kinase/phosphatase domain of osmosensor EnvZ., *J. Bacteriol. 176*, 1157-1163.

128. Cantwell, B. J., Draheim, R.R., Weart, R.B., Nguyen, C., Stewart, R.C., Manson, M.D. (2003) CheZ phosphatase localizes to chemoreceptor patches via CheA-short., *J. Bacteriol. 185*, 2354-2361.

129. Southern, J. A., Young, D.F., Heaney, F., Baumgärtner, W.K., Randall, R.E. (1991) Identification of an epitope on the P and V proteins of simian virus 5 that distinguishes between two isolates with different biological characteristics., *J. Gen. Virol. 72*, 1551-1557.

130. Guzman, L. M., Belin, D., Carson, M.J., Beckwith, J. (1995) Tight regulation, modulation, and high-level expression by vectors containing the arabinose PBAD promoter., *J. Bacteriol. 177*, 4121-4130.

131. Miller, J. H. (1972) *Experiments in Molecular Genetics.*, Cold Spring Harbor, NY.

132. Ward, S. M., Bormans, A.F., Manson, M.D. (2006) Mutationally altered signal output in the Nart (NarX-Tar) hybrid chemoreceptor., *J. Bacteriol. 188*, 3944-3951.

133. Berg, H. C., Block, S.M. (1984) A miniature flow cell designed for rapid exchange of media under high-power microscope objectives., *J. Gen. Microbiol. 130*, 2915-2920.

134. Bormans, A. Intradimer and Interdimer Methylation Response by Bacterial Chemoreceptors to Attractant Stimulus, Ph.D. Dissertation, Texas A&M University, College Station, TX, 2005.

135. Goy, M. F., Springer, M.S., Adler, J. (1978) Failure of sensory adaptation in bacterial mutants that are defective in a protein methylation reaction., *Cell (Cambridge, MA, U. S.) 15*, 1231-1240.

136. Manson, M. D. (2010) Dynamic motors for bacterial flagella., *Proc. Natl. Acad. Sci. U.S.A. 107*, 11151-11152.

137. Zhou, Q., Ames, P., Parkinson, J.S. (2009) Mutational analyses of HAMP helices suggest a dynamic bundle model of input-output signalling in chemoreceptors., *Mol. Microbiol. 73*, 801-814.

138. Zhou, Q., Ames, P., Parkinson, J.S. (2011) Biphasic control logic of HAMP domain signalling in the *Escherichia coli* serine chemoreceptor., *Mol. Microbiol. 80*, 596-611.

139. Manson, M. D. (2011) Transmembrane signaling is anything but rigid., *J. Bacteriol. 193*, 5059-5061.

140. Feng, X., Baumgartner, J.W., Hazelbauer, G.L. (1997) High- and Low-Abundance Chemoreceptors in *Escherichia coli*: Differential Activities Associated with Closely Related Cytoplasmic Domains., *J. Bacteriol. 170*, 6714-6720.

141. Ward, S. M., Delgado, A., Gunsalus, R.P., Manson, M.D. (2002) Chimeric chemoreceptors in *Escherichia coli*: signaling properties of Tar-Tap and Tap-Tar hybrids., *J. Bacteriol. 180*, 914-920.

142. Springer W.R.; Koshland D.E. (1977) Identification of a protein methyltransferase as the cheR gene product in the bacterial sensing system, *Proc. Natl. Acad. Sci. U.S.A. 74*, 533-537.

143. Hessa, T., Meindl-Beinker, N. M., Bernsel, A., Kim, H., Sato, Y., Lerch-Bader, M., Nilsson, I., White, S. H., and von Heijne, G. (2007) Molecular code for transmembrane-helix recognition by the Sec61 translocon, *Nature 450*, 1026-1030.